



Accuracy of Power Curve Measurements

Christensen, Carl Jørgen; Dragt, J.B.

Publication date:
1987

Document Version
Publisher's PDF, also known as Version of record

[Link back to DTU Orbit](#)

Citation (APA):
Christensen, C. J., & Dragt, J. B. (Eds.) (1987). *Accuracy of Power Curve Measurements*. Risø National Laboratory. Risø-M No. 2632

General rights

Copyright and moral rights for the publications made accessible in the public portal are retained by the authors and/or other copyright owners and it is a condition of accessing publications that users recognise and abide by the legal requirements associated with these rights.

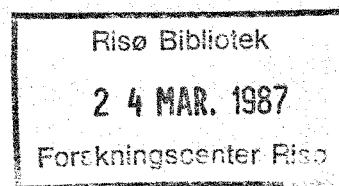
- Users may download and print one copy of any publication from the public portal for the purpose of private study or research.
- You may not further distribute the material or use it for any profit-making activity or commercial gain
- You may freely distribute the URL identifying the publication in the public portal

If you believe that this document breaches copyright please contact us providing details, and we will remove access to the work immediately and investigate your claim.

Accuracy of Power Curve Measurements

C. J. Christensen, Risø and J. B. Dragt, ECN (Editors)

**N. v. d Borg, ECN; O. Carlson, Chalmers; I. R. Derdelinkx, VUB;
R. Hunter, NEL; D. Infield, RAL; M. A. Lodge, AWTS;
J. van Meel, E. Lysen, K. Kieft, CWD; J. P. Molly, DFVLR;
U. S. Paulsen, Risø**



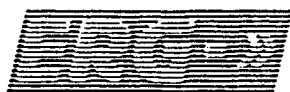
**Report prepared under the auspices of the IMTS
and supported by EEC, DGXVII,
under contract 84/B/7033/II/004/I7**

**Risø National Laboratory, DK-4000 Roskilde, Denmark
November 1986**



ECN

RISØ



ACCURACY OF POWER CURVE MEASUREMENTS

by

C.J. Christensen, Risø and J.B. Dragt, ECN (Editors)

and

N. v.d. Borg, ECN
O. Carlson, Chalmers
I.R. Derdelinkx, VUB
R. Hunter, NEL
D. Infield, RAL

M.A. Lodge, AWTs
J. van Meel, E. Lysen,
K. Kieft, CWD
J.P. Molly, DFVLR
U.S. Paulsen, Risø

November, 1986

Report prepared under the auspices of the IMTS and supported by EEC, DGXVII, under contract 84/B/7033/11/004/17.



COMMISSION
OF THE EUROPEAN
COMMUNITIES

Directorate-General for Energy

ISBN 87-550-1307-4

ISSN 0418-6435

Grafisk Service Center, Risø 1987

ABSTRACT

This report represents a start on the problem of reaching comparability and common acceptability of power curves measured at the different test stations. The problem is essential for establishing a future common set of certification rules. Such common rules in turn will serve the need for opening the internal market for windmills within the EEC. A few non-EEC members of the international IMTS cooperation between test stations have taken part in the project. This has been welcomed, as it will help opening the global market too.

Through the examination of a large number of error source, the test site specific errors were found to be the most important source of uncertainty. This has to do with how well an anemometer in a mast separated from the windmill represents the wind speed that drives the windmill. Three factors create this importance. First, when calculating the progression of errors from a power curve error into an uncertainty on the yearly production prediction, a multiplier of 2-4 must be applied to the velocity uncertainty. Secondly, turbulence induces errors. Thirdly, the terrain around the windmill is almost never homogeneous enough to avoid a flow distortion, that induces errors in the wind speed chosen to represent the driving speed.

A host of measures to be taken by the test station are recommended, aiming at reducing the uncertainties. Without an effort in this direction, the power prediction uncertainty can well be up to 25-30%. But it ought to be possible to reduce this uncertainty to a level of 5-10%.

It is recommended, that the power prediction error is calculated and quoted for a Rayleigh distribution with 7 m/s average wind speed.

<u>CONTENTS:</u>	pag.
1. INTRODUCTION.....	5
2. POWER CURVE DEFINITION AND ERRORS	7
2.1. Aerodynamic power curve	7
2.2. Virtual and driving wind speeds	7
2.3. Turbulence and time averaging	10
2.4. Sources of error	11
3. TERRAIN EFFECTS	13
3.1. Effects of terrain on mean wind speed	13
3.1.1. General description	13
3.1.2. Terrain effect measurements	15
3.1.2.1. The ECN test location for commercial wind turbines	15
3.1.2.2. The HAWT-25 site of ECN	19
3.1.2.3. The AWTs test site	19
3.1.3. Terrain effect estimation	22
3.1.4. Statistical error due to terrain effects	23
3.1.5. Wind gradient and cup anemometer height	24
3.1.6. Conclusions on average terrain effects	25
3.2. The effect of turbulence	26
3.2.1. General assumptions	26
3.2.2. Turbulence effects caused by power curve non- linearity (u^3 -binning)	27
3.2.3. Conclusions and recommendations on turbulence effects	36
3.2.3.1. Power prediction	36
3.2.3.2. Aerodynamic power curves	38
4. MEASUREMENT METHODS IN USE	39
4.1. Introduction	39
4.2. Signals used	39
4.3. Data handling methods	40
5. STATISTICAL TREATMENT OF THE METHOD OF BINS	43
5.1. Review of the method of bins	43
5.2. Statistics within the averaging time τ	44
5.3. Statistics of the averages	50
5.3.1. Statistical errors in power averages	50
5.3.2. WECS dynamics	51
5.3.2.1. Averaging turbulence over the rotor swept area	51
5.3.2.2. Integrating over periodic components	52
5.3.2.3. Averaging by dynamic effects	52
5.4. Statistical description of the method of bins	54
5.4.1. General statement of the problem	54
5.4.2. Normal distribution	54
5.4.3. Frequency domain representation	55
5.4.4. Requirements	56
5.4.5. Discussion of the variance	59
Annex 5A: Statistical definitions	62
Annex 5B: Frequency domain representation	65

6. REVIEW OF ALTERNATIVE METHODS OF ANALYSIS	67
6.1. Method of bins with short averaging time	67
6.2. Boom anemometer method	68
6.3. Power binning	69
6.4. Method of cubic bins	69
6.5. Least squares fitting	70
6.6. Orthogonal regression	71
6.7. Lack-of-correlation correction	71
6.8. Most probable power method	76
6.9. Frequency matching	76
6.10. Additional conditioning	77
6.11. Validity and verification	78
7. ACCURACY OF WIND SPEED MEASUREMENTS	79
7.1. Introduction	79
7.2. Normal calibration of cup anemometers	79
7.3. Calibration changes with time	80
7.4. Cup anemometer overspeeding	81
7.5. Influence on power curve of errors in cup anemometer calibration	82
7.6. Influence on annual production prediction	82
7.7. Recommendations and the need for an intercalibration	83
8. MACHINE CONDITIONS AND POWER SENSOR ERRORS	88
8.1. Machine conditions	88
8.1.1. Deviations from average machine properties	88
8.1.2. Changes in machine properties during measurements .	88
8.1.3. Discontinuities in power curve	89
8.1.4. Influence of climate	90
8.2. Watt-meter error	90
8.3. Reproducibility	91
9. CONCLUSIONS AND RECOMMENDATIONS	93
9.1. Recommendations on machine related errors	93
9.2. Recommendations on cup anemometer calibration and errors .	93
9.3. Representativity of wind measurement	94
9.4. Further work	95
9.5. General conclusion	96
REFERENCES	97
ANNEX A: Site descriptions	100
ANNEX B: Benchmark exercise for power curve measurement	140
ANNEX C: Proposal for the comparison of the accuracy of wind speed measurements at the wind turbine test stations	142

1. INTRODUCTION

Many countries - within the European Community and outside - are supporting test stations for commercial wind turbines. There exists a good cooperation between most of the test stations, centered around the yearly International Meeting of Test Stations of WECS.

It has been recognized by the Commission of the European Communities that it is important to support the uniform development of the performance and function testing, licensing criteria and certification procedures for the approval of wind turbines, through a coordination at Community level of activities undertaken in the National Test Stations. For that reason the Commission has commissioned some contracts with test stations in the European Community for conducting specific studies during 1985-1986. These are finally aimed at a European standardization of wind turbine requirements and testing. Some test stations from outside the Community joined in these studies.

One of the study contracts was on "Power curve computation and accuracy of power curve measurements". The final report on this study is made in two parts:

- A. Power curve computation benchmark tests.
- B. Accuracy of power curve measurements.

The second part of this contract had the following purpose.

The study should review and evaluate the methods used by different test stations for power curve data handling and for the determination of statistical uncertainties in order to formulate community recommendations to the test stations on the advisable power curve statistics and uncertainty calculations to be used. This will enable reliable power production predictions and secure the mutual acceptance of test reports from all test stations.

The participating test stations in this part of the study have been:

- Risø National Laboratory, Roskilde, Denmark (the main contractor),
- Netherlands Energy Research Foundation ECN, Petten, the Netherlands (contract management together with Risø),
- Consultancy Services Wind Energy Developing Countries CWD (with test stations at Eindhoven, Vriezenveen and Almere, the Netherlands),

- Deutsche Forschungs- und Versuchsanstalt für Luft- und Raumfahrt DFVLR (test station Schnittlingen, BRD),
- Vrije Universiteit Brussel, Dienst Stromingsmechanica, VUB, Belgium,
- National Engineering Laboratory NEL, Glasgow, in cooperation with Rutherford Appleton Laboratory, UK.

From outside the European Community the following test stations participated:

- Atlantic Wind Test Site, operated by Resources Ventures Inc., Prince Edward Island, Canada,
- Chalmers University of Technology, Dept. of Electrical Machinery, Göteborg, Sweden.

The work has proceeded as follows:

During the work on a contract with the EEC, DGXVII for the preparation of the IMTS-meeting in Lannion (June 1984), the need for a study of power curve measurement accuracy was revealed and the IMTS-meeting agreed to pursue the study. A detailed proposal for the study was accepted by the EEC and support was granted in a contract with the EEC in early 1985.

The work was started with a questionnaire distributed to the test stations in July 1985. The questionnaire was reproduced in the intermediate report on the project (ref. [1]). After a visit to most of the participating test stations by the editors (May 1986), a draft report was discussed at the IMTS-meeting at Schnittlingen, October 1986.

2. POWER CURVE DEFINITION AND ERRORS

2.1. Aerodynamic power curve

In aerodynamic calculations (and to a degree also in wind tunnel measurements) the power curve is defined and thought of in the following way (illustrated in fig. 2.1). In a suitable distance upstream of the windmill a wind of velocity v is streaming towards the machine, giving off energy to the rotor (thereby losing speed). The power curve is then seen as the relation between the power $P(v)$ produced by this undisturbed upwind wind speed v .

This definition is, however, of very doubtful value for a windmill in the natural wind. The main difficulty is that it assumes a smooth laminar flow of a high degree of homogeneity and symmetry. In nature the surrounding landscape will inevitably distort this picture. The ground surface will resist the wind, making sure to set up a vertical wind velocity gradient. Any kind of hills, valleys, trees, buildings, etc. in the landscape will prevent the stream lines from being straight lines even without the windmill. This in turn sets up horizontal gradients of wind speed also and produces focusing effects. On top of this turbulence is created by the rough surface and by thermal effects. This turbulence will make sure that local disturbances are created that are of course not equal at two points in space at the same time.

2.2. Virtual and driving wind speeds

We will therefore adopt a different philosophy. As was evident in fig. 2.1, the machine distorts the field. Therefore the wind field in the rotor plane is not interesting as a reference in a power curve measurement. The upstream velocity was really chosen as representative of the free-field velocity, that is the velocity in the rotor plane, if the windmill were removed. This "virtual" wind speed is the interesting velocity, as it is this wind, that decides the resources of a site. Even then it must be remembered that the free field velocity is not constant over the rotor plane. Therefore we define the wind velocity as a vector function $\underline{v}(\underline{r})$. The wind driving the windmill will then be some suitable average over the rotor area of $\underline{v}(\underline{r})$. Let us call the component along the rotor axis

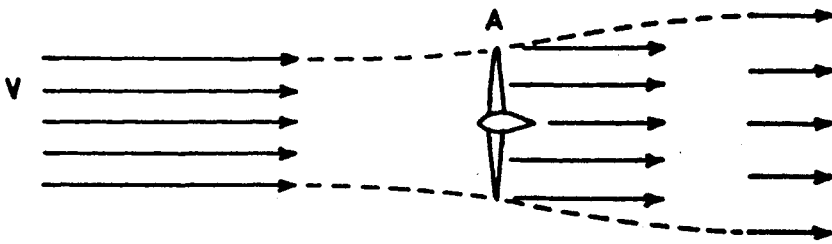


Fig. 2.1. Aerodynamic flow picture around a windmill rotor (idealized power curve definition).

(direction \hat{n}) of this average the "driving" wind speed

$$v = \int_A \underline{v}(\underline{r}) \cdot \hat{n} dA$$

In case of a linear wind shear and with negligible turbulence, the driving wind speed is equal to the virtual speed at hub height.

This average velocity is of course fictional and therefore not useful in practice either, but it is theoretically useful when trying to understand the situation. In practice, we will place an anemometer in a mast at some suitable distance in a position, where we can convince ourselves, that the wind speed u as measured is a good representation of the driving speed v . We will then measure P (windmill power) as a function of u , i.e. $P=P(u)$. If we have chosen a good representation of v , we can assume that the correct power curve $P(v)$ is $P(u)$ with $u = v$.

The notion of a virtual wind speed driving the windmill was introduced by Akins [2] but in the simpler form of one virtual speed in the rotor center with the machine removed. The usefulness of the virtual wind speed is twofold. First when doing performance predictions at a site, you start out with measurements of wind speeds in a mast without the machine present, i.e. a "virtual" free field wind speed is measured. Then the performance can be calculated simply as

$$= \int_0^{\infty} P(v) f(v) dv$$

where $f(v)$ is the established probability distribution for the virtual wind speed. Then, of course, also the power curve $P(v)$ has to be a function of the virtual wind speed.

Further, the error analysis is facilitated by the extra complexity in our use of the driving wind speed. In this case the major error sources, for statistical errors in particular, are in evaluating how representative the measured wind speed u is for the driving wind speed.

2.3. Turbulence and time averaging

The power curve $P(v)$ should ideally be based on momentaneous and simultaneous measurements of v and P . But here we meet insurmountable difficulties because of turbulence.

Turbulence (which is an alternative description of wind gusts) introduces uncertainty in the measurements by creating not fully coherent disturbances of the driving speed v and of u . In an oversimplified description of turbulence one can visualize a steady air flow with a velocity $\langle \bar{u} \rangle$ (average wind speed) with eddies of different sizes embedded, floating along with the air (so-called "frozen turbulence"). Assume that a cup anemometer is located at a distance D upstream of (in front of) the turbine. A large eddy will cause a slow fluctuation usually experienced by the wind sensor and by the total rotor area. The high frequency fluctuation) will be seen first by the wind sensor and D/\bar{u} secs. later by only a part of the rotor. It may miss the wind sensor but hit part of the rotor, or it may die out before reaching the rotor. This causes incomplete coherence and gives rise to scatter in the power curve. These effects are discussed in the chapters 5-6.

It should be made clear here, that turbulence could have two very different effects. The one we are talking about here is the fact, that turbulence causes the wind hitting the blade to vary in speed and direction quite rapidly. This is assumed to cause the present power production to vary with the wind speed variations as described by the power curve.

The main problem as far as power curve measurements is concerned, is that the similar changes in the wind speed at the anemometer are not fully coherent with the driving wind speed, thus causing power curve scatter.

Another effect could be envisioned, however. The present understanding of the aerodynamic basis for the power curve assumes a laminar flow around the blades. Turbulent disturbances of the flow could possible change the aerodynamic forces and thereby the power curve. This would mean that even if the turbulence did not disturb the measurement as such, the power curve could depend on the turbulence. Very little is known about this possibility of power curve change with turbulende. Therefore we can not prescribe an uncertainty element for this possibility. It actually means that the power curve uncertainty calculated does not represent a "true" value but rather a state-of-the-art value.

2.4. Sources of error

When analysing power curve measurements there are many sources of error. In table 2.1 these errors are listed. The main error groups are 1) machine conditions and power sensor errors (production errors or climatic effects), 2) wind sensor errors, and 3) representativity of measured wind speed (terrain effects or data handling errors). Most of the errors are concerned with how good a representation the mast wind speed is.

This report deals with these errors.

Chapters 3-7 deals with the representativity of the chosen wind velocity, 8-9 with machine and sensor errors.

In chapter 3 the terrain effects are treated. The systematic errors stemming from misrepresenting the driving wind speed because of inhomogeneities in the terrain are reviewed. Secondly the influence of turbulence is discussed.

In chapter 4 an overall discussion of the methods currently used by test stations is given. Particular emphasis is put on signal conditioning and data handling.

Chapters 5-6 deals with statistical problems (mostly caused by turbulence). Chapter 5 describes the popular method-of-bins with velocity-binning. The method and in particular its possible errors are described from a statistical point of view. Chapter 6 reviews other alternative data handling methods.

In chapter 7, the cupanemometer inaccuracy problem is treated. The consequences for power curve and power production prediction errors are discussed also.

Chapter 8 discusses the errors having to do with machine conditions and power sensor errors.

Chapter 9 summarizes conclusions and recommendations.

Annex A gives maps and pictures describing the test stations.

In two further appendices two possibilities for intercomparing methods in use are discussed: B: data handling benchmark and C: cup-anemometer intercalibration.

Table 2.1. Sources of error

Machine conditions and power sensor errors

Pitching error

Yawing error

Dirty blades

On/off problem

2-generator operation

Watt-meter - 3 phases, unbalanced loads

Machine conditions - climatic effects

- air density

- rain

- icing

Wind sensor errors

Cup-anemometer - calibration

- constancy

- dynamic behaviour (overspeeding)

Representativity-terrain effects

Vertical component of wind velocity

Velocity errors

- wind gradient

- anemometer height

- landscape

- flow distortion by windmill

Turbulende-coherence

- wind direction

- degree of turbulence ($\overline{v^3}$ or $\overline{v^2}$)

Representativity-signal handling

Sampling rate

Transmission errors

Filtering

- analog

- digital

Averaging time

- machine dynamic

- coherence

- resolution

- aliasing

Erroneous (u,P)-points

Experimental time

Possible corrections

Calculation of yearly production

Statistical method

- statistical error

- systematic error

3. TERRAIN EFFECTS

3.1. Effects of terrain on mean wind speed

3.1.1. General description

Irregularities in the terrain of a test station will disturb the homogeneity of the air flow. The effect of turbulence will be discussed in section 3.2. Here we consider the problem that the mean flow at the reference anemometer and the undisturbed (virtual) flow at the wind turbine location (i.e. the driving wind) may be affected in a different way by terrain features. This would result in an erroneous power curve. The error will generally depend on wind direction and height above the terrain.

It is not the intention in this report to present comprehensive test station descriptions, but mainly to describe their features and possibilities as far as power curve accuracy is concerned. Therefore extensive references to test station features will be found throughout the report emphasizing the particular error source discussion rather than the single test station. In Annex A a collection of maps and pictures of the participating test stations is given. These can be referred to in the discussion of the terrain features discussed here.

In establishing wind turbine test stations one has usually tried to find good locations, but in actual practice often compromises had to be accepted. In considering the test stations, participating in this project, it is easy to list a number of terrain features that might lead (but not necessarily do so!) to systematic differences between anemometer and wind turbine locations.

ECN : The test station for commercial machines is located on a North-South dune ridge, 12-15 m high, with flat land to the East and dune terrain to the West (dominating wind). There are large buildings in the north-west direction.

Risø : The test station is located on a terrain with slight slopes in Western direction (dominating wind) coming up from the fjord, which contains in the Southwest a peninsula with low hills.

NEL : The test station is very open, at the flat top of a hill (330 m), with 10-15% slopes on the West. The dominating winds come up these slopes, meeting the anemometer and wind turbines at dif-

ferent distances, so possibly affecting them differently.

- RAL : The test location has several severe irregularities in the near surroundings: a hill on one side, and on another side a complex of buildings (like nuclear reactors) of the atomic energy research establishment of Harwell.
- VUB : This test station has several terrain problems. It is on a hill near Brussels, and apart from the (lower lying) buildings of the medical faculty of the university and a row of trees and bushes on the other side, a large fire brigade building was erected next to the test station. The new test location at Zeebrugge promises to be much better.
- DFVLR: The Schnittlingen test station is also located on top of a hill with slopes on several sides, which perhaps might lead to inhomogeneities. Some effect of the (low) measurement building, close to the test bed for commercial machines, cannot be excluded.
- CWD : The test station at the Technological University of Eindhoven is close to university buildings on one side and has trees (10 to 20 m high) on other sides. The new test station in Almere seems to be better, both in wind regime as with regard to possible terrain effects.
- AWTS : This large field is located at the Northern end of the Prince Edward Island. It is almost triangular, flat, but on two sides surrounded by cliffs (6-12 m) coming up from the ocean, and on the third side by a forest.
- Chalmers: The test station is located in rough terrain in an area of small rocky islands in a fjord at Sweden's West Coast. The dominating wind direction (SW) is more-or-less over the town of Hönö at a distance of 500-1000 m.

It has appeared that in most cases the possible terrain effects have not been evaluated qualitatively (with the exception of AWTS and ECN). The possible magnitude of the effects is not known. So this constitutes a large unknown error source for the power curve measurements.

Three possible approaches are possible to account for the effects:

- a. detailed wind mapping of the terrain (preferably before the erection of the wind turbine), using a set of several anemometers;

- b. detailed flow-measurements in a wind tunnel for an accurately made physical model of the terrain and its surroundings.
- c. detailed computer-modeling of the complex terrain and numerical computation of the flow field. (The CEC supported European wind atlas project includes activities with regard to computer models for flow field calculation.)

Results of such studies are summarized in the section 3.1.2, namely made at ECN (a and b) and AWTS (b). These studies give some general insight in the complexity of the problem and in the orders of magnitude of resulting effects. Order of magnitude estimates can also be obtained by the methods developed for wind turbine siting, using idealised models of the terrain (section 3.1.3).

There is no standard way of taking terrain effects into account. In some places (RAL, DFVLR, ECN, ...) measurements with wind from obviously disturbed directions are excluded. Criteria for that are often rather subjective. Standardization of power curve measurements certainly requires some more objective criteria. The international test station cooperation is recommended to take up this discussion.

3.1.2. Terrain effect measurements

3.1.2.1. The ECN test location for commercial wind turbines

The situation has been shown in Annex A. A 1:500 model of this terrain with its 5 test locations and central anemometer mast location has been placed in a wind tunnel of MT-TNO, Apeldoorn, with simulated boundary flow [4]. Detailed flow mapping was made using hot wire anemometry. For the 5 test locations the ratio of local wind speed to the wind speed at the anemometer mast has been determined for several altitudes and wind directions. An example is shown in fig. 3.1. In some directions the errors may be of the order of 10%, in particular for Northwest to North directions, due to a large building. The building was also shown to increase the turbulence intensity.

In power curve measurements such wind directions are excluded from the analysis. For the acceptable wind directions the wind tunnel data are used to translate the anemometer wind speed (interpolated to hub height) into undisturbed wind speed at the test location.

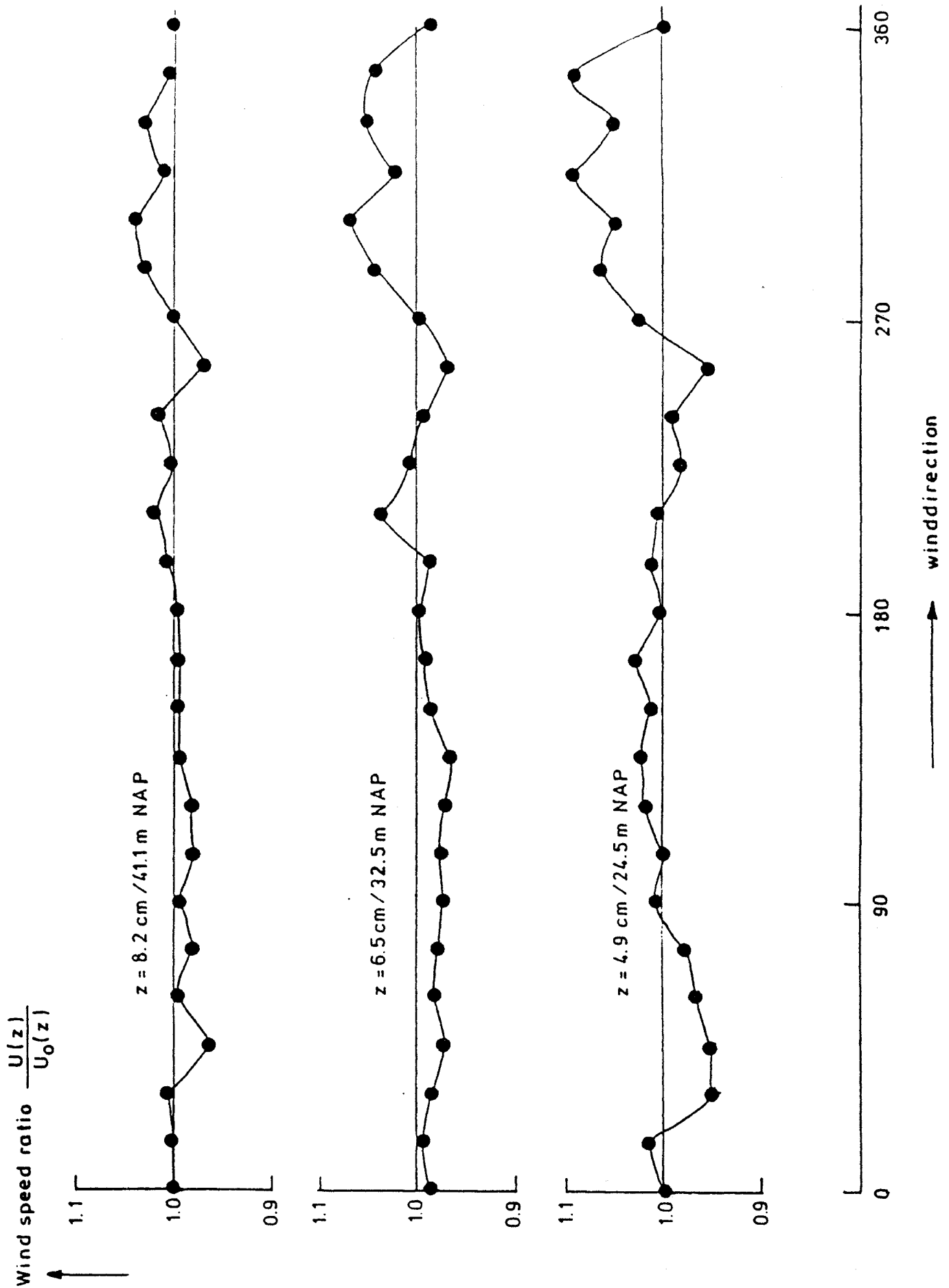


Fig. 3.1. Ratio of wind speeds at a test location and at the anemometer mast for 3 different heights and 25 wind directions, as measured by TNO-MT in a windtunnel model of the ECN test station [4].

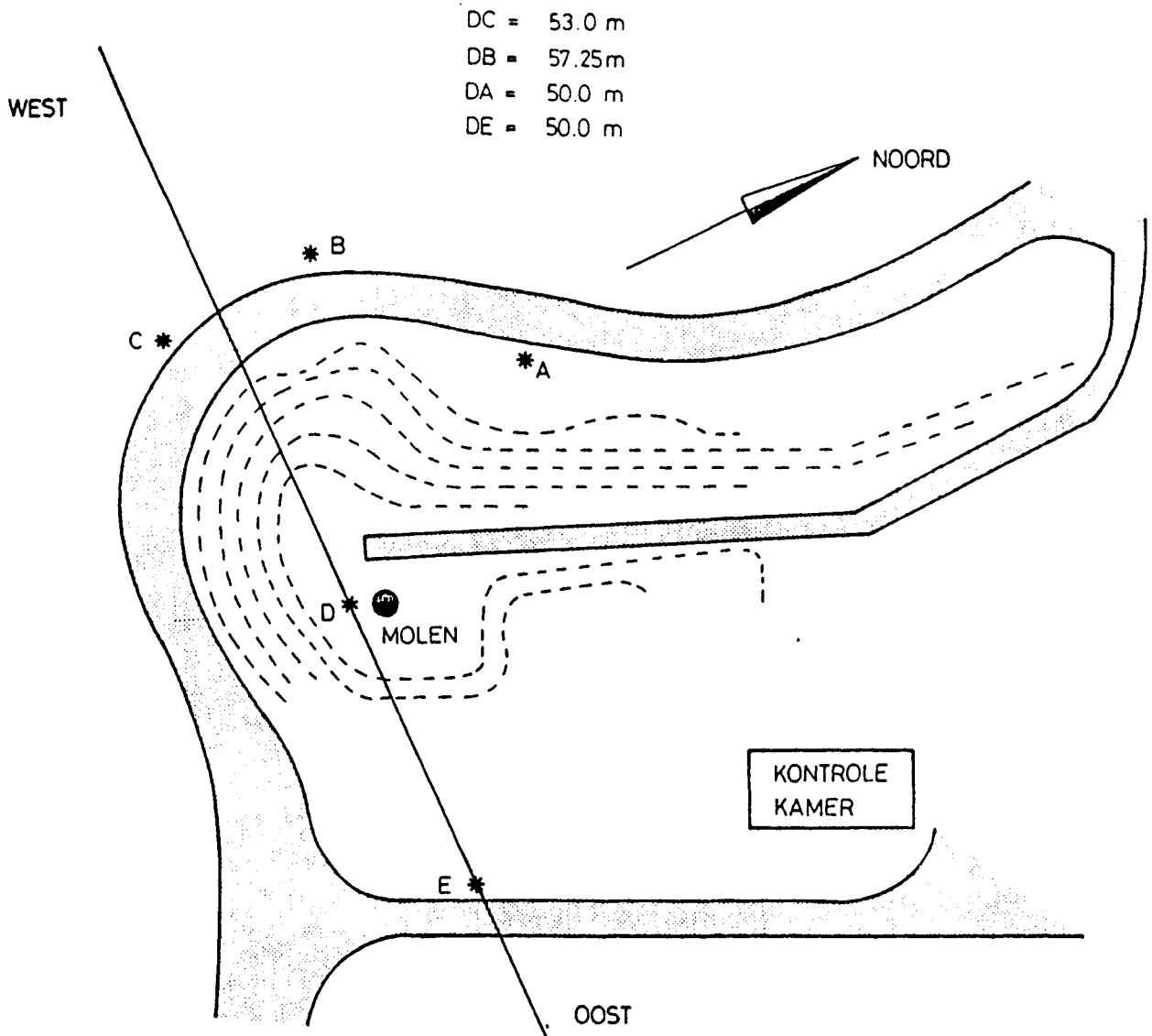


Fig. 3.2. Position of wind masts (stars) for the measurements of figure 3.3. (from [5]).

POLE B VERSUS POLE D

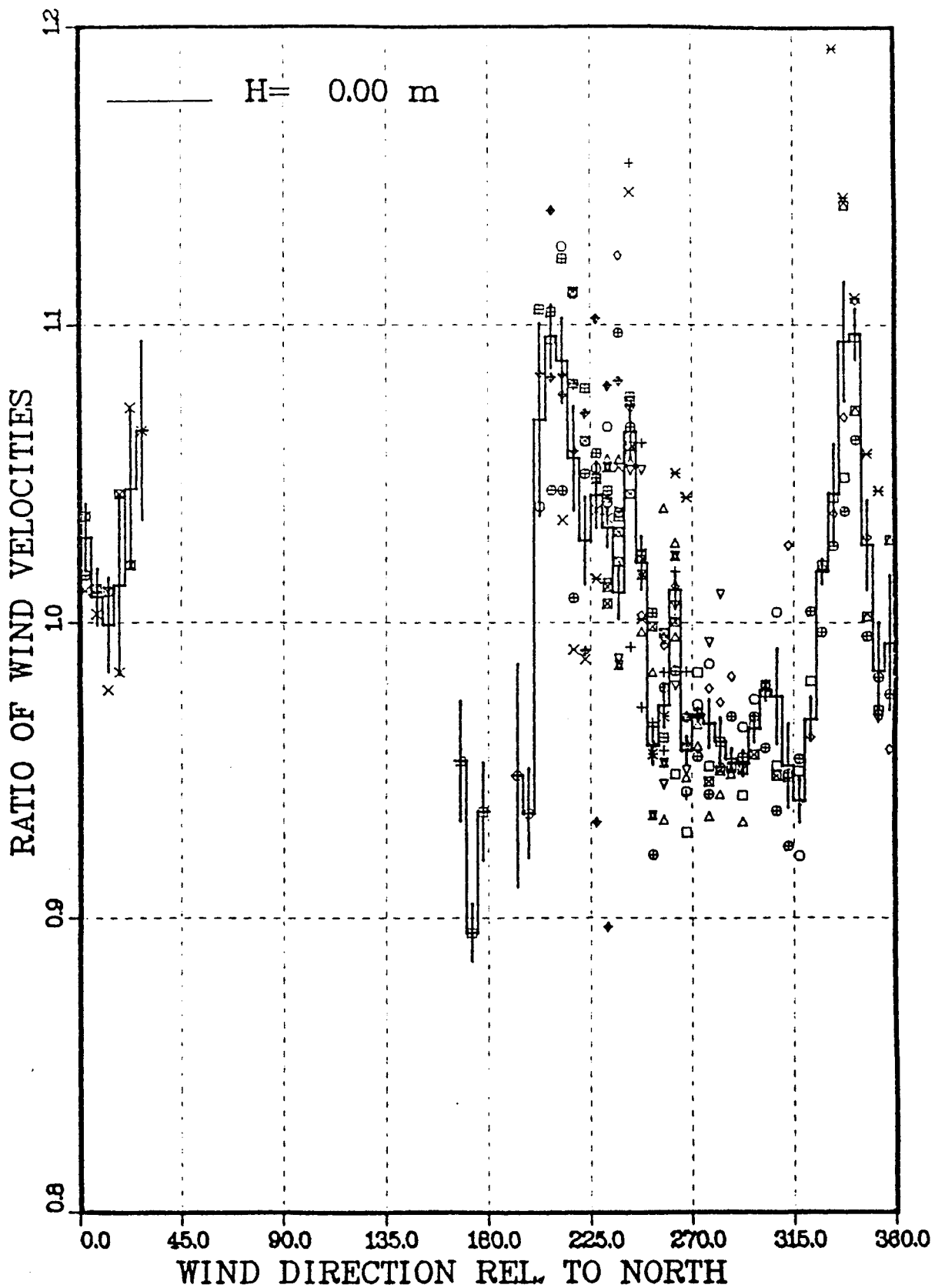


Fig. 3.3. Measured wind speed ratios at hub heights as a function of wind direction (different symbols denote different measurements series, the lines are the averages with standard deviations), [5].

3.1.2.2. The HAWT-25 site of ECN

This wind turbine is surrounded by 4 meteorological masts, A, B, C and E in fig. 3.2. Before the erection of the machine a fifth mast, D, was placed at that location. During several months wind speed ratios have been measured [5] between masts A, B, C, E and the reference mast D, at different heights (3 for each mast) and selected according to wind directions. One typical result is shown in fig. 3.3, where different samples represent different measurement series. The irregularities can be related to peculiarities in this rather inhomogeneous terrain. It is concluded that accurate performance measurements can only be made in the wind direction interval 240° - 350° , which corresponds to open, relatively smooth terrain. In this range a correction of about 5% has to be applied (due to the slope of the small hill where the machine is located).

Outside this range the deviations are large and highly irregular.

For one sector, around North, i.e. 310° - 30° , these measurements could be compared to the wind tunnel tests mentioned in section 3.1.2.1. [6].

There turned out to be a general agreement for the velocity ratios in a horizontal plane. But the field data exhibited a much larger scatter than the wind tunnel data, so that no final conclusion on agreement between the two methods could be reached.

3.1.2.3. The AWTS test site

Extensive wind tunnel testing has been performed for this test station in 1980 [7]. This clean, open terrain has 6-12 m cliffs on two sides, and scrub brush of 5 m height (at that time!) on the other side. A scale 1:500 model of this terrain was placed in a 2x3 m wind tunnel of the National Research Council of Canada (Ottawa). The flow field was mapped in detail, for many wind directions. The following conclusions were reached:

- The wind velocity is uniform, except near the scrub brush and close to the cliff edge.
- There was no dependence on wind direction at the anemometer site, and a little at the large wind turbine site.
- Very near to cliff or scrub brush large effects may occur.

This is illustrated in fig. 3.4 (from [7]). Differences of the order of 5-10% over distances, representative for wind turbine to anemometer distance, are frequent. Near the forest the effect can be larger. An unexpectedly large effect was found for row 1, which is nearly tangent to the East cliffs. A special flow pattern, with flow separation, supposed to

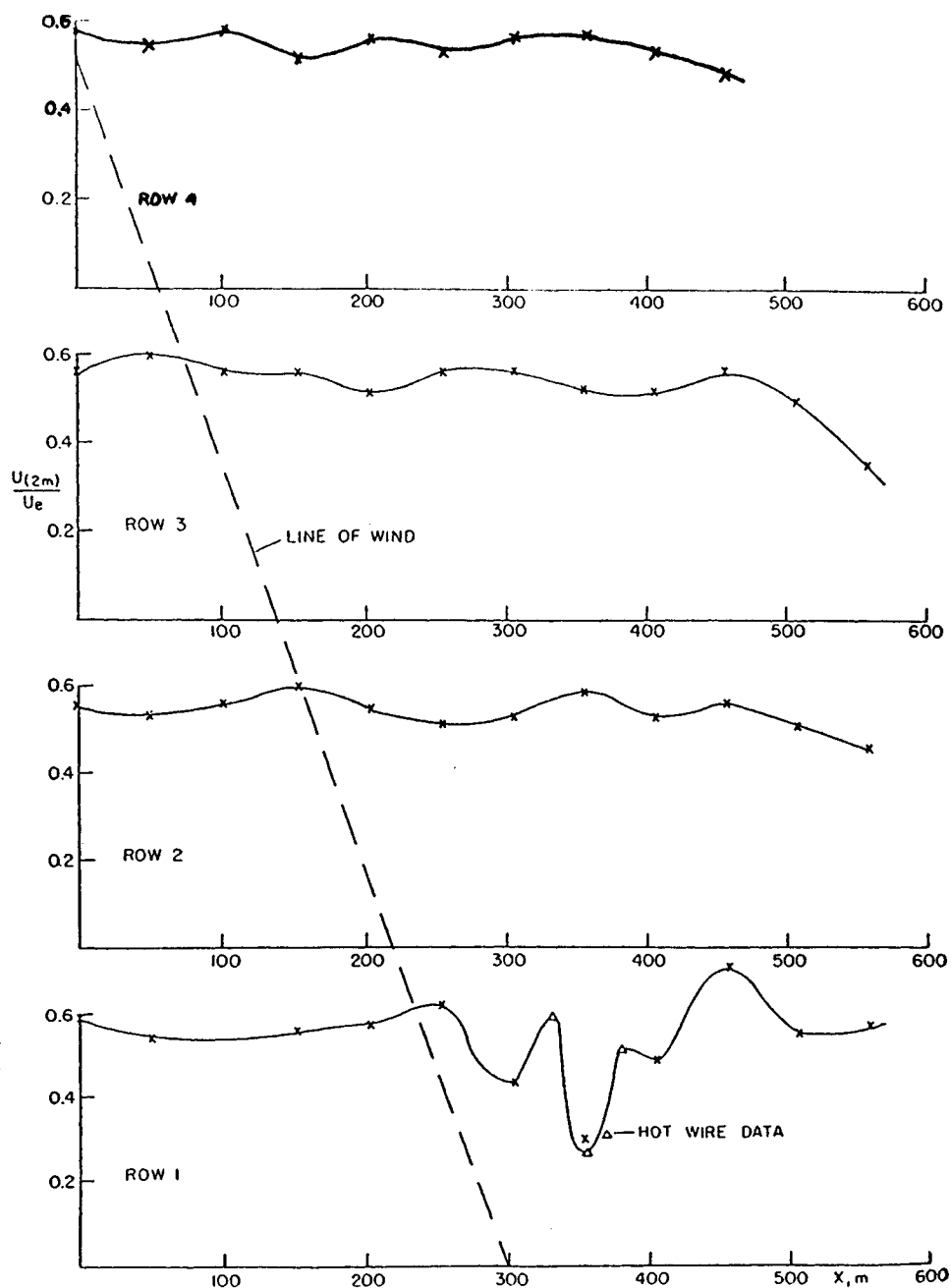


Fig. 3.4. Wind speed ratio at 2 m obtained for a wind tunnel model of the Atlantic Wind Test Site for 4 rows of sensors in the direction $\phi = 275^\circ$.

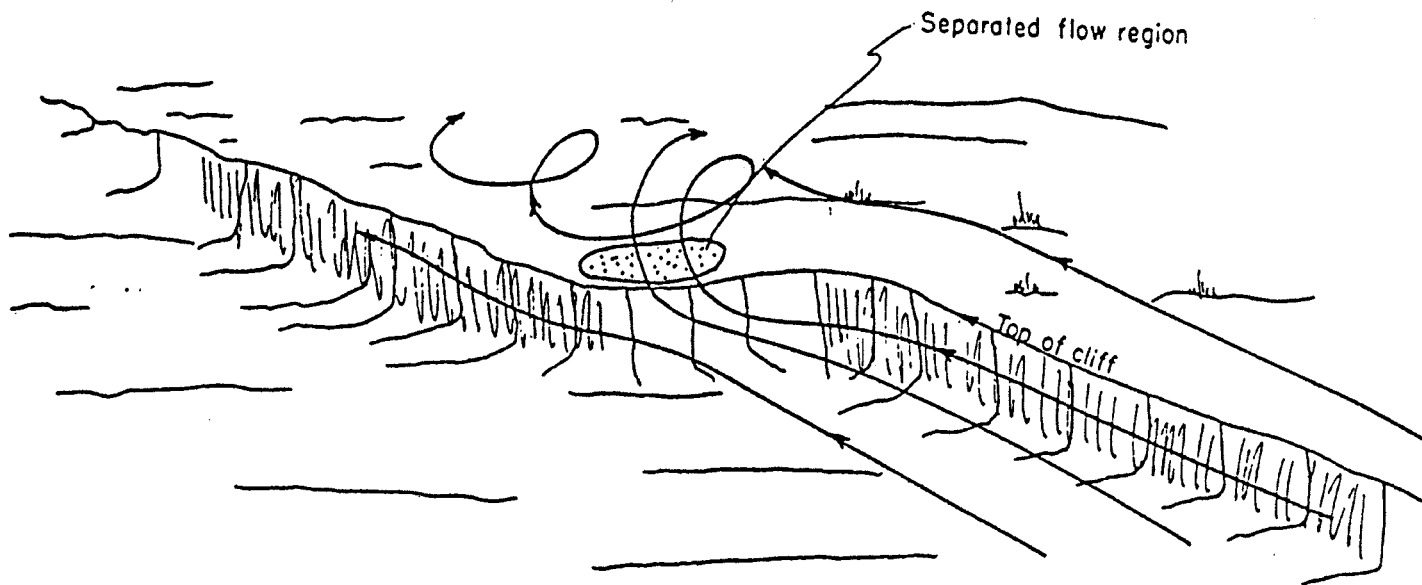


Fig. 3.5. Postulated flow pattern when the wind meets a turn of the cliff face at the Atlantic Wind Test Site.

behave like fig. 3.5 may cause these very large effects, which would lead to completely erroneous power curves, if measured at that place with that particular wind direction.

It may be mentioned that supplementary measurements corresponding to higher altitudes are now under consideration.

3.1.3. Terrain effect estimation

For wind turbine siting methodologies have been developed to account for local terrain effects [8,9]. It is suggested that such methods may also be used to obtain an order-of-magnitude estimate of the effect of certain terrain features on power curve measurements.

This is illustrated with the following idealized situation (somewhat resembling one feature of the VUB test station). In a flat grassland test station the anemometer (height 20 m) is located at 65 m from a very large 8 m high forest, the wind turbine to be tested at 100 m.

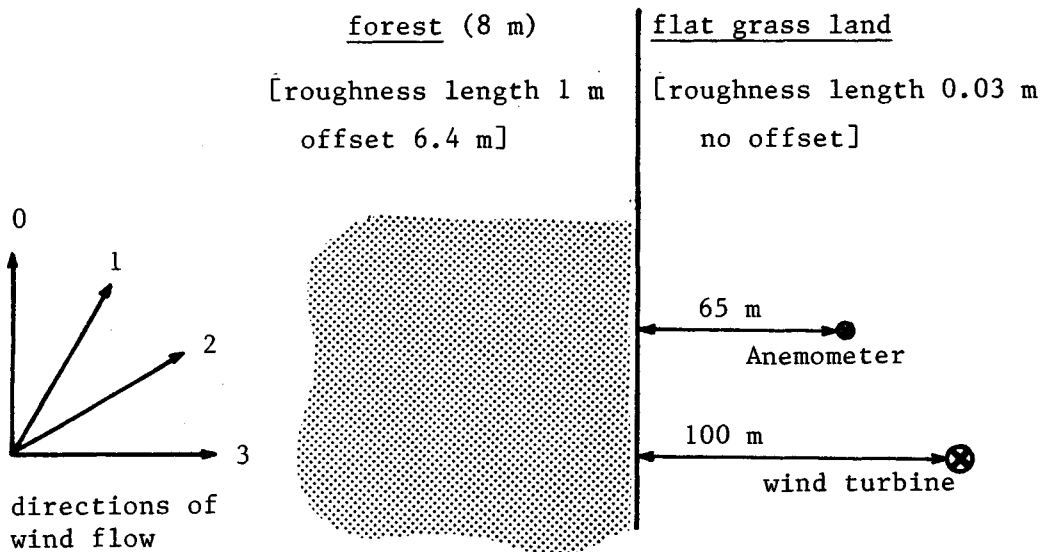


Fig. 3.6. Sketch of an idealized situation for which a terrain effect is estimated by calculation.

The following correction factors were calculated, using Appendix 7 of [9].

Correction factors for wind speed relative to undisturbed case (direction 0)			
Wind direction	Correction factor anemometer, C_{R1}	Correction factor wind turbine, C_{R0}	C_{R0}/C_{R1}
3	0.75	0.90	1.21
2	0.87	0.92	1.06
1	0.93	0.98	1.05

The large correction for the anemometer for direction 3 (perpendicular to the forest) is due to the fact that the thickness of the local boundary layer due to the roughness transition is smaller than the anemometer height.

3.1.4. Statistical error due to terrain effects

A statistical analysis of the measurement points in the lower plot of fig. 3.1 shows, that the velocity ratio has an average value of 1.01 over all wind directions and a scatter (standard deviation) of $0.04 = 4\%$.

Such site characteristics can introduce a statistical error in the velocity scale of the power curve measurements. Assume that we measure a power curve in a single experiment with a randomly selected, but constant wind direction during the experiment. This means, that we start a T hours measurement without looking at the weather. In this case we have several possibilities in the error analysis as discussed in the following. In all cases you have the knowledge of fig. 3.1 available.

1. The wind direction is not measured. In this case we would have to assign the uncertainties to the velocity measurements in the form $\pm 1\pm 4\%$, where the first is a correction for a systematic error of 1%, that comes from the average difference between mast and windmill wind speeds. But also a statistical uncertainty of 4% originates from picking up a random direction, that according to fig. 3.1 could give a 10% error in the extreme case.

2. If we repeat the experiment N times with wind directions randomly selected from the range $0-360^\circ$, we will have a spread in velocity error (s.d.) of 4%. If the N experiments are averaged, the velocity deviation will be much better determined namely with a statistical uncertainty of $4\%/\sqrt{N}$. Making say $N=16$ repetitions reduces the uncertainty on the mean to $\pm 1\%$.
3. If instead the wind direction is measured - or a "good" direction is selected - you are much better off. In this case the information of fig. 3.1 can be used to correct the velocity measurement and you get down to an uncertainty, that is determined rather by the quality of the determination of the error in fig. 3.1.

This remaining uncertainty when a velocity correction is measured is, however, very difficult to evaluate. This problem is very tricky and needs further studies. Two important points need examination.

The use of wind tunnel modelling is being questioned because of the inherent difficulty of scaling both the average flow and the turbulence correctly in the wind tunnel flow. This is particularly important, as the accuracy required for the modelling is very high. Another difficulty if using the field measurement method of fig. 3.3 instead of wind tunnel modelling is the scatter in the velocity ratios measured at each direction. The basic difficulty here could be the variation in climatic parameters other than wind speed and direction. It could for instance be humidity (rain) or the stability of the planetary boundary layer (stable when air temperature at hub height is higher than at lower levels).

3.1.5. Wind gradient and cupanemometer height

The wind speed usually varies with height z , typically proportional to $\ln(z/z_0)$. For a roughness length z_0 of 0.3 m, this would mean, that the blade tip would see a wind speed 23% higher with the blade pointing up than when pointing down for a 20 m rotor on a 24 m tower. This large variation is important. It has been shown [10] that if the variation were linear, the hub height wind speed would be the ideal measure of the average over the rotor. With the logarithmic wind profile, the error on the average energy flow through the rotor deviates very little (2%) from energy flow assuming a constant wind speed over the rotor equal to the hub height speed. The anemometer should therefore be placed in the mast at hub

height. In sloping terrain this is to be understood as hub and anemometer at same height over ground (not in the same horizontal plane).

The accuracy of the anemometer height should be evaluated as follows.

A height error of Δz (z is hub height) gives

$$\frac{u+\Delta u}{u} = \frac{\ln(z+\Delta z) - \ln z_0}{\ln z - \ln z_0}$$

From which:

$$\frac{\Delta u}{u} = \frac{\Delta z/z}{\ln z - \ln z_0}$$

The following table shows the relative velocity error for $\Delta z/z = 5\%$ (e.g. 1 m in 20 m) for different landscapes.

z_0 [m]	$\ln(z/z_0)$	$\Delta u/u$ ($\Delta z/z = 0.05$)
0.01	7.6	0.7%
0.05	6.0	0.8%
0.30	4.2	1.2%

It is clear, that $\Delta z/z$ should be kept below 5% (or $\Delta z < 1$ m for a 20 m tower) to ensure a less than 1% velocity error, which is a reasonable requirement.

3.1.6. Conclusions on average terrain effects

It appears from sections 3.1.2. and 3.1.3. that terrain effects of the order of 5% in wind velocity are easily possible. Under unfavorable conditions the effects may exceed 10%. Such situations should be absolutely avoided.

How serious is a 5% wind velocity uncertainty? Clearly the effect on a C_p - measurement would be 15%, which is unacceptably high. For such a measurement the terrain effects have to be evaluated carefully and to be corrected for. The effect of a 5% velocity error on the annual energy production is investigated in chapter 7. There it is concluded that the effect may be somewhat smaller than 15%, but still quite high, and certainly unacceptable from the point of view of predicting (or even guaranteeing) the economics of specific wind energy projects.

So the terrain effect problem deserves more attention. The applicability of the "terrain effect estimation method described in section 3.1.3. has to be investigated. More work should be done on wind tunnel testing of test site models. The wind tunnel tests need careful validation against properly selected field measurements.

3.2. The effect of turbulence

3.2.1. General assumptions

As mentioned in chapter 2, turbulence introduces fluctuations in u and in P (wind speed and power). This was illustrated by the "frozen turbulence" picture. In this section we shall adhere strictly to this picture more than usually in order to illustrate time delay effects and the effect of power curve nonlinearity.

We shall assume that the eddies causing fluctuations are unchanged while floating with the wind from anemometer to windmill.

Furthermore, we will assume that our representative wind speed is somehow measured as an average over an area that is the projection of the rotor area onto a plane parallel to the rotor and containing the mast, that is at a distance D in front of the rotor.

With these extra assumptions we try to be left with mainly coherent fluctuations in power and wind speed. The power fluctuations would be an exact copy of the measured wind speed fluctuations except that the non-linearity of the power curve to be measured will distort the power fluctuations.

As a start on the discussion in this chapter, fig. 3.7 shows typical time traces for wind speed and power.

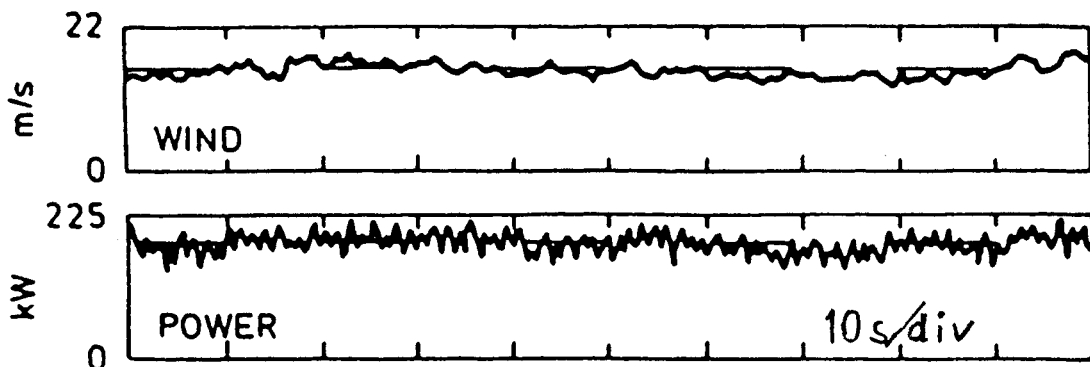


Fig. 3.7. Typical time traces of power and wind speed.

In order to reconcile these pictures with the notion of "frozen turbulence" we need to decide which wind speed drives which fluctuations along. Usually this is done by using a time average (T secs) wind speed.

$$\bar{u} = \frac{1}{T} \int_t^{t+T} u(t') dt'$$

to drive along fluctuations

$$u'(t') = u(t') - \bar{u}$$

Which is valid within the time averaging period $t/t+T$. Average values and fluctuations in P are separated analogously

$$P'(t') = P(t') - \bar{P}$$

with

$$\bar{P} = \frac{1}{T} \int_t^{t+T} P(t') dt'$$

3.2.2. Turbulence effects caused by power curve non-linearity (u^3 -binning)

Assume that an experiment along the idealized lines described in the introduction to this chapter is set up. In this experiment we measure T-averaged values \bar{u} , \bar{P} of wind speed and power. We can assume that the instantaneous values of u and P follows the mathematical power curve shown in fig. 3.8 in a region around \bar{u} .

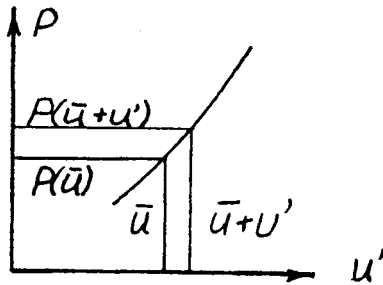


Fig. 3.8. Idealized non-linear power curve

The question is whether (\bar{u}, \bar{P}) is a point on the power curve. To answer this question we will calculate the expected \bar{P} .

If $P(u)$ were linear around \bar{u} , (\bar{u}, \bar{P}) would be a point on $P(u)$, because representing $\bar{P}(u)$ with $a+bu$, P can be simply calculated from:

$$\bar{P} = \frac{1}{T} \int_0^T (a+bu) dt = a + \frac{b}{T} \int_0^T u(t') dt' = a+b\bar{u} \quad (1)$$

When $P(u)$ is not linear the situation is different. In this case let us do, a series expansion of $P(u)$ around \bar{u} to find relations between \bar{P} , $P(\bar{u})$ and \bar{u} :

$$P(\bar{u}+u') = P(\bar{u}) [1 + u'P'(\bar{u})/P(\bar{u}) + \frac{1}{2}u'^2 P''(\bar{u})/P(\bar{u}) + \epsilon] \quad (2)$$

Terms of 3rd or higher order in \bar{u} will normally be small and may be discarded.

Averaging (2) over the averaging period T we find \bar{P} :

$$\begin{aligned} \bar{P} &= \overline{P(\bar{u}) + u'P'(\bar{u}) + 1/2 u'^2 P''(\bar{u})} \\ &= P(\bar{u}) + \overline{u'P'(\bar{u})} + 1/2 \overline{u'^2 P''(\bar{u})} \\ &= P(\bar{u}) [1 + 1/2 \overline{u'^2 P''(\bar{u})}/P(\bar{u})] \end{aligned} \quad (3)$$

Here it was used that $\bar{u}' = 0$, as is easily seen from the definition of u . Now, expressing $P(u)$ in terms of $C_p(u)$ and differentiating to find $P'(\bar{u})$ and $P''(\bar{u})$ we have

$$P(\bar{u}) = 1/2 \rho \bar{u}^3 A C_p(\bar{u}) \quad (4)$$

$$P'(\bar{u})/P(\bar{u}) = \frac{3}{\bar{u}} [1 + \frac{\bar{u}}{3} C'_p(\bar{u})/C_p(\bar{u})] \quad (5)$$

$$P''(\bar{u})/P(\bar{u}) = \frac{6}{\bar{u}^2} [1 + \bar{u} C'_p(\bar{u})/C_p(\bar{u}) + \frac{\bar{u}^2}{6} C''_p(\bar{u})/C_p(\bar{u})] \quad (6)$$

Inserting (4)-(6) into (3) we get

$$\bar{P} = P(\bar{u}) [1 + 3(\frac{\sigma_u}{\bar{u}})^2 (1 + \bar{u} \frac{C'_p(\bar{u})}{C_p(\bar{u})} + \frac{\bar{u}^2}{6} \frac{C''_p(\bar{u})}{C_p(\bar{u})})] \quad (7)$$

where $\sigma^2(\bar{u})$, \bar{u}^2 , C_p , C'_p and C''_p are all evaluated for the actual T-averaging period, i.e. at the point $u = \bar{u}$.

Eq. (7) clearly shows that (\bar{u}, \bar{P}) is not a point on $P(u)$. Such a point can, however, be found by using (7) for correcting \bar{P} as follows:

$$\begin{aligned} P(\bar{u}) &= \overline{P(u)} \left[1 + 3 \left(\frac{\sigma_u}{\bar{u}} \right)^2 \left(1 + \bar{u} \frac{C'_p(\bar{u})}{C_p(\bar{u})} + \frac{\bar{u}^2}{6} \frac{C''_p(\bar{u})}{C_p(\bar{u})} \right) \right] = \\ &= \bar{P} [1 - \Delta P/P(\bar{u})] \end{aligned} \quad (8)$$

Instead of correcting P for the "overshoot" \bar{P} , one could choose to correct the \bar{u} value, e.g. think of using something like. To do this we calculate:

$$\begin{aligned} \bar{u} + \Delta u &= \bar{u} + \Delta P/P'(u) = \bar{u} \left[1 + \frac{\Delta P/P(\bar{u})}{\bar{u} P'(\bar{u})/P(\bar{u})} \right] \\ &= \bar{u} \left[1 + \frac{\frac{\sigma^2}{\bar{u}^2} \frac{1 + \bar{u} C'_p/C_p + \frac{\bar{u}^2}{6} C''_p/C_p}{1 + \frac{\bar{u}}{6} C'_p/C_p}} \right] \end{aligned} \quad (9)$$

Both kinds of correction (i.e. ΔP or Δu correction) have been used occasionally. But in such cases it is customary to assume, that $P(u)$ is strictly proportional to u^3 . If this were so, we would find $C_p = \text{constant}$ and $C'_p = C''_p = 0$, in which case (8) and (9) reduce to the simpler well known forms:

$$P(\bar{u}) = \bar{P} [1 - \Delta P/P] = \bar{P} \left[1 - 3 \left(\frac{\sigma}{\bar{u}} \right)^2 \right] \quad (8a)$$

$$\bar{u} + \Delta u = u \left[1 + \left(\frac{\sigma}{\bar{u}} \right)^2 \right] \sim \sqrt[3]{\bar{u}^3} \quad (9a)$$

Here the use of $\sqrt[3]{\bar{u}^3}$ as suggested by Mengellkamp (ref.) has been introduced as found by using (3) with a $P = \text{const } u^3$. Either using (8a) or (9a) or in particular using $\sqrt[3]{\bar{u}^3}$ as velocity would produce an accurate power curve point, if and only if $P = \text{const } u^3$. We will, however, not recommend to use these simplifications in general, as the error is deemed to be too large.

Writing (3) slightly differently ($\sigma_u^2 = \bar{u}'^2$)

$$\overline{P(u)} = P(\bar{u}) + 1/2 P''(\bar{u})\sigma_u^2 \quad (10)$$

To illustrate the order of magnitude involved we have chosen one particular windmill, whose power curve has been measured by T.F. Pedersen [12]. Fig. 3.9 shows the power curve $P(u)$ and $C_p(u)$ deduced from this $P(\bar{u})$ without correction for turbulence. The C_p -curve of course in itself illustrates how much the power curve deviates from a u^3 -curve ($C_p = \text{const } P(u)/u^3$). In fig. 3.10 different approximations to $P(\bar{u})$ are plotted together with the measured power curve. The curve marked $P(u)$ serves to illustrate the relative importance of various wind speeds for the yearly production prediction, as

$$\text{expected yearly production} = 8760 \cdot \int_0^{\infty} P(u)f(u)du$$

It is clear, that in the u -region where $P(u) \cdot f(u)$ is high, a power curve error is least acceptable, so clearly the u^3 approximation is very bad. It is seen that $P(u) = \text{const } u^3$ deviates considerably already from $\bar{u} = 9$ m/s, and increasingly so at higher u 's.

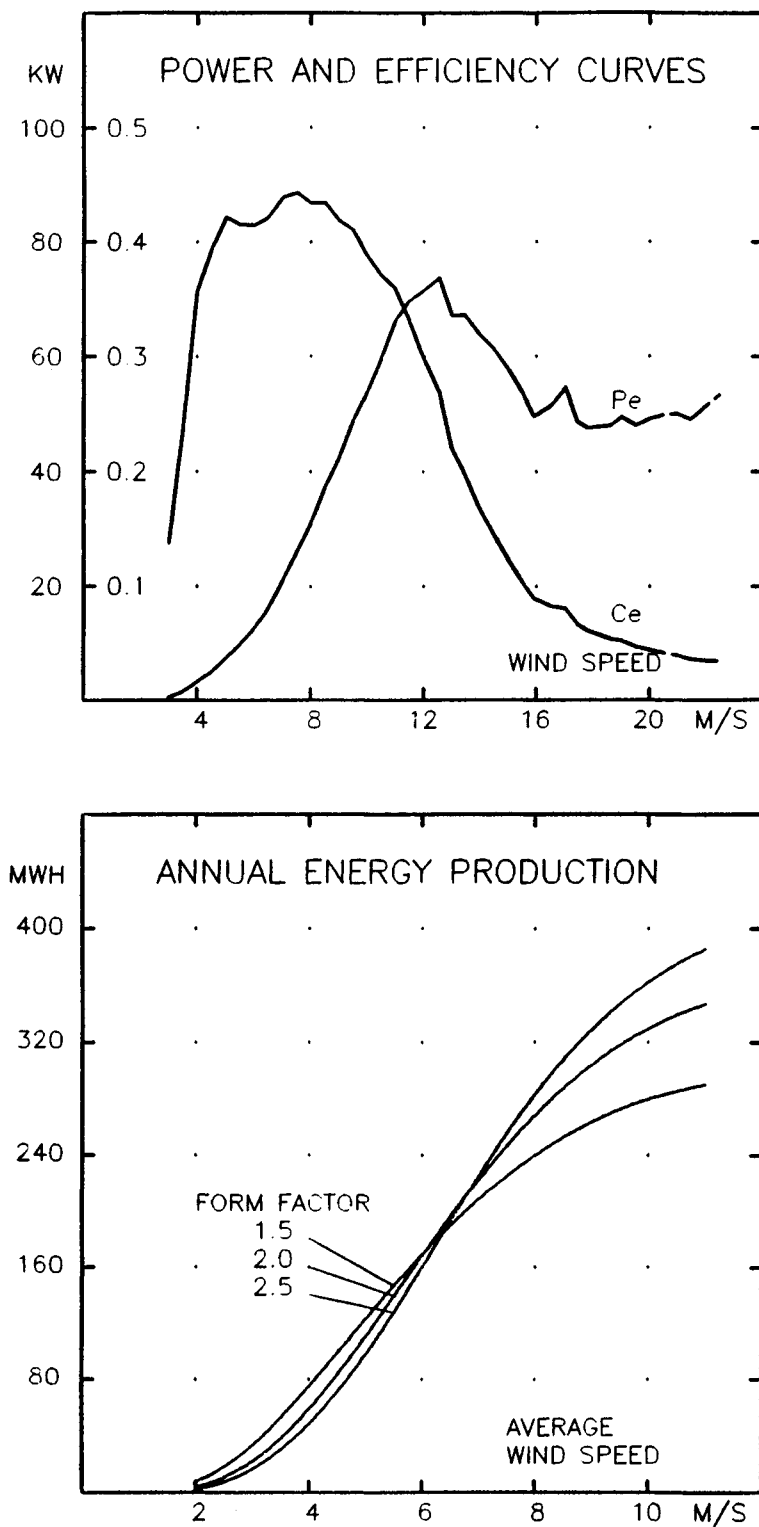


Fig. 3.9. Power curves and annual energy production of WM17 S.

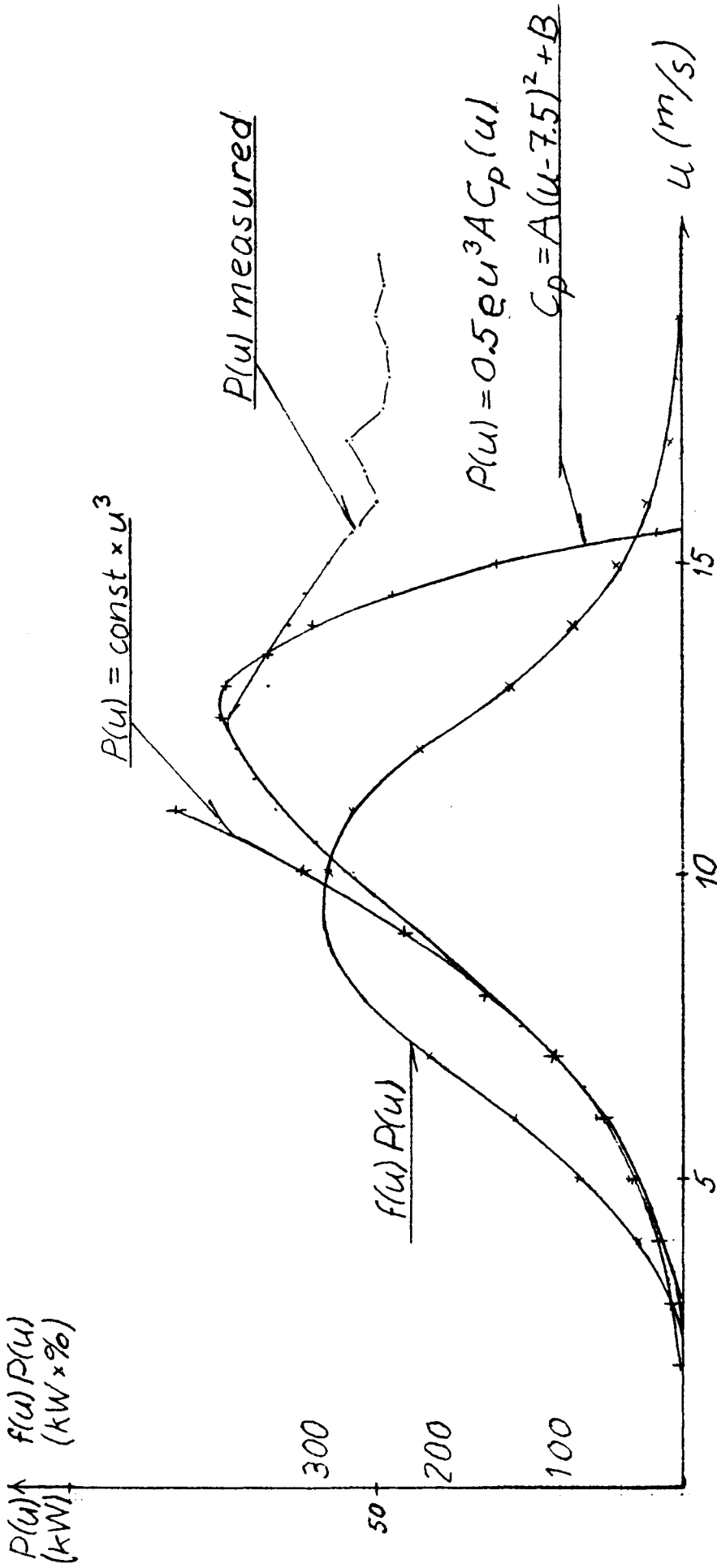


Fig. 3.10. Approximated power curve.

Another possible approximation is illustrated in fig. 3.10, namely assuming C_p parabolic of the form:

$$C_p = A(v - v_o)^2 + B \quad (11)$$

v_o is the wind velocity, where C_p peaks. The constant A and B are found by fitting to the measured C_p -values between 4-11 m/s. These constants are used for comparing fitted and measured C_p -Values in fig. 3.11 and for approximating (\bar{u}) in fig. 3.10. This fit is definitely not perfect, but much better than the u^3 -approximation. Using these A and B-values, the correction to the power curve from (8):

$$P(\bar{u}) = \bar{P}(\bar{u}) [1 - 3\left(\frac{\sigma}{\bar{u}}\right)^2 \cdot \delta] \quad (12)$$

was calculated. The results are shown in table below.

\bar{u}	C_p	$\bar{u}C'_p$	$\bar{u}^2/6 C''_p$	δ	$\delta \cdot 3\left(\frac{\sigma}{\bar{u}}\right)^2 \%$
4	0.358	0.187	-0.036	1.42	7
5	0.398	0.167	-0.036	1.28	6
6	0.425	0.120	-0.080	1.09	5
7	0.438	0.047	-0.109	0.86	4
8	0.438	-0.054	-0.143	0.55	3
9	0.425	-0.181	-0.181	0.15	1
10	0.398	-0.335	-0.223	-0.40	- 2
11	0.358	-0.515	-0.270	-1.20	- 5
12	0.304	-0.723	-0.321	-2.34	-13

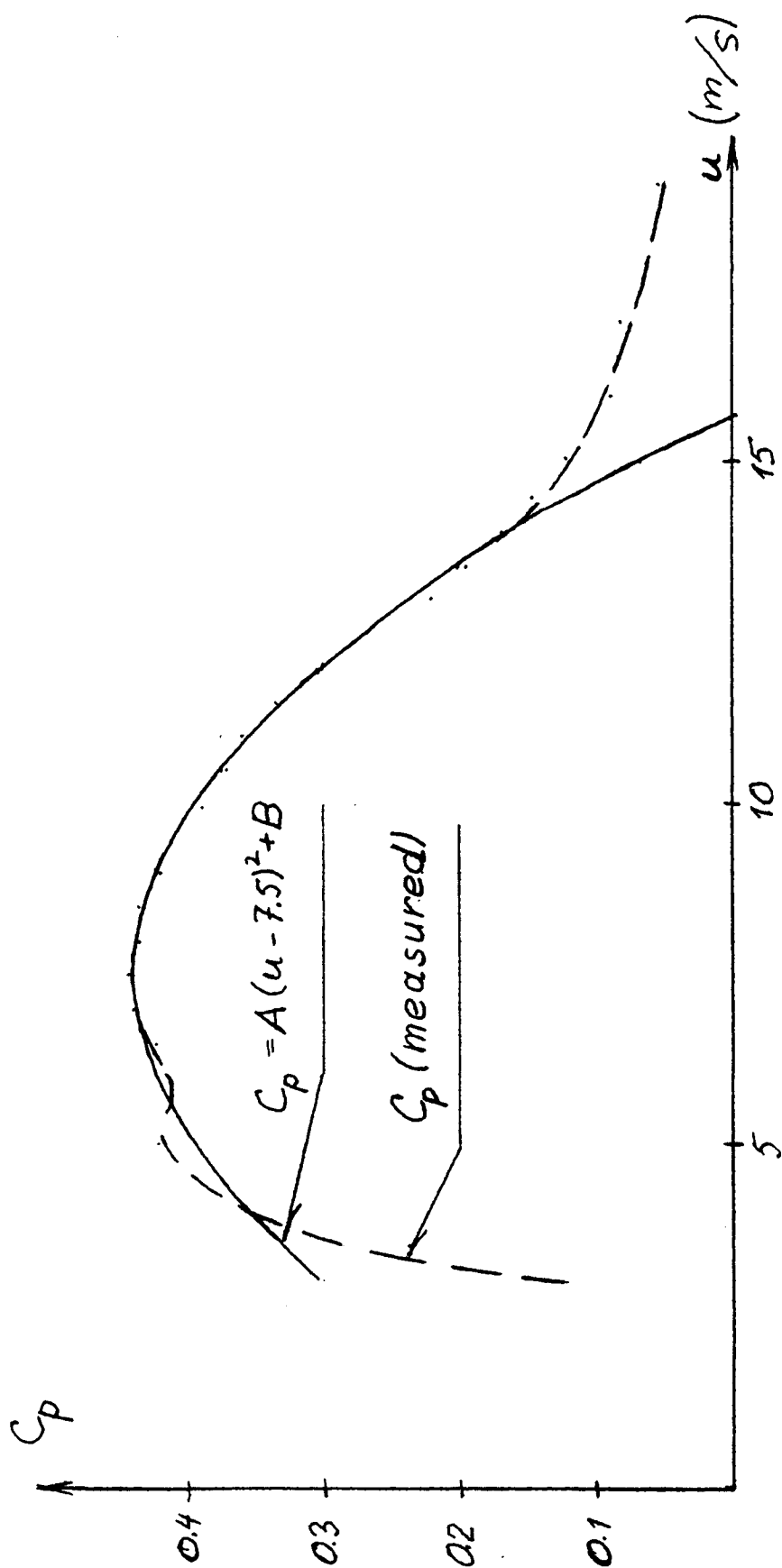


Fig. 3.11. Fitting C_p to a parabola.

Here we have used the expected "normal" turbulence:

$$\frac{\sigma_u}{u} = \frac{1}{\ln(z/z_0)} \quad (13)$$

which for a site with $z_0 = 0.01$ m gives $(\sigma_u/u) = 13\%$ and $3(\sigma_u/u)^2 = 0.05$

with $z = 24$ m.

If the u^3 -approximation were valid, $C_p = 1$ for all u would be expected. Not surprisingly this goes particularly wrong where power limitation sets in. The ΔP even changes sign so the normal correction goes the wrong way.

To illustrate the error introduced in power predictions when neglecting the turbulence correction, we will evaluate the error for the WM 17S measurement shown above.

We will assume as above

$$\sigma_u^2 = \epsilon^2 u^2 = 0.017 u^2 \quad (14)$$

The wind distribution is taken as a Weibull distribution with $C = 2$, $A = 7.5$ (Rayleigh-distribution). We will express the power curve as (from 10)

$$P(\bar{u}) = \bar{P}(u) - 1/2 \sigma_u^2 P''(\bar{u}) \quad (15)$$

The prediction error is now

$$\Delta = \int_0^{\infty} 1/2 \sigma_u^2 P''(u) P(u) du = 1/2 \epsilon^2 \int_0^{\infty} P''(u) u^2 P(u) du \quad (16)$$

To evaluate this integral two integrations by parts are performed, where the differentiations of $P(u)$ are removed at the expense of differentiating the relatively simple distribution function $u^2 f(u)$ twice. It can be shown that

$$\Delta = 1/2 \epsilon^2 \int_0^{\infty} P(u) f_2(u) \left[6 - 14 \left(\frac{u}{A} \right)^2 + 4 \left(\frac{u}{A} \right)^4 \right] du \quad (17)$$

where $f_2(u)$ denotes the Rayleigh distribution with the scaling parameter A .

$$f_2(u) = \frac{2}{A} \left(\frac{u}{A}\right) e^{-\left(\frac{u}{A}\right)^2}$$

The 4th order polynomial in (u/A) is the extra weighting factor that allows the evaluation of the correction factor without differentiating $P(u)$. For the WM 17S we have evaluated Δ and got $\Delta = -0.35$ kW. Here $A = 7.5$ m/s has been chosen. At that A -value the $P(\bar{u})$ yields 190.000 kWh/yr or $\langle P \rangle = 21.7$ kW. Thus the turbulence error in the power prediction amounts to 1.6%.

If the simple correction (8a) assuming $P \propto u^3$ were applied uncritically to a measurement at a site with turbulence characteristics as here assumed (eq. 13) a relative correction to each P -value of $3 \cdot \epsilon^2 = 5.1\%$ which will then in turn be the total correction also to $\langle P \rangle$. This is a much too big correction.

3.2.3. Conclusions and recommendations on turbulence effects

3.2.3.1. Power prediction

It is clear, that turbulence together with power curve non-linearity gives rise to a significant error. It is equally clear, that the often used correction method, that assumes $P \propto u^3$ overcorrects considerably and at least as long as used for correcting the yearly energy prediction value should not be used. Correcting u by using u^3 -binning has some of the same principal errors, but to a lesser degree. Therefore, the u^3 -binning warrants further investigations. We cannot recommend this method either, before such investigations have shown the validity and shortcomings more clearly.

The basic reason to discard the $P \propto u^3$ assumption and therefore at least in principle also the $\sqrt[3]{u^3}$ method is that when trying to correct for power curve non-linearity errors induced by turbulence, one must work with the real shape of the measured curve and not with a seemingly nice, but clearly wrong shape $P \propto u^3$. That P is certainly different from a u^3 shape is clear, when remembering that C_p -curves, which we are so interested in,

are certainly never constant as they should then be. Particularly when going into the high wind power regulation region P is far from proportional to u^3 .

As far as the practical use of power curves for power production predictions is concerned a few further arguments are needed.

It is recommended that a power curve measurement when reported should have a measure of the turbulence level at the site included. In this way the possibility is still open for the windmill buyer to make his own turbulence correction.

The exact formulation of a standard for this turbulence measurement remains to be examined.

All power curves measured are to a certain degree distorted by turbulence but so are the sites where the predictions are done. If the turbulence level at installation sites is about the same as the test site, no correction is needed and not wanted. This is so because at potential sites one often uses wind distributions measured for meteorological purposes and no turbulence measurements exist. Therefore it seems better to take the test site power curve without turbulence correction than taking turbulence into account. If this uncorrected power curve is used together with uncorrected wind speed data at the site of installation the correct power prediction is obtained - if the turbulence characteristics are the same at the two sites.

Ideally of course a correction for turbulence yields a "better" power curve. But for practical use, it is then left to the prediction process to make much more elaborate measurements of turbulence characteristics and a consequent recorection of the power curve to include turbulence. But at the present stage this elaborate process is not to be recommended. On the contrary, if the test station decides to include the correction (e.g. for aerodynamic reasons) it ought to give both corrected and uncorrected curves and an evaluation of the difference in predictions using the two curves should be included. This serves to avoid confusing the matters for the users of the power curves.

For the particular case discussed here, the correction was 1.6%. Much higher turbulence levels can be expected at certain sites in practical use for wind energy production. Presumably 2-3 times higher σ_u/u -values could be expected (mountainous areas), giving rise to 5-15% turbulence correction.

3.2.3.2. Aerodynamic power curves

It is our belief, that in respect to the arguments in a) the power curve should not be corrected without making very clear, that this was done. The C_p -curves often requested by aerodynamics research, however, ought to be corrected. It must, however, be clear that assuming $P \propto u^3$ is incorrect and

that the correction has to use the measured shape of the power curve. It could be argued, that in one point (where C_p is max) the power curve is proportional to u^3 , so here the usual simple correction (8a) could be valid. The example in the table after eq.(12), however, shows that this is not true. In this example the correction should only be 2/3 of the simple correction. This stems from the fact, that even though $C_p' = 0$, $C_p'' \neq 0$ into this changes the correction, i.e. the curvature of C_p has to be taken into account. So in order to correct for turbulence, we see no way around more elaborate correction procedure outlined here.

4. MEASUREMENT METHODS IN USE

4.1. Introduction

Before the project was started it was clear already that most test stations follow the IEA recommendations [11] rather closely. The questionnaire had a set of questions to investigate in some more detail how the measurement of the power curve is performed in the different stations. The main results are summarized in this chapter. They are presented in three groups:

- the signals used for the measurements;
- the processing of the signals;
- the way of performing the bin analysis.

In the following tables the test stations are ordered alphabetically. The different CWD-test sites follow the same practices: they are combined in one line. The RAL has two lines due to the differences in HAWT and VAWT testing. The Zeebrugge test site, which has not yet been fully established, is not included.

4.2. Signals used

Only the signals which are relevant for power performance measurements are included in the following table.

Test station	wind measurements			power measurements		
	velocity	anemometer height	direction	output power	shaft torque	rotor speed
AWTS	>2	hub/equator <u>+1</u> m		el:AC 1 or 3 phase DC		
Chalmers	x	hub	x	el: 3 phase AC		x
CWD	x	hub (and 10 m)	x	water flow		x
DFVLR	3	hub,top,bottom of rotor		el: 3 phase AC		
ECN	3	3 levels (interpol. to hub)	3	el: 3 phase AC		
NEL	x	hub, to max. 20 m	x	el: 3 phase AC	x	x
RAL-HAWT	3	2 at hub, 1 on boom		el: 3 phase AC		
-VAWT	2	hub			x	x
Risø	3	hub	1	el: 3 phase AC	x	x
VUB	x	hub/equator	x	el: 3 phase AC	x	x

Table 4.2.1. Overview of signals for power curve measurements. Crosses mean that the signal is used. Figures indicate the number of sensors used.

In all test stations atmospheric conditions (at least pressure and temperature) are monitored in order to correct for air density variations. For stations near sea level these corrections are small. It is common to use the IEA recommendation for the correction. The most elevated test station is the one of DFVLR at Schnittlingen, where the density correction is substantial. It has been observed by J.P. Molly [14] that the density correction according to the IEA does not properly account for the control mode in pitch controlled machines. He proposed and demonstrated an alternative air density correction method.

In specifying the anemometer height with respect to the hub of the wind turbine rotor there is some ambiguity in definition for sloping terrains. It is most common to specify the heights with respect to the ground.

4.3. Data handling methods

The main specifications on the processing of the signals before digitizing are given in the following table:

Test station	Signal preprocessing	Sampling
AWTS	filter for spurious noise	1 Hz
Chalmers	no filter	1 Hz
CWD	analog signals: no filter	1 Hz
	pulse frequency (a.o. flow): 1 sec integration	
DFVLR	filter for wind signals	10 Hz
ECN	low pass filter 10 Hz	4 Hz
NEL	low pass anti-alias. Analog data link	5-10 Hz
RAL -HAWT	no filter	30 s aver.
-VAWT	low pass filter 2 sec	0.5 Hz
Risø	low pass filter 0.4 Hz	1 Hz
VUB	no filters	0.3 Hz

Table 4.3.1.: Signal processing.

The method of bins may be used (and is in use) for the analysis of several possible signals against several other signals, but here we restrict ourselves to the analysis of power (either electrical or mechanical - see the

table of section 4.2) as a function of wind speed. Details of the analyses, performed in the participating test stations, are summarized in table 4.3.2.

It appears that the IEA recommendations are followed more-or-less. The bin width (below rated wind speed 1 m/s and above 2 m/s, according to IEA) is usually chosen much narrower, but in such a way that data can be combined to obtain the IEA-mesh.

The most significant deviations occur in selecting the wind directions, for which data are excluded from the analysis. The IEA recommendation is to exclude the wake of the turbine over a 90° sector ($\pm 45^\circ$). Some test stations have no limitation. In many cases terrain features, like buildings or other wind turbines, exclude some directions. Much more restrictive than the IEA recommends is the Risø test station. Clearly there is a need for some further study on this point (also see chapter 3), in order to arrive at a generally acceptable standardization.

There appears to exist a clear lack of quantitative understanding of the accuracy of the power curves obtained from the analysis. There is some insight in the error sources, but not in their magnitudes.

Annual energy production calculations are routinely made for measured power curves by AWTS, CWD, ECN, Risø and VUB, but usually for Weibul-distributions of wind velocity with parameters characteristic for the site, rather than for $k=2$ as recommended by the IEA. There are no reliable estimates for the accuracy.

test station	averaging time τ	parameters computed over averaging time τ	wind directions excluded from bin analysis	bin width	total measuring time	parameters computed for the data in each bin
AWTS Chalmers	10 min 10 min(?)	mean mean of V,P,direction rotor speed, V^3	turbine wake $\pm 45^\circ$ no limitation	$\Delta V = 0.5$ m/s $\Delta V = 1$ m/s	in discussion 500 h operation	mean, s.d. mean
CWD	10 min (or less)	mean, peak, s.d., max(rotor* γ aw speed)	turbine wake $\pm 45^\circ$	$\Delta V = 0.5$ or 0.25 m/s	>2 weeks	mean, s.d.
DFVLR	10 min	mean, freq.distr., min., max.	south directions	$\Delta V = 1$ m/s	months	mean, s.d., freq. distr.
ECN	10 min	mean, s.d., min., max.	turbine wake $\pm 45^\circ$ other turbine $\pm 45^\circ$, large building	$\Delta V = 0.5$ m/s	months	mean, s.d., max., min.
NEL	10 min or less	mean, max., min. V^2 , V^3	turbine wake $\pm 45^\circ$ other turbines	$\Delta V = 1-2$ m/s	variable	several possibilities
RAL-HAWT	30 s	mean	direction of build- dings	$\Delta V = 0.5$ m/s	75h op.	mean
-VAWT	10 min	mean	wake of other turbines	$\Delta \lambda = 0.25$ m/s	42 h op.	mean
Risø	10 min./ 30 s.	mean, s.d.	outside 90° west sector	$\Delta V = 0.5$ m/s	200 h operation	mean, s.d.
VUB	10 min.	mean	no limitation	$\Delta V = 1-2$ m/s	no spec.	mean

Table 4.3.2.: Bin analysis

(Note: s.d. = standard deviation, sometimes measured as a variance).

5. STATISTICAL TREATMENT OF THE METHOD OF BINS

5.1 Review of the method of bins

After averaging over a time τ , pairs of wind speed and power averages (V_k, P_k) are obtained. The wind speed range has been subdivided into a set of intervals (bins). To each bin correspond some registers. The data are collected in the registers of the bin to which V_k belongs (velocity binning). This data collection finally results in average power values in each bin, average velocity values of each bin (often the midpoint of the bin is taken instead), number of data pairs per bin, and (sometimes) variance of power values per bin. These results are either obtained by straightforward summing of the data and their squares, or - preferably, due to accuracy problems - by a recursive algorithm (see Annex). The final averaged bin power values versus the average bin velocity values constitute the power curve.

Some specific features of the recommendations made in 1982 by an expert group for the International Energy Agency [13] are as follows.

Averaging time is 10 minutes. The anemometer (distance constant ≤ 5 m; $\leq 5\%$ inaccuracy) should be between 2 and 8 rotor diameters from the wind turbine and as much as possible at hub height (otherwise a small correction has to be applied), and free of the wake of the tower, supposed to extend over a 90° sector behind the tower. The power curve is to be determined for the net output power (3% accurate), and it is only intended to predict the annual energy output at a site to be characterized by a Rayleigh wind speed distribution and assuming 100% windturbine availability. To this end at least 3000 data pairs (V_k, P_k) have to be collected, with a minimum of 10 data per bin, where bin widths are 1 m/s below the lowest wind velocity where maximum power is generated and 2 m/s above.

It may be noted that there is often need for other power curves. For instance the rotor power or shaft power (usually measured as shaft torque times rotor angular speed) is important for comparing performance with aerodynamic predictions. Such power curves are often converted to aerodynamic efficiency C_p versus tip speed ratio λ . One may desire a better velocity resolution or a shorter total measurement time than 3000×10 minutes. That is possible in principle by taking shorter averaging time τ than 10 minutes, e.g. 30 seconds. This has actually been done in several test stations and research

establishments (see section 4.3). Some pitfalls may be met, however. Their discussion will be included in the following sections, along with the discussion of the "standard" method, which in our opinion should be closely following the IEA-recommendations.

5.2. Statistics within the averaging time τ

In statistical considerations we have to distinguish between the statistical behaviour within the averaging time τ (i.e. the 10 minutes according to IEA, or shorter for special purposes), and the statistics of the data after averaging over τ . In this section we consider the former case.

Average and variance of some signal $x(t)$ over interval τ are defined by:

$$\bar{x}(t) = \frac{1}{\tau} \int_t^{t+\tau} x(t') dt'$$

and

$$\sigma_x^2 = \frac{1}{\tau} \int_t^{t+\tau} \{x(t') - \bar{x}(t)\}^2 dt' .$$

Note that the variance over the interval is obtained with respect to the mean over the same interval.

In the digital data collection and analysis systems of most test stations these calculations are replaced by discrete sampled data equivalents, either directly or recursively according to the equations of the Annex, where $N\Delta t = \tau$ (Δt = sample interval).

In sampled data systems signals have to be appropriately filtered first, in order to remove all fluctuations above half the sample frequency. If not, these fluctuations are folded back to low frequencies ("aliasing"). In the long run they will not spoil the expectation of mean values, but the accuracy (variance) may be seriously spoiled. For anemometers the inertia takes care of this filtering to a certain extent. A distance constant of the anemometer between 2 and 5 m fits well to the frequently used sample rate of 1 sample/second over the most significant wind speed range.

Faster anemometers might require an extra filter or faster sampling.

The filter on the other hand also reduces the variance σ_x^2 , in particular if the cut-off is not very sharp, as it is the case with the cup anemometer (basically a first order filter). For wind measurements the variance may easily have a systematic error of 10%, i.e. 5% in the degree of turbulence (see below). At the present time this error does not seem to be of real concern.

The fluctuations within averaging time τ may also cause a systematic error in the mean wind speed due to the "over-speeding" effect: the cup anemometer is a non-linear device, which responds faster to increasing wind than to decreasing wind, on the average giving rise to an over-estimation, see section 7.4.

The variance is most important for the wind speed signal. It is of interest to express it (i.e. the continuous version) in the APSD (the frequency spectrum or Auto Power Spectral Density, see Annex 5A). The expectation of the variance, eq. (A.1), is then:

$$\sigma_u^2 = \int_0^\infty S_{uu}(f) \cdot [1 - F_\tau(f)] df ,$$

where $F_\tau(f)$ expresses the filtering due to averaging, given in eq. (A.8) of the Annex 5A.

The fluctuation spectrum S_{uu} is sketched in fig. , in an area preserving form, namely $f \cdot S(f)$ versus $\ln f$. The high frequency part is due to turbulence. It is separated from lower frequency parts by the "spectral gap". The filter $[1 - F_\tau(f)]$ acts as a high-pass filter with a 50% point at frequency $0.44/\tau$. For $\tau = 10$ minutes (600 seconds) it just passes the turbulence part of the spectrum, so in that case σ_u^2 is the variance due to turbulence. Due to the spectral gap this value is relatively insensitive to the value of τ in the range of 10 minutes to 1 hour. For shorter τ this is no longer true.

The degree of turbulence, $\epsilon = \sigma_u / \bar{u}$, turns out to be fairly independent of \bar{u} over the range of wind speed of interest for wind turbine operation, as it is illustrated in fig. 5.2 [11]. It is primarily a terrain characteristic,

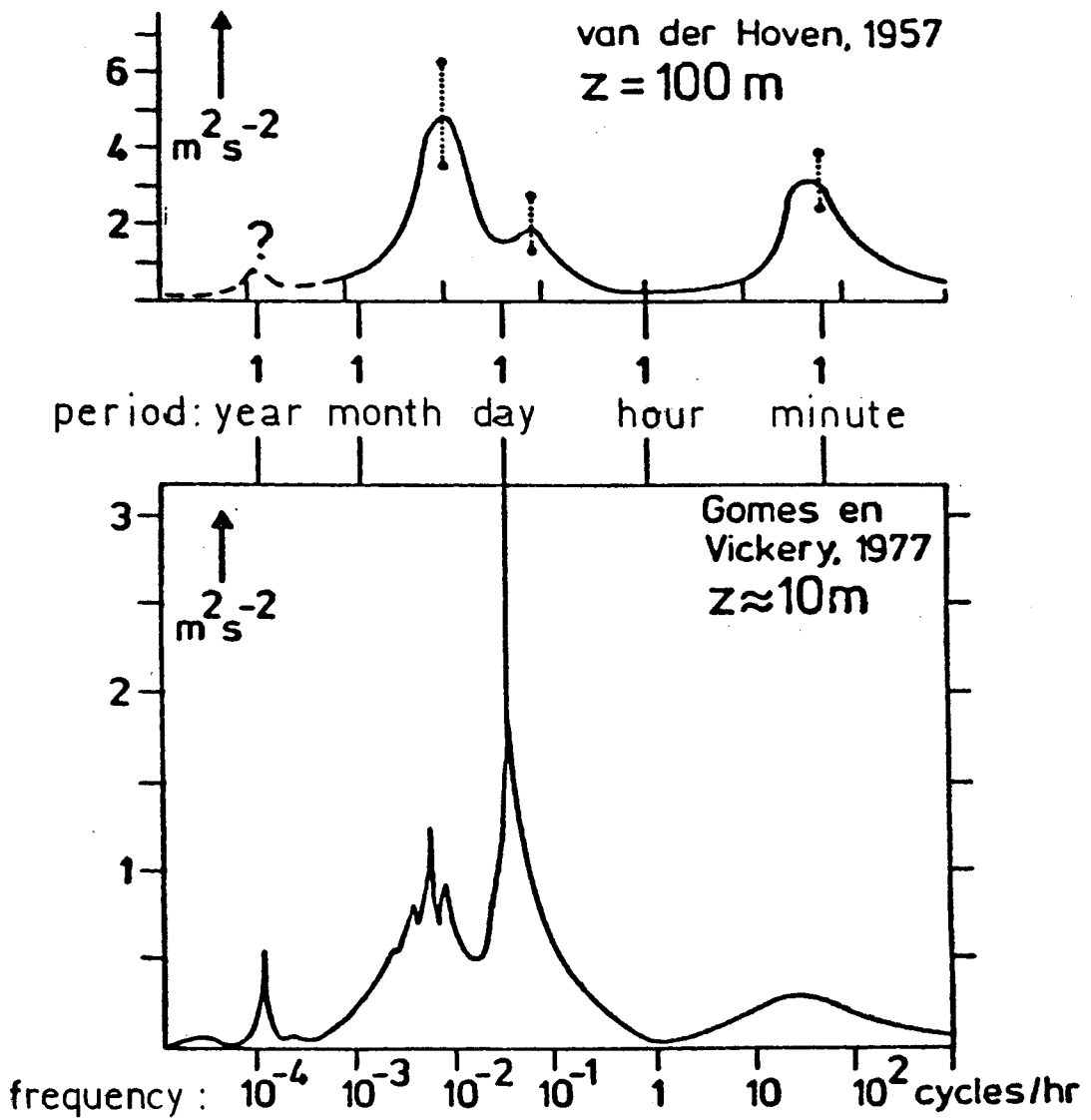


Fig. 5.1. Long term wind velocity spectra according to two different evaluations (taken from [15]).

as shown by the empirical relationship

$$\epsilon = 1/\ln\left(\frac{z}{z_0}\right) ,$$

where z = height above ground, and z_0 = roughness length.

It has been recommended in section 3.2.3.1. to measure this parameter along with the average values for the power curve, as it is a measure for the extent to which a power curve is influenced by the turbulence. If this number is quoted together with the power curve, this value can be used to improve the energy production prediction at an other site, where the degree of turbulence is known.

Due to turbulence the wind speed during time τ is fluctuating over a certain interval, in a way that can be closely approximated by a normal (or Gaussian) distribution. This means, for example, that if $\epsilon = 13\%$,

$\bar{u} = 9.5$ m/s, the average power coming into the bin of 9-10 m/s, actually is due to wind speed values belonging to neighbouring bins, as follows:

bin: 6 - 7 m/s	2%	} of the data
7 - 8 m/s	10%	
8 - 9 m/s	22%	
9 - 10 m/s	32%	
10 - 11 m/s	22%	
11 - 12 m/s	10%	
12 - 13 m/s	2%	

It is to be noted that the possible lack-of-correlation - to be discussed in section 5.4.5 - may even increase this spread. Furthermore it should be clear that this limited resolution is the reason for the turbulence disturbance, discussed in section 3.2. A shorter averaging time improves the resolution, and this might be one reason to choose a shorter τ -value for the aerodynamic power curve.

The fluctuations of the power signal within the averaging time are of less importance for the power curve problem. Of course these fluctuations are important as one of the factors determining the quality of the power, but that is another matter. Also the power signals require an appropriate anti-

aliasing filter. Otherwise high frequency fluctuations (e.g. due to mechanical resonancies) will be observed as low frequency disturbances, which may spoil the accuracy. Often a "natural" filter is present due to the dynamical inertia of the WECS. This will be briefly discussed in section 5.3.2.3. with regard to its relevance for the statistical behaviour of the averaged power values. On the other hand the power signal may contain the AC grid frequency. The worst aliasing problem would occur if sampling would be synchronized with this frequency in such a way that it is folded to frequency zero, i.e. gives rise to a bias. This situation appears to be forbidden in the IEA-recommendation.

There is one contribution to the standard deviation of averaged power, that is a typical consequence of the method of bins. Suppose that the real power curve is linear within a bin (slope dP/du) and that the wind speed distribution is uniform over the bin width (Δu).

Then:

$$P = \bar{P} + \frac{dP}{du}(u - \bar{u}) \quad \text{for } \bar{u} - \frac{1}{2}\Delta u \leq u \leq \bar{u} + \frac{1}{2}\Delta u$$

and

$$\sigma_p^2 = \overline{(P - \bar{P})^2} = \left(\frac{dP}{du}\right)^2 \cdot \int_{\bar{u} - \frac{1}{2}\Delta u}^{\bar{u} + \frac{1}{2}\Delta u} (\bar{u} - u)^2 du = \left(\left|\frac{dP}{du}\right| \cdot \frac{\Delta u}{2\sqrt{3}}\right)^2$$

This contribution is small above the rated wind speed, and below it will be of the order of 3% for current wind turbines using the 1 m/s bin widths.

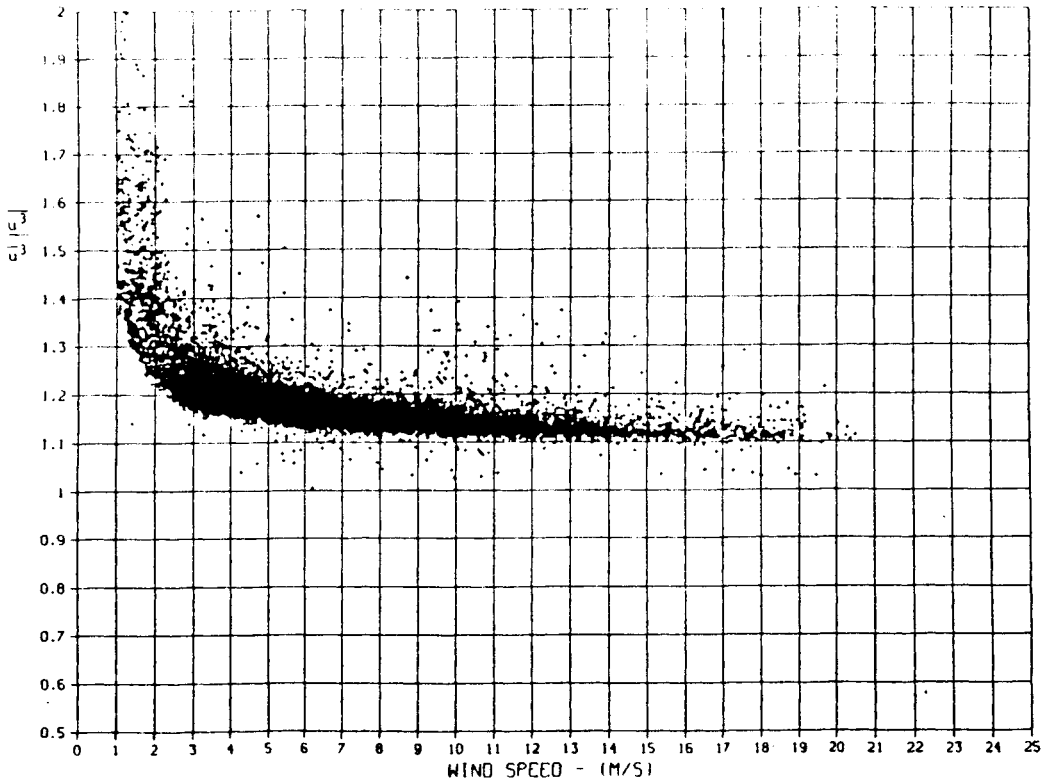


Fig. 5.2. The ratio $\frac{u^3}{\bar{u}^3}$ or $(1+3\sigma_u^2/\bar{u}^2)$ measured at Pellworm for every 10-minute averaging interval from November 1983 to February 1984 [11].

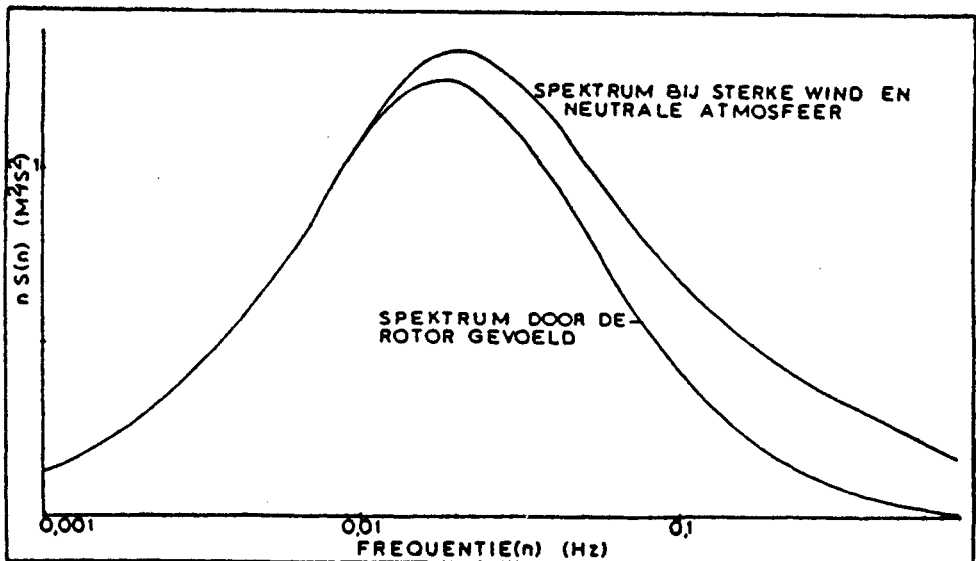


Fig. 5.3. The power spectrum of wind speed fluctuations felt by the rotor (lower curve), compared to the undisturbed spectrum (upper curve). Data $u=13$ m/s, $z=20$ m, $z_0=0.03$ m, rotor diameter = 16 m. Taken from [21].

5.3. Statistics of the averages

In this section we consider the statistical deviations of the data after averaging over the averaging time interval τ (600 s in the IEA recommendation, down to tens of seconds for special purposes).

5.3.1. Statistical errors in power averages

The power averages show a spread which may be due to many error sources. Many of the errors, summarized in Table 2.1 of chapter 2, have an unpredictable, stochastic component.

Examples are the following:

- Differences in machine conditions, like dirt, rain or ice on the blades, hysteresis around cut in or during switching between two generators, poor yawing control, etc.;
- Some dynamic effects in WECS, which will be briefly discussed in section 5.3.2.3.;
- Irregularities in sensors (like change in calibration of anemometers) and further instrumentatin (amplification, electronic noise, etc.);
- Differences in wind conditions, like changes due to terrain effects in fluctuating wind (see section 3.2), turbulence effects and the fundamental non-measurability of the driving wind (chapter 2) which produces the power. These matters will be discussed more extensively in section 5.4.

It should be noted that an irregular effect, giving rise to statistical errors, may become a regular systematic effect, if proper monitoring is performed. A well-known example is the anemometer calibration, where frequent recalibrations in principle reduce the calibration errors to a negligible level. Another very recent example is the monitoring of rain during power curve measurements. It has been observed in the Schnittlingen test station [16] and at the NEL test station by Howden people [17] that systematic differences occur between power curve measurements with and without rain.

5.3.2. WECS dynamics

5.3.2.1. Averaging turbulence over the rotor swept area

The turbulence fluctuations, as they are measured with the anemometer (of sufficient band width), are not all felt by the rotor, as the rotor integrates the fluctuations over its swept area. Slow fluctuations correspond to large scale turbulent structures and will be felt by the rotor, but fast small scale fluctuations are more-or-less averaged out. This integrating effect acts as a frequency filter, having a low pass characteristic. We will denote its transfer function by $H_r(f)$. Its effect is included in the definition of "driving wind speed" in chapter 2.

The function $H_r(f)$ has been estimated for the first time in ref. [18]. Since then in several places computer programs have been made for its computation, commonly based on an integration of the lateral coherence function of the turbulence over the rotor swept area.

In reality slightly more happens. It is not only true that the turbulence fluctuations are attenuated at higher frequencies, but the removed components are actually shifted to higher frequencies, for a B-bladed rotor around the values of B, 2B, 3B, times the frequency of the rotor rotation (ref. e.g. [19]). These higher components are usually of little concern in power curve measurements (see discussion in the next section). It has been found [20] that the turbulent load spectra can be expanded in "rotational modes", and that the zero order mode term just accounts for the rotor swept area averaging. An example of the filter $H_r(f)$ is given in fig. 5.3, as obtained from a computer code of TNO, Apeldoorn, by geometrical averaging over the rotor area, taking the lateral coherence into account. The filter is real, there is no phase shift.

5.3.2.2. Integrating over periodic components

If Ω is the angular speed of the B-bladed rotor, periodic or nearly periodic fluctuations in power may occur at frequency:

- Ω due to aerodynamic or gravitational unbalance;
- $B\Omega$ and harmonics, due to wind shear, tower shadow, improper yawing and turbulence (see section 5.3.2.1) for HAWT's whereas the torque ripple due to periodic changes in angle of incidence causes a dominating effect for VAWT's.

The worst case is a 100% modulation, that may occur in the aerodynamic power of a VAWT, but certainly will be less in the output power (section 5.3.2.3). One could think that averaging over an integral number of cycles would be desirable. It is easily seen however that in the worst case of $P(t) = \bar{P}(1 + \sin 2\Omega t)$, when averaging over $(N + \frac{1}{2})$ periods, i.e. $\tau = (N + \frac{1}{2})\frac{2\pi}{\Omega}$, the relative error will be 3% for $N=10$ and 1% for $N=30$. So it is reasonably safe to take the averaging time larger than 10-15 rotor revolutions. If not, the bin averaging may still largely remove the error, but the standard deviation of bin averages will increase.

5.3.2.3. Averaging by dynamic effects

The problem to be discussed in this subsection arises if rotor speed is variable. Then the power of the wind is not only used to drive the shaft and the load (generator, pump), but also to accelerate (or decelerate) the rotor. The wind speed history will (in a sense) be stored in rotor kinetic energy and later be delivered to the load as part of the power.

In a linear approximation,

$$P_{\text{meas}}(t) = \int_{-\infty}^t h_d(t-t')P(u(t'))dt',$$

where in this case $u(t)$ is the driving wind speed.

If the response function $h_d(t)$ extends over a time interval which is not small with respect to the averaging time, errors may occur in the bin analysis.

This can be visualized as follows. Suppose that at a certain moment a wind speed bin at u_1 is selected well above the mean wind speed of that measure-

ment. Then there is a high probability that the rotor during the previous time experienced a lower wind speed than u_1 , so the rotor speed is likely to be lower than the speed corresponding to u_1 , so at this moment the rotor will probably accelerate, delivering a lower power than $P(u_1)$ to the shaft and load.

The effect is equivalent to (and in fact a special case of) the "lack-of-coherence" problem be discussed in section 5.4: it appears in the situation that the correlation between the measured pair u and P (both averaged over τ) becomes poor.

The degree to which this happens depends on the extent of the function $h_d(t)$, or its Fourier transform $H_d(f)$, which is a filter with low pass characteristics. For a wind turbine with induction generator it is in first approximation a first order filter, for a grid coupled synchronous generator a second order filter. In these cases the cut-off frequency is determined by the effective moment of inertia I of the rotating parts, relative to the stiffness of the system (shaft and generator). In these situations the effects are usually small. They can be evaluated from a simplified dynamical model of the WECS.

For a variable speed machine (e.g. constant λ -operation) the filter $H_d(f)$ largely depends on the method of control. The time constant can be quite high in principle. In that case a careful dynamical analysis is required to estimate the lack-of-correlation effect. Another way around the problem is an experimental one: measure power and rotor speed $\Omega(t)$ simultaneously, and correct the power with a dynamical contribution $I\Omega \cdot \frac{d\Omega}{dt}$.

5.4. Statistical description of the method of bins

5.4.1. General statement of the problem

In what now follows the samples of power measurement and wind speed measurement will be the averages over averaging time τ , where possibly the power may be slightly shifted in time in order to account for the transport lag between anemometer and wind turbine. The probability to find power and wind speed in intervals $(P, P+dP)$, $(u, u+du)$ is given by a two-dimensional frequency function $f(P, u)$.

Analysis by the method of bins means selecting and averaging the power samples which belong to wind speed samples in a small interval, say $u_i - \frac{1}{2}\Delta \leq u \leq u_i + \frac{1}{2}\Delta$. The frequency function for the power samples in this bin is then equal to

$$f_i(P) = \int_{u_i - \Delta/2}^{u_i + \Delta/2} f(P, u) du / \int_{-\infty}^{+\infty} dP' \int_{u_i - \Delta/2}^{u_i + \Delta/2} f(P', u) du,$$

where the denominator takes care of normalization. It is convenient to consider in particular the conditional distribution, which corresponds to very narrow bins, defined by

$$f(P|u_i) = f(P, u_i) / \int f(P', u_i) dP'.$$

The expected bin average is the mean of this distribution, while its second central moment is the variance of the bin data. In the following sections these two aspects will be considered in more detail.

The basic assumption of the method of bins is that the conditional mean, i.e. $\int P \cdot f(P|u_i) \cdot dP$, is equal to the power belonging to u_i , i.e. $P(u_i)$. Is there any reason for this belief? And if so, what is the accuracy?

5.4.2. Normal distribution

Divide the total measurement time for a power curve into pieces of data, collected under more-or-less stationary meteorological conditions, for a measurement time T (which may be several hours).

The averages of power and wind speed samples during this time are denoted by (P_o, u_o) , which is a point of the power curve.

Then it is often a reasonable assumption that $f(P, V)$ for this sub-set of data becomes a bivariate normal distribution,

$$f(P, U) = \frac{1}{2\pi\sigma_p\sigma_u\sqrt{1-r^2}} \exp\left[-\frac{1}{2(1-r^2)} \left\{ \left(\frac{P-P_o}{\sigma_p}\right)^2 - 2r\left(\frac{P-P_o}{\sigma_p}\right)\left(\frac{u-u_o}{\sigma_u}\right) + \left(\frac{u-u_o}{\sigma_u}\right)^2 \right\}\right].$$

This function is characterized by 5 parameters: u_o, P_o , the variances σ_u^2 and σ_p^2 , and the covariance σ_{Pu}^2 or correlation coefficient $r = \sigma_{Pu}^2 / \sigma_p \sigma_u$. From this the conditional distribution $f(P(u))$ is easily found (see e.g. ref. [Cramér]). This is a one-dimensional normal distribution in P , with mean

$$\overline{P_i} = P_o + \frac{r\sigma_p}{\sigma_u} (u_i - u_o) = P_o + \frac{\sigma_{Pu}^2}{\sigma_u^2} (u_i - u_o),$$

and variance

$$\sigma_i^2 = \sigma_p^2(1-r^2),$$

independent of u_i .

We now have to consider the possible errors made in identifying $\overline{P_i}$ with $P(u_i)$, or in first order approximation with $P(u_o) + \frac{dP}{dV} (u_i - u_o)$.

To this end we have to make further physical assumptions.

5.4.3. Frequency domain representation

It is most convenient to continue the treatment of the problem in the frequency domain. This is done in some detail in the Annex 6.B. Here we summarize the main points.

The requirement of the last sections was:

$$\sigma_{Pu}^2 = \left(\frac{dP}{du}\right) \cdot \sigma_u^2.$$

We consider in linear approximation the factors determining σ_{Pu}^2 and σ_u^2 . They act like (low-pass) frequency filters, acting on the wind speed fluctuation spectrum $S_o(f)$. The filters are:

- in both σ_{Pu}^2 and σ_u^2 :
time averaging and
measurement time: $F_\tau(f) - F_T(f)$
- in σ_{Pu}^2 :
coherence: $\gamma(f)$
transport delay,
as far as uncompensated: $\exp(-2\pi ifd)$
rotor area averaging: $H_r(f)$
wind turbine dynamics: $H_d(f)$
- in σ_u^2
anemometer response: $H_w(f)$.

Now σ_{Pu}^2 and σ_u^2 contain $S_o[F_\tau - F_T]$, both filtered by several filters. The above requirement is only satisfied if the filter responses are 1 over the range where $S_o[F_\tau - F_T]$ exists, i.e. essentially from $1/T$ to $1/\tau$. The filters are illustrated in fig. 5.4. The physical requirements, following from the filter requirement, are treated in section 5.4.4.

5.4.4. Requirements

The requirements on the filters lead to a set of physical requirements.

- a. The averaging time τ must be large enough not to feel the rotor area filtering. For the situation in the sketch (where $R/\bar{u} \approx 2.2$) this is still the case for $\tau \approx 60$ seconds. Since $H_r(f)$ primarily depends on $f \cdot R/\bar{u}$ the averaging time must be increased proportionally for larger rotors or lower mean wind speeds.
- b. Due to $H_d(f)$ the dynamic time constant of the WECS will start to play a role if its order of magnitude becomes larger than about 0.1τ .
For the IEA-averaging time of 600 seconds this is usually no problem, but for shorter averaging time it should be checked that the turbine is reacting fast enough on wind fluctuations. If not, the $I\Omega \frac{d\Omega}{dt}$ - correction (section 5.3.2.3) might be considered.

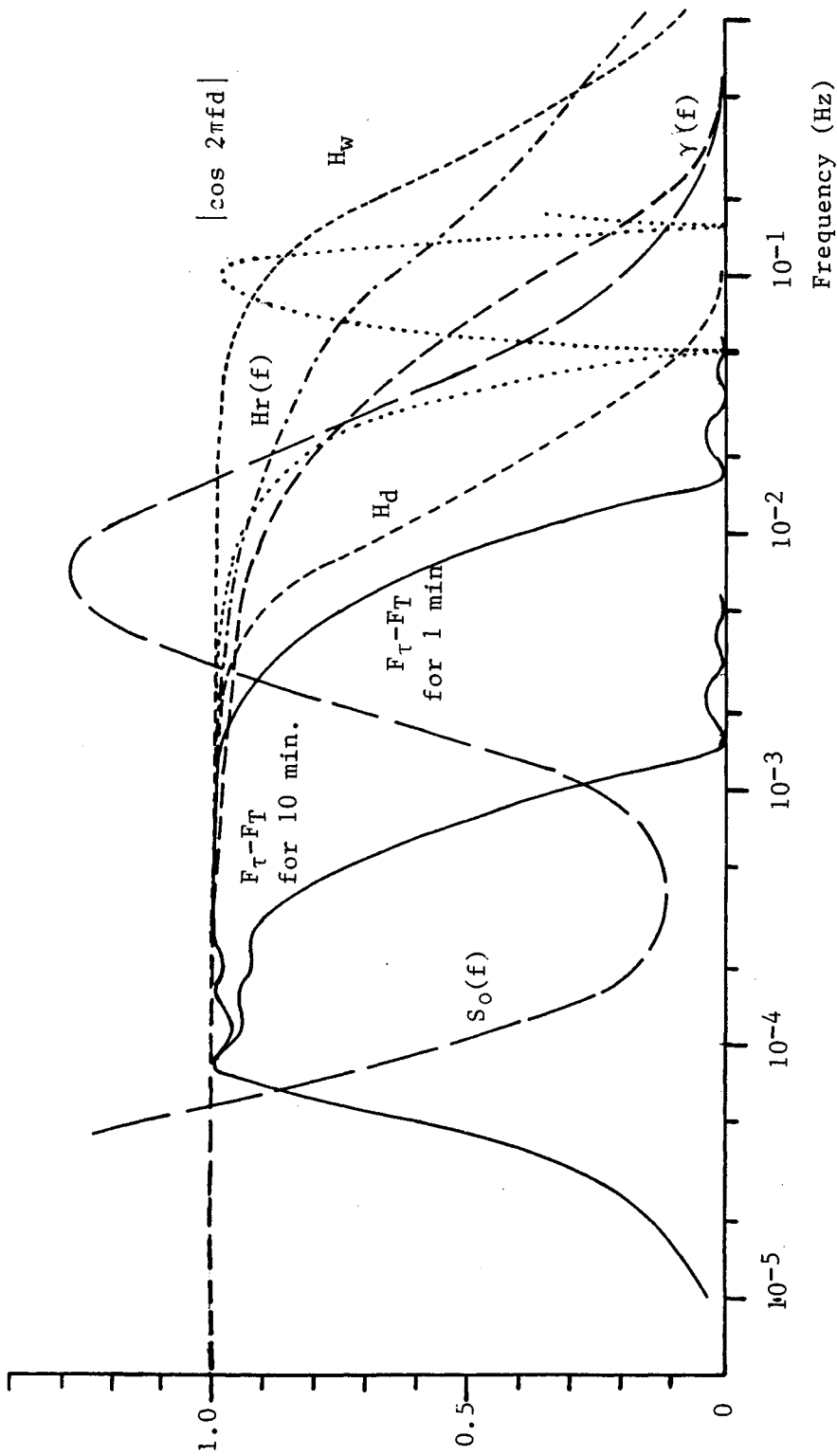


Fig. 5.4. Sketch showing a wind spectrum $S_0(f)$ and the "filter" functions involved: time averaging ($F_T - F_T$), coherence ($\gamma(f)$), rotor area averaging (H_r), transport lag ($\cos 2\pi f d$), wind turbine dynamics (H_d) and anemometer dynamics (H_w).

c. The anemometer time-constant (in filter $H_w(f)$) will only cause problems if averaging time comes in the seconds range. So this effect will not play a role in practical situations.

d. The coherence $\gamma(f)$ must be close to 1 down to the frequency $1/\tau$. In the often used expression

$$\gamma(f) = \exp\left(-\frac{aDf}{\bar{u}}\right),$$

where D is the distance between anemometer and the wind turbine, while a is a constant, about 10 if the anemometer is in front of the turbine (longitudinal coherence) and about 2 if it is across (lateral coherence). For $\tau=600$ s this condition is easily met. But for instance for the anemometer across the turbine at 100 m distance, the condition would be clearly violated for an averaging time of 1 minute.

e. The transport lag effect, $\cos 2\pi f d$, is negligible for current anemometer distances at the 10 minute averaging. But for shorter τ - in the range of 10-20 times the transport time - the effect will increase. So for shorter averaging times the transport lag correction should be applied.

It is concluded that under the IEA recommendations the different effects will not play a significant role, so the method if bins is valid.

For shorter averaging time errors may appear, especially of the anemometer is besides the wind turbine at a larger distance. These errors are systematic errors for a measurement under a particular wind condition. It is true that errors may cancel to a certain extent, when many measurements under many different wind conditions are combined. But one has to be careful in this respect.

The formulas given in this chapter allow a quantitative evaluation of such errors. If the conditions are fulfilled the correlation coefficient r between P and u will be very close to 1. In principle this can be checked experimentally.

If the transfer function $H_d(f)$ is sufficiently flat over the frequency range of interest, and without phase shifts, then P is a deterministic function of the driving wind speed v . In that case the linearity assumption can be dropped (P may be any function of v). It is now sufficient to assume a bivariate distribution for u_0 and v_0 and the whole argument will be as before.

5.4.5. Discussion of the variance

It seems that not much attention has been given up to now to the evaluation of the variances of the power samples and the statistical accuracy of the final bin average of these samples.

To illustrate some pertinent point we will use here some simple analytical approximations.

First, we calculate variances for very narrow bins (the contribution of finite width was considered in section 5.2 already). Then it follows from section 7.3.2 that the (conditional) variance of power in the bin belonging to velocity u_i is

$$\sigma_i^2 = \sigma_p^2(1-r^2).$$

Now assume for simplicity that the transfer functions $|H_w|$, $|H_r|$, $|H_d|$ and $\cos 2\pi f d$ are all equal to unity. The lack of correlation in this case is only due to the coherence function $\gamma(f)$. Then

$$1-r^2 = 1 - \frac{\int \gamma(f) S_o(f) \{F_\tau(f) - F_T(f)\} df}{\int S_o(f) \{F_\tau(f) - F_T(f)\} df}.$$

This means: the power variance of the whole measurement over time T is to be multiplied by this factor to obtain the variance of the power samples that go into the bin analysis. Also assume that $S_o(f)$ is constant over the relevant frequency range from $\frac{1}{T}$ to $\frac{1}{\tau}$. Then the integrals can be evaluated analytically. If $T \gg \tau$ the assumption of constant S_o makes the contribution of the terms $F_T(f)$ negligible, and one finds

$$1-r^2 = \frac{2}{\pi} \left\{ \arctan \alpha + \frac{1}{2} \alpha \ln \left(1 + \frac{1}{\alpha^2} \right) \right\}$$

with

$$\alpha = a \cdot \frac{D}{u} \cdot \frac{1}{2\pi\tau},$$

where the symbols have their previous meanings (a is constant in exponential coherence function, D is distance anemometer to WECS, τ is averaging time). For σ_p we can make an estimation in the assumption that the power follows the wind fluctuations ($H_d=1$). Then

$$\sigma_p / \bar{P} = k \cdot \epsilon$$

with ϵ = degree of turbulence

$$k = \left(\frac{dP/\bar{P}}{du/\bar{u}} \right).$$

The following table has been calculated for $\epsilon=13\%$ and $k=1$ (which is the correct order of magnitude below the rated power and wind speed). We take $\bar{u} = 8$ m/s. The turbine under test has a 20 m rotor diameter, and the distances are 2 and 8 diameters from the turbine (limits of IEA recommendation).

anemometer	a	distance d (m)	averaging time τ (s)	r	$\sqrt{1-r^2}$	σ_i / \bar{P} (%)
up-wind	2	40	600	0.991	0.136	1,8
up-wind	2	160	600	0.970	0.243	3.2
lateral	10	40	600	0.977	0.212	2.8
lateral	10	160	600	0.890	0.457	5.9

It is concluded that in following the IEA-recommendations acceptable standard deviations will be obtained, as far as wind statistics is concerned. One has to realize that for the 10 minutes averaging the statistical errors of the N samples going into a particular bin will be relatively uncorrelated, so the errors are reduced by a factor $1/\sqrt{N}$, which is $< 0,32$ as $N \geq 10$.

For short averaging times the situation will be different.

It is clear that a careful error analysis is to be recommended here.

There is another point to be made. In comparing the 2nd and the 4th line of the table it is seen that the accuracy for an up-wind anemometer may be nearly twice as small as for a lateral one.

In the IEA-recommendations such measurements are considered to be of equal value: they enter the final bin analysis with equal weights. There is a danger here: care should be taken that inaccurate data are not spoiling the accurate ones. To give a trivial example: if two measurements 101 ± 5 and 89 ± 10 are combined with equal weights the result is 95.0 ± 7.9 , whereas a proper statistical weighting leads to the much better estimate of 98.6 ± 4.5 .

Therefore, further study is required to investigate to what extent some method of weighted averaging has to be recommended for power curve measurements. For short averaging times this recommendation holds even stronger.

A final remark concerns the velocity resolution of the measured power curve. In section 5.2. it was seen that the wind speed fluctuations within the averaging time determine the resolution.

But even if this spread were small, the lack of correlation might spoil the resolution, since in that case a fixed anemometer reading would correspond to a range of wind speeds at the WECS. This would occur if the wind spectrum $S_0(f)$ would be low above $1/\tau$ and high below with poor coherence.

It is the same factor $(1-r^2)$ that determines the ratio of the conditional variance of wind speed at the WECS (driving wind) and the total variance. It follows from the 6th column of the above table, that this lack-of-correlation resolution is much narrower than the resolution due to fluctuations within τ for the case of IEA recommendations. In case of short time averaging this point deserves some closer attention.

It has been concluded that statistical errors should be small if IEA specifications are followed. We recommend, however, that this should be checked by determining (and reporting) the standard deviations of the mean values per bin. The effect of these errors on the yearly energy production should also be calculated, assuming the statistical errors of the bin averages to be independent.

ANNEX 5A: Statistical definitions

Consider a stationary process with two variables $X(t)$ and $Y(t)$, fluctuating around their mean values m_x and m_y with standard deviations σ_x and σ_y . For a large number of N samples X_i and Y_i ($i = 1, \dots, N$) from $X(t)$ and $Y(t)$ the means and variances (σ^2) can be estimated by

$$\begin{aligned} m_x &= \frac{1}{N} \sum_{i=1}^N X_i \\ \sigma_x^2 &= \frac{1}{N} \sum_{i=1}^N (X_i - m_x)^2 \end{aligned} \quad , \quad (A.1)$$

(similarly for Y), or by equivalent recursive relations, after n samples:

$$\begin{aligned} m_x(n) &= m_x(n-1) + \{X_n - m_x(n-1)\}/n \\ \sigma_n^2(n) &= \frac{n-1}{n} [\sigma_x^2(n-1) + \{X_n - m_x(n-1)\}^2/n] \end{aligned} \quad \text{for } n = 1, 2, \dots, N \quad (A.2)$$

In case of on-line computation the recursive computation is to be preferred over a computation based on (A.1), where numerical inaccuracies may arise in σ^2 due to subtraction of nearly equal large numbers.

The covariance can be estimated by

$$\sigma_{xy}^2 = \frac{1}{N} \sum_{i=1}^N (X_i - m_x) (Y_i - m_y) \quad (A.3)$$

(or an equivalent recursive relation). The correlation coefficient is defined by:

$$r = \sigma_{xy}^2 / \sigma_x \sigma_y \quad (A.4)$$

In the main text of Chapter 7 we use these concepts at two different levels. First (section 7.1) averaging is performed for the directly measured data (typically sampled at intervals Δt of 1 second), over averaging times of $\tau (=N\Delta t)$, (typically 1 to 10 minutes). In section 7.2-3, however, the samples are the τ -averaged data, for which means and variances of the total measurement time T (say several hours) are to be obtained.

In theoretical considerations it is convenient to express the fluctuating parts of the signals, $x(t)$ and $y(t)$, in their frequency components. In this

report we follow definitions and conventions of ref. [22].

The correlation function $R_{xy}(t')$ is the expectation value of $x(t).y(t+t')$ and the cross power spectral density (CPSD) its Fourier transform,

$$S_{xy}(f) = \int_{-\infty}^{+\infty} R_{xy}(t') e^{-2\pi i f t'} dt' , \quad (A.5)$$

with the inverse

$$R_{xy}(t') = \int_{-\infty}^{+\infty} S_{xy}(f) e^{2\pi i f t'} df' \quad (A.6)$$

for frequencies $-\infty < f < +\infty$ (two-sided). Autocorrelation functions $R_{xx}(t')$ $R_{yy}(t')$ with auto power spectral density functions (APSD) $S_{xx}(f)$, $S_{yy}(f)$ are defined correspondingly. The (complex) CPSD can be expressed in a (real) coherence function $\gamma(f)$ and phase $\theta(f)$ by:

$$\frac{S_{xy}(f)}{\sqrt{S_{xx}(f) \cdot S_{yy}(f)}} = \gamma_{xy}(f) \cdot \exp[-i\theta(f)] \quad (A.7)$$

Note that the spectra extend over positive and negative frequencies. In integrations one has to bear in mind that APSDs are even functions of frequency, and that CPSDs are complex with even real part (and coherence) and odd imaginary (or phase) parts.

If a linear systems responds to a $\delta(t)$ -input by a filter response function $h(t)$, then for a stochastic excitation of that system the CPSD of output and input is obtained as the product of the input APSD and the transfer function $H(f)$ of the filter, which is the Fourier transform of $h(t)$. The output APSD is equal to input APSD times $|H(f)|^2$.

From its definition for $t'=0$ it follows that $R_{xy}(0)$ is a covariance, and (A.6) then shows that $S_{xy}(f)$ gives a spectral decomposition of the covariance. Note that the imaginary part of S_{xy} does not contribute in the case of $t'=0$, so that the integrand may be replaced by $\text{Re}S_{xy}$. Similarly the APSD gives the spectral decomposition of the corresponding variance. Note that these (co)-variances are defined with respect to their true mean values. In measurements, however, we have to use the mean over some averaging time.

In section 5.2 this is the time τ . Therefore, to obtain the spectral decomposition of a (co-)variance within averaging time τ , a contribution has to be subtracted which corresponds to this averaging, i.e. filtered by a filter with response function a "box car" wave of duration τ (i.e. $h(t) = 1$ for $0 \leq t \leq \tau$ and $h(t) = 0$ elsewhere). The square modulus of the corresponding transfer function is denoted by $F_\tau(f)$ in this report, and is readily found by Fourier transformation to be

$$F_\tau(f) = \left(\frac{\sin \pi f \tau}{\pi f \tau} \right)^2. \quad (\text{A.8})$$

It follows that a (co)variance within averaging time τ is expressed in the corresponding spectrum in the frequency domain by

$$\sigma^2 = \int S(f) [1 - F_\tau(f)] . df \quad (\text{A.9})$$

On the other hand, using similar arguments, the (co)variance of the τ -averaged values, measured over the total measurement time T , is:

$$\sigma^2 = \int S(f) . [F_\tau(f) - F_T(f)] . df. \quad (\text{A.10})$$

(also see ref. [7]).

ANNEX 5B: Frequency domain representation

Consider the undisturbed winds at the anemometer and at the center of the wind turbine rotor, $u_o(t)$ and $v_o(t)$ respectively. In homogeneous terrain their means and fluctuation spectra will be equal, \bar{u} and $S_o(f)$.

Their cross-power spectrum can be written as $S_o(f) \cdot \gamma(f) \cdot \exp(-2\pi i f d_o)$, where $\gamma(f)$ is the (real) coherence function, which is a function of distance and wind direction with respect to the two locations. The complex exponential expresses a possible transport lag time d_o , which gives a phase shift of $2\pi f d_o$ radians.

The spectrum of the anemometer signal, $S_{uu}(f)$, is now the spectrum $S_o(f)$, multiplied by the anemometer response transfer function $|H_w(f)|^2$, which is approximately a first order filter with time constant equal to distance constant (≤ 5 m) divided by mean wind speed. Then

$$\sigma_u^2 = \int S_o(f) \cdot |H_w(f)|^2 \cdot [F_\tau(f) - F_T(f)] \cdot df$$

where the F-filters express the averaging over τ during measurement time T (see Annex 5A, eq. (A.8)).

Furthermore we assume the following physical model. The momentaneous power $P(t)$ is determined by the driving wind speed $v(t)$ (see section 2), which follows from the (point) wind speed in the center of the rotor $v_o(t)$ by the rotor area averaging filter $H_r(f)$, introduced in section 5.3.2.1. These driving wind speed fluctuations cause the power fluctuations through the filter $H_d(f)$, discussed in section 5.3.2.3. Only the power signal is measurable, not the virtual (non-existing) wind speeds $v(t)$. There is not a deterministic relation between v and u , and therefore between u and P , but only the statistical one, expressed in the correlation coefficient or covariance.

From the definitions, assuming linearity between P and v for the moment (see end of section 5.4.4),

$$\sigma_{Pu}^2 = \left(\frac{dp}{dv}\right) \int S_o(f) \cdot H_r(f) \gamma(f) \cdot \text{Re}[H_d(f) e^{-2\pi i f d}] \cdot [F_\tau(f) - F_T(f)] \cdot df$$

This expresses the covariance for the averages over time intervals τ . In defining the averaging intervals it is possible to compensate for the transport delay phase of $2\pi f d_0$, by delaying the power averaging intervals by a similar amount with respect to the anemometer averaging intervals. Certainly for short-time averaging this is recommendable. In the general formula above the transport delay effect is expressed in the delay time d , which is the difference between d_0 and the interval shift time (ideally $d=0$).

For completeness we give the formula for the variance in P ,

$$\sigma_p^2 = \left(\frac{dP}{dv} \right)^2 \cdot \int S_O(f) \cdot H_r(f)^2 \cdot |H_d(f)|^2 \cdot [F_\tau(f) - F_T(f)] \cdot df.$$

This equation is not used in the analysis of this subsection.

From the discussion in section 5.4.2. and the expressions for σ_u^2 and σ_{Pu}^2 it now follows immediately that the method of bins is valid, provided that

$$\int S_O(f) \cdot \gamma(f) \cdot H_r(f) \cdot \text{Re}[H_d(f)e^{-2\pi i f d}] \cdot [F_\tau(f) - F_T(f)] df =$$

$$\int S_O(f) \cdot |H_w(f)|^2 \cdot [F_\tau(f) - F_T(f)] df.$$

Fig. 5.4 illustrates the situation. It sketches the different spectra and filter characteristics involved. It is clear from the figure that the above equality is closely valid if the filters $|H_r(f)|$, $|H_d(f)|$ and $|H_w(f)|$ are close to 1 over the relevant frequency interval from $\frac{1}{T}$ to $\frac{1}{\tau}$, where the upper frequency, the inverse of averaging time, imposes the heaviest requirements, especially so if τ becomes much smaller than 600 s. The same applies to $\gamma(f)$ and $\text{Re}[e^{-2\pi i f d}] = \cos 2\pi f d$.

6. REVIEW OF ALTERNATIVE METHODS OF ANALYSIS

It appears that in the different test stations the IEA recommendations are followed as close as possible for the routine measurement of power curves. Nevertheless a variety of other methods of data analysis has been proposed and tried in several institutes, mainly to improve upon some of the drawbacks of the standard method, namely:

- very long measuring time;
- few measurements at high wind velocities;
- poor resolution in wind speed;
- possibility of systematic errors.

Below a number of variants are summarized. Mutual relationships are indicated. Note that combinations of these methods can be (and have been) made.

6.1. Method of bins with short averaging time

The obvious way to increase the speed of the measurement is to use a much shorter averaging time than 10 minutes.

Though not standard practice, this has been tried in many test stations and research institutes. Averaging times are usually taken in the range of 10 seconds to 1 minute. A shorter averaging time makes no sense due to the disturbing effect of local turbulence and of the dynamics of the wind turbine. Advantages are the shorter measurement time, the broader wind velocity range, and better resolution. This makes the method more suitable for the aerodynamic studies; the compatibility with WMO wind measurement standards is lost.

Main disadvantages are:

- increased statistical error (chapter 5);
- lower correlation between power and wind data, and therefore the possibility of notable systematic errors.

In order to improve on the latter point a rather careful planning of the measurements is required. It is important to have the anemometer mast in the upwind direction (because of the much higher longitudinal than lateral coherence in turbulent flow), as close as possible to the rotor, but yet not feeling the flow disturbance (distance of 2-3 rotor diameters), and the anemometer should be at hub height. For real fast measurements a transportable

anemometer mast would be nearly a prerequisite. The most extreme way to realize this is to attach the anemometer on a beam fixed to the turbine (see section 6.2).

It is recommendable to determine the correlation coefficient between power and wind speed in such fast measurements. If this coefficient is below 1 (say, about <0.9) one may try to apply a correction for lack-of-correlation (section 6.7).

Special care is required for variable speed rotors, where dynamic effects are likely to disturb results. A correction for rotor acceleration and deceleration should be envisaged here, by increasing the output power by $\eta I \Omega \frac{d\Omega}{dt}$ (I = rotor moment of inertia, Ω = rotor angular velocity, η = conversion efficiency).

6.2. Boom anemometer method

Very good correlation between power and wind velocity is obtained with the anemometer on a boom attached to the wind turbine at a very short distance (e.g. 1 rotor diameter at SERI, 0.5 rotor diameter at RAL). The problem with this method is of course that the anemometer reading may be disturbed by the presence of the rotor. The best way to account for that is to "calibrate" the boom anemometer against a far field anemometer in some separate measurement runs (RAL).

The idea of a very close anemometer has been applied in practice in a number of different ways. Noteworthy examples are the 17 m VAWT of Sandia National Laboratory (Albuquerque) with an anemometer on top of the turbine, the 9 m Northwind HAWT at RAL with an upwind anemometer at only 0.5 rotor diameter distance ([23] and [24]), and an airfoil testbed of the SERI Wind Energy Research Center (5 m diameter HAWT) with 2 anemometers on the two sides (1 rotor diameter from the hub) [25].

It has been shown that the method may lead to accurate power curves. Note however that in all cases mentioned the primary interest of the measurements was to determine the aerodynamic characteristics of the rotor, rather than determining power curves for energy production prediction.

6.3. Power binning

Instead of averaging the power measurements in wind velocity bins, it is also possible to average the wind velocities which belong to the same power bin. This method has been used in several places ([26] and [27]).

Since the wind velocity constitutes the dominating source of error there is a certain logic in this method. The power curve obtained in this way turns out to cover a somewhat larger power range than for a conventional bin analysis of the same data.

It should be noted that also in this method a high correlation between power and wind velocity is required. If not, systematic errors will occur as in conventional binning, but with opposite signs. This last property may be used to set a "quality criterion" on measured data: the set is acceptable if normal binning and power binning yield the same piece of power curve.

The main drawback of this method is that it requires a monotonous power curve. A power curve with downward slope at high wind velocities (e.g. a stall controlled machine) can not be measured in this way, unless more sophisticated analysis of the distribution of data in a power bin is made, in order to distinguish the two wind speed values that belong to a chosen power (see section 6.8).

6.4. Method of cubic bins

It has often been tried - especially for aerodynamic performance studies - to apply the method of bins to C_p (aerodynamic efficiency) versus λ (tip speed ratio), after conversion of power and wind velocity samples to C_p and λ -values. It gives some difficulties to do this for strongly fluctuating winds. In ref. [28] the effect of wind speed uncertainty on both C_p and λ was investigated. It was shown to be better to choose bins in the C_p - λ -plane, which are not bounded by straight lines but by cubic functions, $C_p = k_n \cdot \lambda^3$ for a sequence of values of k_n , as shown in fig. 6.1. This was called "method of cubic bins".

It is easy to see that the method is basically equivalent to power binning. Namely, by transforming the (C_p, λ) -plane into a $(K_p, \frac{1}{\lambda})$ -plane by $K_p = C_p / \lambda^3$, the cubic functions become straight lines $K_p = k_n$. For a constant speed machine the parameters K_p and $1/\lambda$ are just the power and the velocity, normalized to

dimensionless parameters by division by the constants $\frac{1}{2}\rho A(\omega R)^3$ and (ωR) , which are constants depending on tip speed ωR .

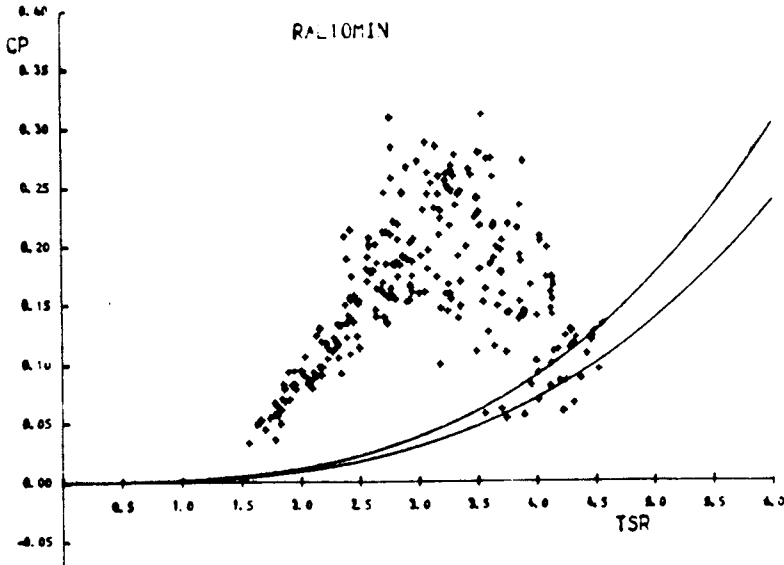


Fig. 6.1. Illustration of cubic binning of C_p as a function of tip speed ratio TSR.

Another feature of the method of cubic bins is that the data in the bins are not simply averaged, but their frequency distribution is considered. The most probable C_p/λ^3 is derived from the maximum of this distribution. The possible occurrence of two maxima in the same bin can be recognized in this way, which is a very important feature.

It is concluded that the method of cubic bins is equivalent to a combination of power binning and most probable power method (sections 6.3 and 6.8).

6.5. Least squares fitting

In order to smooth out the fluctuations in the different bin values of a power curve, one often fits a polynomial to the data by the method of least squares. This analysis can be done afterwards after the bin selections, but it is also possible to skip the intermediate step of bin selection and instead to calculate parameters which determine the polynomial coefficients directly.

The procedures may be followed both for velocity binning and for power binning [27]. Together with short time averaging a very fast power curve estimation can be realized in this way. Polynomials of different degrees may be chosen, usually not higher than three [29], and often only for limited pieces of the power curve.

In case of linear least squares fitting it simply boils down to a classical least squares regression analysis: velocity binning then corresponds to regression of power on velocity, power binning (section 6.1) to regression of velocity on power (e.g. [30]). Linear fitting is certainly not useful for the collection of all measured data, but for the sub-sets of data taken under more-or-less stationary wind conditions such a regression may be quite useful.

6.6. Orthogonal regression

It is well known that a regression analysis between two variables is not symmetric in the two if their correlation coefficient is less than 1. The effect is easily explained if one considers the joint probability distribution, with its elliptic equal probability contours if normal statistics holds. The long main axis of this ellipsis corresponds to the true relationship between power and velocity. The least squares linear regression line of power on velocity likewise passes through the center of the ellipses, but with smaller slope. The regression of velocity on power on the other hand is steeper than the correct line. To circumvent this problem it has been proposed [10] to use orthogonal regression [30] instead, i.e. not minimizing the sum of squares of distances along one of the coordinates, but perpendicular to the regression line. This has been tried for the Gedser wind turbine, for which correlation ellipses and regression lines are shown in figure 6.2.

A problem in this method is a choice of the scales of power and velocity: orthogonality depends on this choice. Christensen's recommendation is to choose them in such a way that the line will have a slope around 45° . If we assume the physical model that power is a function of driving wind speed with the same mean and standard deviation as the anemometer reading, this recommendation corresponds to equal standard deviations in both directions and the estimate of the piece of power curve is free of systematic errors.

6.7. Lack-of-correlation correction

Under the assumption of normal statistics estimates can be obtained for the systematic difference (bias) between a bin mean value and the true value belonging to that bin (see chapter 7 and ref. [26]). If it is again assumed that the mean and variance of the driving wind speed felt by the rotor and the observed anemometer wind speed are equal, corrections can be derived for either way of binning, on wind speed or on power.

Key parameter in these corrections is the correlation coefficient between the

power and wind speed values (after averaging, for the data as they go into the bin analysis). If the bin selection algorithm calculates both means and standard deviations per bin, then these correlation coefficients can be obtained afterwards. It is also possible to determine a correlation coefficient during the measurement, over an integration time which is moving with the sampling, and to apply the lack-of-correlation correction directly, in real time [31]. For instance, with a sample averaging time of 16 seconds, satisfactory corrections are obtained with correlation integration times of 300-600 seconds.

An example of the corrections - both for power and velocity binning, and applied afterwards - is given in fig. 6.3. It turns out that power binning gives slightly better results with regard to approximations involved and measurement range resulting.

If averaging time is long enough (under the IEA recommendations this usually is the case) then the correlation coefficient will be close to unity. Nevertheless, it is generally recommended to determine the correlation coefficient during the analysis as a check. Another way of checking is to make bin analysis in the two directions (wind speed and power) for the same data, and to check that resulting power curves coincide.

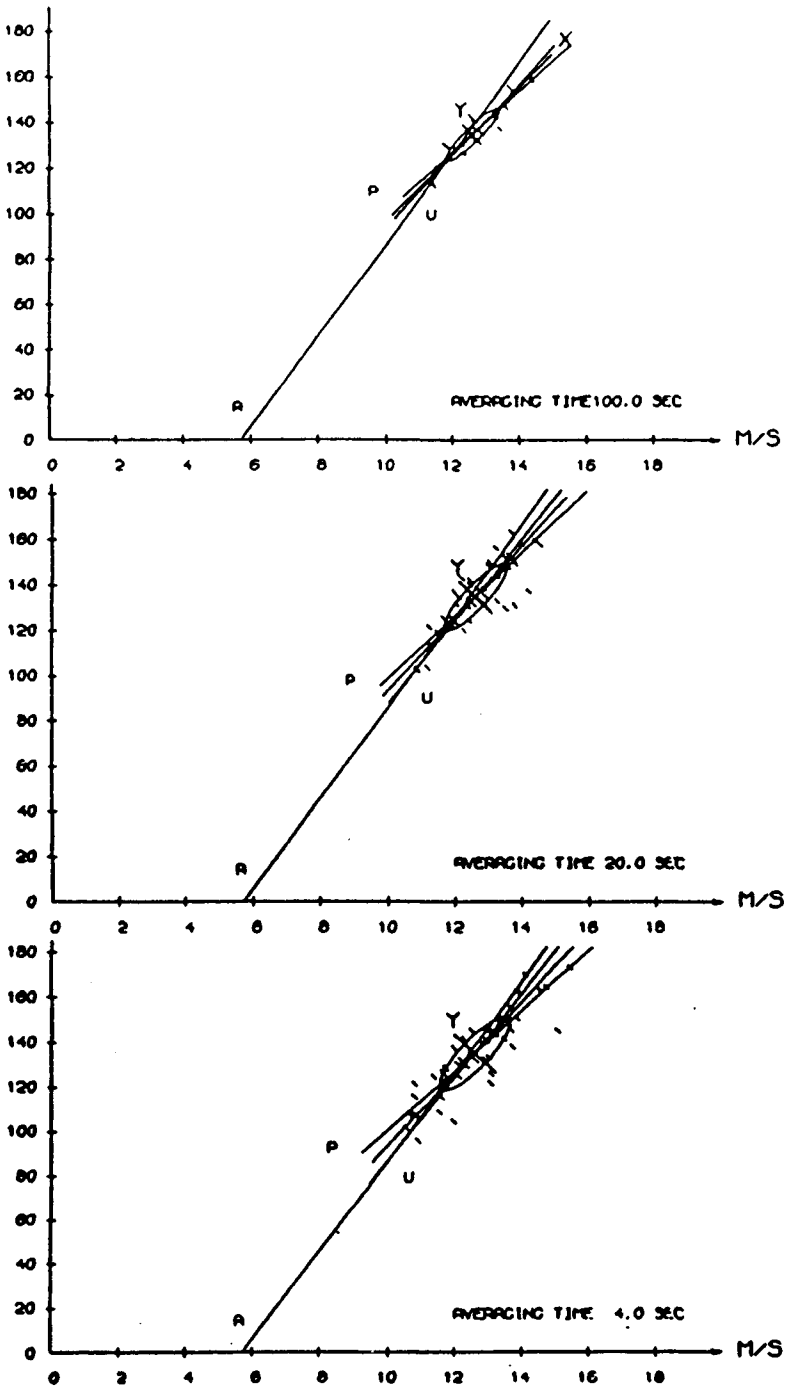


Fig. 6.2.A. Correlation ellipses and regression lines for power versus wind speed, using Gedser windmills data for different averaging times. Good correlation case (wind mast to mill).

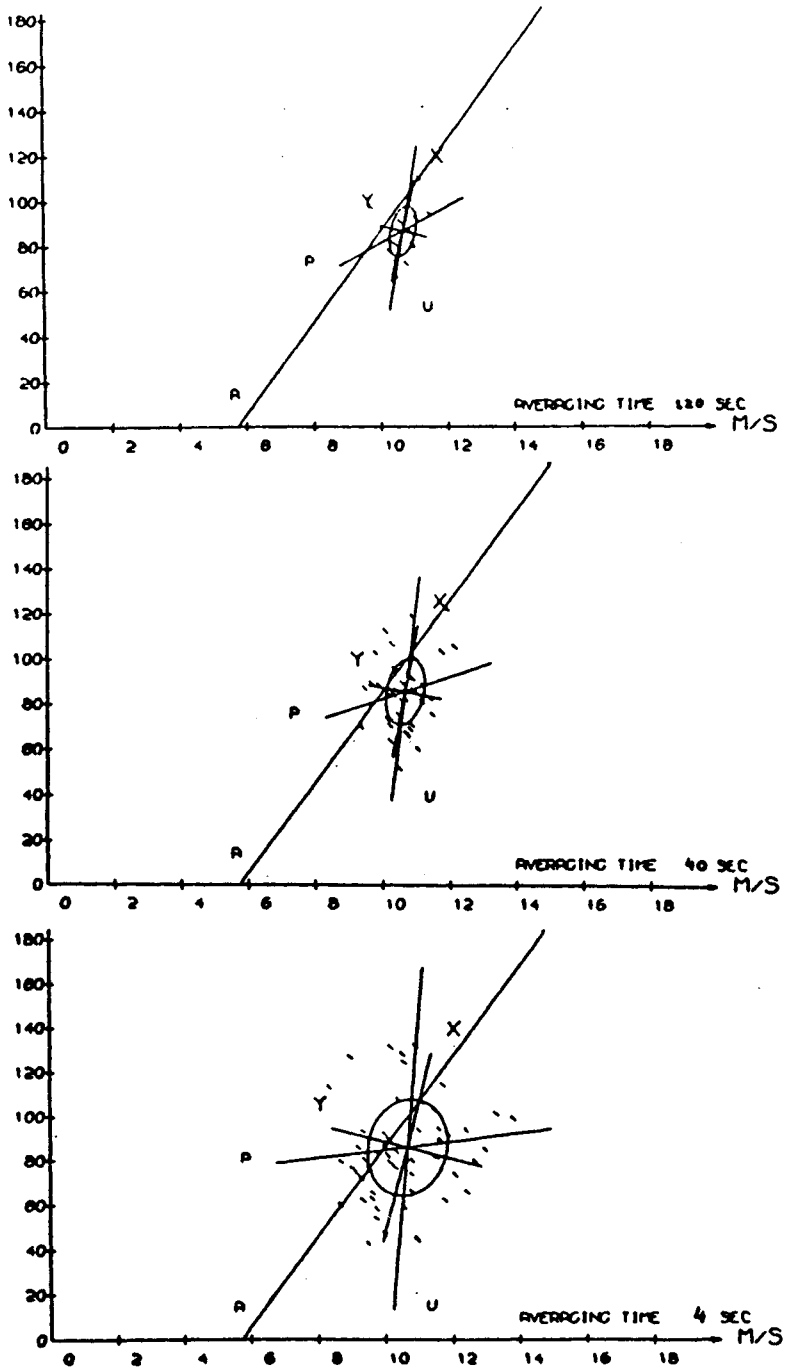


Fig. 7.2.B. Same as 7.2.A. Bad correlation case (wind 50° off mast to mill direction).

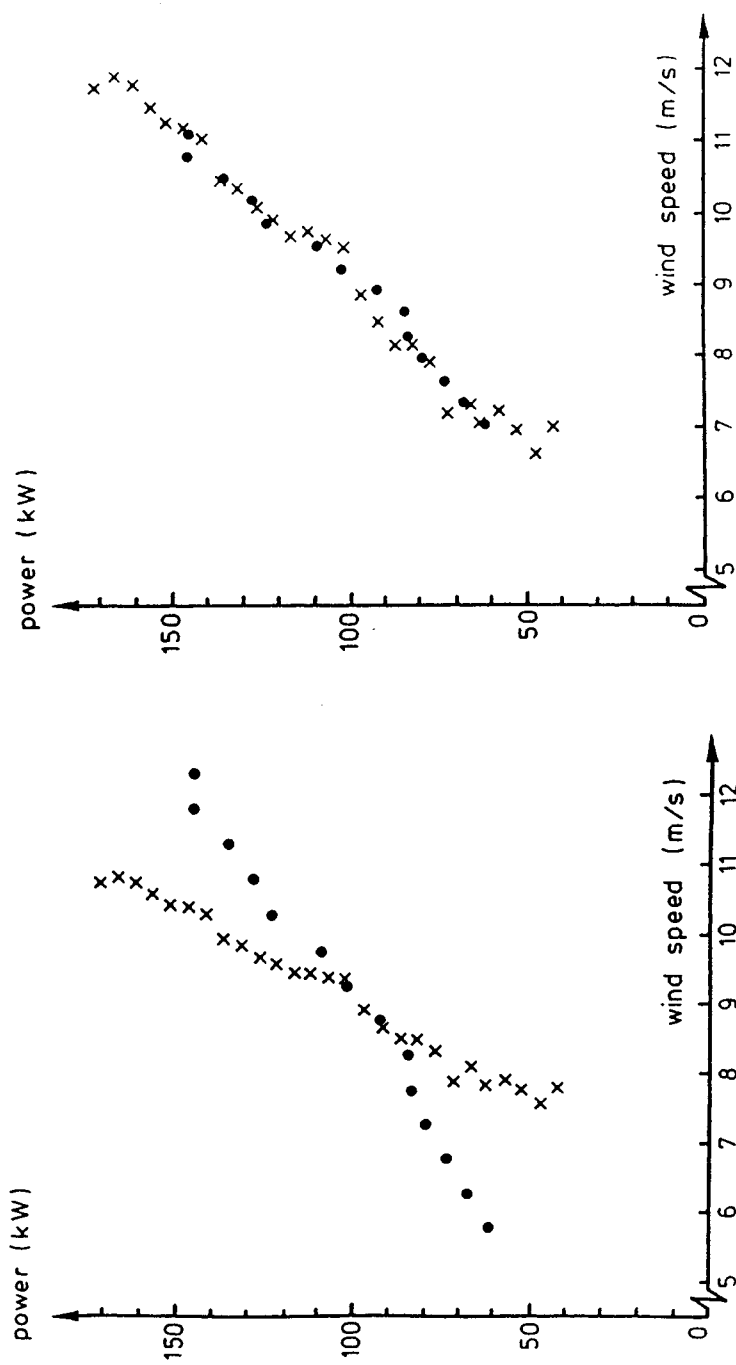


Fig. 7.3. Power curve with poor correlation (4 seconds averaging time), showing wind velocity binning (dots) and power binning (crosses). The right hand figure shows the same data, but correction for lack of correlation.

6.8. Most probable power method

The most common way of analysis is to take the mean value of the data collected in a bin as the best estimate. A more refined way is to analyse the frequency distribution of the data in the bin and to take the most probable (actually most frequent) value as the best estimate. For symmetrical frequency distributions (e.g. normal) this value coincides with the mean. But there are cases where this is not the situation. For instance: if there is some hysteresis in the power versus wind speed, in particular near cut-in [32]. For that situation it was proposed to use the most probable-power method around cut-in in combination with the conventional method of bins at higher wind velocities. Another situation occurs when there actually belong two different values to a particular bin. This situation is found in case of power binning for a power curve going through a maximum, as it may be found for stall controlled machines. It has been pointed out (in connection with the methods of cubic bins, section 6.4) that in such cases the two maxima in frequency may be identified.

6.9. Frequency matching

This is a method quite different from all others and not a variant of the method of bins. To the authors' knowledge it was invented at the Rocky Flats test station (USA). One simply determines the cumulative distribution functions (i.e. the integral of the frequency distribution) for both wind velocity and power. Then one tries to find a mapping of power on velocity in such a way that the two distribution functions become coincident.

The algorithm is very simple:

count the number of samples with wind speeds below a certain level. Then the power belonging to this wind speed is that power below which an equal number of power samples is found [33].

This analysis can only be made if the power curve is a monotonous (ascending) function, which is a certain limitation.

A drawback of this method might be that the simultaneity between power and wind speed is not used in the analysis. It is not known to what extent this loss of information deteriorates the accuracy. Some experimentation indicates good results, free of the lack-of-correlation type of error found in the bin analysis. The method certainly deserves some further study.

6.10. Additional conditioning

In addition to the conditioning of power samples on the observed velocities, as it is done in the method of bins, there have been proposals for extra conditioning on other parameters, usually with the aim to take some special physical conditions into account. A detailed treatment cannot be given here, but it is certainly worthwhile to summarize some significant and important cases.

- Around cut-in hysteresis effects occur. To study them the data may be selected according to belonging to a "start series" (increasing wind, and - depending on the system - increasing rotor speed) or to a "stop series" (the reverse). This has been proposed and tried [34] for water pumping wind mills (with piston pump), which show this hysteresis very strongly. An example is shown in fig. 6.4. Also for electricity producing turbines this development may be of interest.
- In variable speed systems dynamic effects may be important (see chapter 5 and section 6.1). It has been suggested to improve the accuracy in this situation not by the complication of an extra correction, but by the condition that $\frac{d\Omega}{dt}$ is small enough.

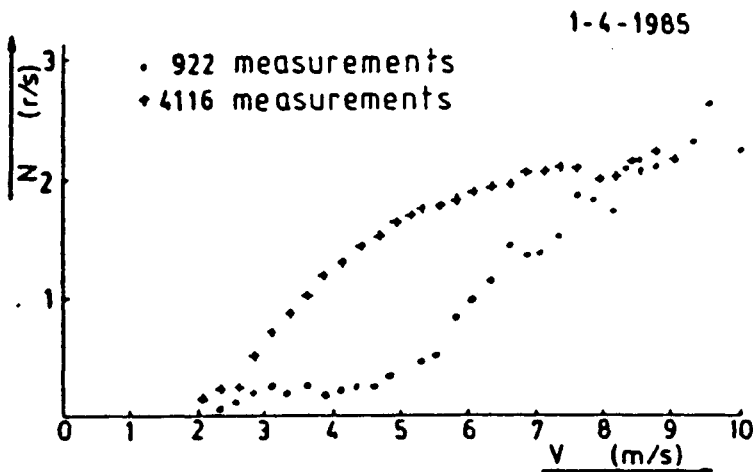


Fig. 6.4. Measurements of hysteresis behaviour of a water pumping windmill
..... start series
+++++ stop series

6.11. Validity and verification

It is our view that a good standard for power curve determination, aimed at the estimation of energy production, will be very close to the IEA recommendations. It will have to be accepted that a proper measurement will take a fairly long time. So what is the use of the alternatives? There are two main objectives to deviate from the IEA:

- measurement of aerodynamic characteristics;
- quick, first look power curves.

The latter are not to be recommended with the present knowledge, since it is not possible to attach good figures on accuracy and reliability. But it is certainly worthwhile to collect experience and to perform further studies with the alternative methods, treated in this chapter. This might lead, for example, to a standard for aerodynamic performance testing.

One study that may be proposed in this connection is a systematic study on some of the alternative methods and their combinations, by an intercomparison, using the same source data. So one might collect some well-defined sets of measurements (with short averaging time) and to use them to obtain power curves including estimates of their accuracies, using different averaging times and different ways of analysis (velocity binning, power binning, regression methods and lack-of-correlation corrections, frequency matching, etc.).

Such an experience, together with experience in the conditioning possibilities mentioned in section 6.10 for which further study is recommended, will deepen the insight and lead to improvements of the power performance standards.

7. ACCURACY OF WIND SPEED MEASUREMENTS

7.1. Introduction

The accuracy of the power production depends strongly on the cup anemometer accuracy as will be discussed in section 7.6. But even worse is the accuracy in efficiency C_p . C_p is usually found by dividing measured power values with u^3 . Therefore the relative error in C_p due to wind speed errors is 3 times the relative wind speed error. The production prediction does depend on Δu in a usually somewhat lower power (1-3) but enough, that the wind speed error is critical. Therefore calibration of the cup anemometer is very critical.

7.2. Normal calibration of cup anemometers

Relative calibration of cup anemometers (relative to a well-known (standard) cup anemometer) can easily be done in the free atmosphere. A series of cups, among them a standard, can be mounted on one boom and be datalogged in parallel for an extended period. A spacing between the cups of a few cup diameters makes sure that the lack-of-correlation problems is limited. But still a fairly long running time is needed for good results. Furthermore, in the end at least the standard cup needs an absolute calibration, which will then be the critical one. Therefore, it is advisable and often faster to rely on absolute measurements in a wind tunnel, which will be described here.

For calibration in a wind tunnel a reliable tunnel type is essential and warrants careful investigations. Both for open tunnels and for circulating (closed) tunnels it may be difficult to obtain a sufficiently homogeneous and accurately known wind speed across the tunnel cross section. In many cases a tedious accurate mapping across the cross section used is needed. The easiest type of tunnel to use is a straight large area tunnel.

In order to have a homogeneous area across the cup anemometer, the tunnel cross section ought to be at least $4 \times$ the diameter of the cup assembly (typically a $0.6 \times 0.6 \text{ m}^2$ tunnel is needed).

Typically the cup anemometer (diameter D) is mounted in the tunnel e.g. $D/4$ under the tunnel centre. The wind speed is measured with a pitot tube mounted $D/4$ above the centre and $2-3D$ upwind of the cup anemometer. Conse-

quently the wind speed homogeneity must be good for a tunnel segment of more than 0.5 m length.

To check the homogeneity, the cup anemometer is replaced by another pitot tube mounted in the same position and on a stand as closely identical as possible to the cup anemometer stand. In this way a possible inhomogeneity in the air flow (that can be caused either by the tunnel or by the instrument set-up) is copied in the test set-up and thus removed from the calibration measurement.

The pitot tube reduces the wind speed measurement into a pressure difference measurement. The manometer used for this pressure measurement must be a precise and well-calibrated instrument. It should be calibrated both before and after the experiment against a precision instrument.

A cup anemometer is a relatively slow instrument and often actually an integrating type, e.g. emitting a pulse train that is counted over a finite time (10-100 sec) to yield not speed but "meters of wind passed". It is therefore advantageous to use an electrical manometer with integration built in.

When going from one wind speed in the tunnel to another one should allow for ample time for the tunnel to stabilize (> 30 sec). The calibration itself should follow a procedure that emphasizes the wind speeds that are most important for the wind energy production (say 5-10 m/s). As the measurement of difference pressure at low wind speeds is very uncertain it is suggested that no measurements under 5 m/s (wind mill cut-in) are allowed in the determination of the calibration curve. A reasonable choice of measurement points could be 5, 6, 7, 8, 9, 10, 12, 16, 20 m/s. A linear regression to a line $u = af+b$, where f is the cup anemometer frequency, fits the measured points. It should be checked that the correlation coefficient $R \geq 0.9990$. Otherwise the anemometer is non-linear or the measurement of too low quality and should be improved.

A non-linear cup anemometer should not be used. It would be dependent on Reynolds number and air density and therefore too inaccurate.

7.3. Calibration changes with time

Several laboratories have observed changes in cup anemometer calibration constants when the instruments are recalibrated after some time. No syste-

matic examination of this subject seems to exist. We have, however, recorded the experience of several people and will on the basis of this attempt to draw some conclusions.

In [34] available information has been gathered on repeated calibrations by ECN both at different times and in different tunnels. About different tunnels see section 7.1. The results of these examinations are that if the calibration results are believed, the derived wind speeds in the range 5-10 m/s of wind speed at a certain anemometer reading can change by 3-5% after use for some years.

The experience at Risø can be summarized as follows [35]. In new cup anemometers the bearings tend to be fairly tight and different. If a running-in period of a few months is allowed, the anemometers will have gone through their changes and a calibration made after running-in will hold for years. This presupposes, however, that the cups are sharp-edged (minimizes dirt sensitivity), that they are of a stable material that does not suffer permanent stress-induced deformations due to the centrifugal forces, and finally that the bearings are well protected against moisture, salt, dust, etc.

7.4. Cup anemometer overspeeding

It is well-known that the cup anemometer used in a turbulent wind (i.e. not in wind tunnels!) gets slightly non-linear (runs too fast). This so-called overspeeding has been treated in [36].

The basic reason for this effect is the following. When the wind speed fluctuates, the cups have to accelerate and decelerate under the influence of the moment induced by the difference between the present wind speed and the wind speed corresponding to the present speed of rotation. This induced moment is non-linear around zero moment. If the cup anemometer is very heavy and therefore reacts slowly to wind speed changes, rather large speed correcting moments must come into play and the non-linearity will therefore induce errors just like discussed in Section 3.2.

The best way to avoid this error is to use small, light weight cup systems. The cup response to wind speed changes is well described by a distance constant L . The response time of the cup is then L/u , i.e. the response is faster if \bar{u} is high. A practical way to evaluate the error has

been given in [37]. It appears that for $L < 2$ the correction can nearly always be neglected. It also follows that for $L < 5$ m - which is the IEA recommendation [13] - the error is below about 1% for heights above 10 m in a terrain with a roughness length of 0.05 m. This actually has been the background for the IEA recommendation on the distance constant. For larger z_0 , however, the error may become larger. Therefore our recommendation is:

- for $L < 2$ m neglect the overspeeding error;
- for $2 \text{ m} < L < 5 \text{ m}$ check for the possibility of an overspeeding error using [36] or [37];
- anemometers with $L > 5 \text{ m}$ are not recommended to be used for power curve measurements.

7.5. Influence on power curve of errors in cup anemometers calibration

If a systematic wind speed error were the only error on the power curve measurement, of course the only influence would be to stretch, compress or shift the power curve along the u-axis. With errors of a few per cent the effect is barely visible.

If we have a u-error that is of the form $u' = Au$, where u' (the corrected wind speed) deviates from u with a constant percentage error at all u-values, most characteristic wind speed values will change by the same percentage. This is so for e.g. cut-in, cut-out and rated wind speeds. The same is the case for the speed at maximum efficiency (i.e. the maximum C_p wind speed).

The maximum efficiency, however, does change with 3x the relative u-change, i.e. by 3% for a 1% u-error.

7.6. Influence on annual productions prediction

An error in the wind speed measurement of course results in an error in the power prediction calculation:

$$\text{annual production} = 8760 \cdot \int_0^{\infty} f(u)P(u)du$$

as $P(u)$ is changed along the u-axis. The resulting error has to be calcu-

lated using a typical wind speed distribution. The result will depend on both the power curve and the wind speed distribution of the site.

As examples we shall look at the prediction of yearly power production for the ECN-machine 25 m HAT (fig. 7.1) and the WM 17S (fig. 3.9). Especially fig. 7.1 shows the change in power curve when assuming a constant relative u-error for all u's. Fig. 7.2 (from [34]) shows the influence of u-errors up to 5% on the prediction for a Rayleigh-distribution with mean wind wind speeds of 5, 6, 7 m/s, respectively.

Fig. 7.3 shows the same calculation for WM 17S.

It is seen that at 6-6.5 m/s average wind speed, a 2% error in velocity for the 25 m HAT means a 7% change in prediction and for WM 17S a 3.5% change. This means that the shape of the power curve is of vital importance and that a calculation of the derived error in the prediction has to be done using the integration formula with distorted power curves for the actual machine. It should be recommended that we agree on a definite wind distribution, e.g. a Rayleigh-distribution with $\bar{u} = 7$ m/s.

The derived error is then only one example and the user of the power curve measurement must re-evaluate the error for his site.

7.7. Recommendations and the need for an intercalibration

It has been found that cup anemometer calibration needs extensive care and that each test station should make sure that their procedure for calibrating is adequate.

The following recommendations can be spelled out at the present time.

- It is to be preferred to use a small, light cup anemometer in order to avoid overspeeding effects caused by turbulence. If the distance constant is longer than 2 m an overspeeding correction should be considered, anemometers with distance constant of more than 5 m are not recommended for power curve measurements.
- The cup system should be sharp-edged to avoid dirt problems. The material should be strong and stiff and should not be easy to deform plastically.
- A 3-month period of running-in should be allowed before calibration. The calibration of at least a few anemometers in a badge should be repeated at least once a year.

- The calibration procedure is important. As many institutions do such calibrations it is advisable to set up an intercomparison (round robin test of cup anemometers) between the normal procedures of the different test stations (see appendix C).
- A measured power curve should always be followed by a prediction of annual power production using measured power curves and corrected power curves together with a 7.0 m/s Rayleigh-distribution yielding the prediction error as a consequence of an error in wind speed.

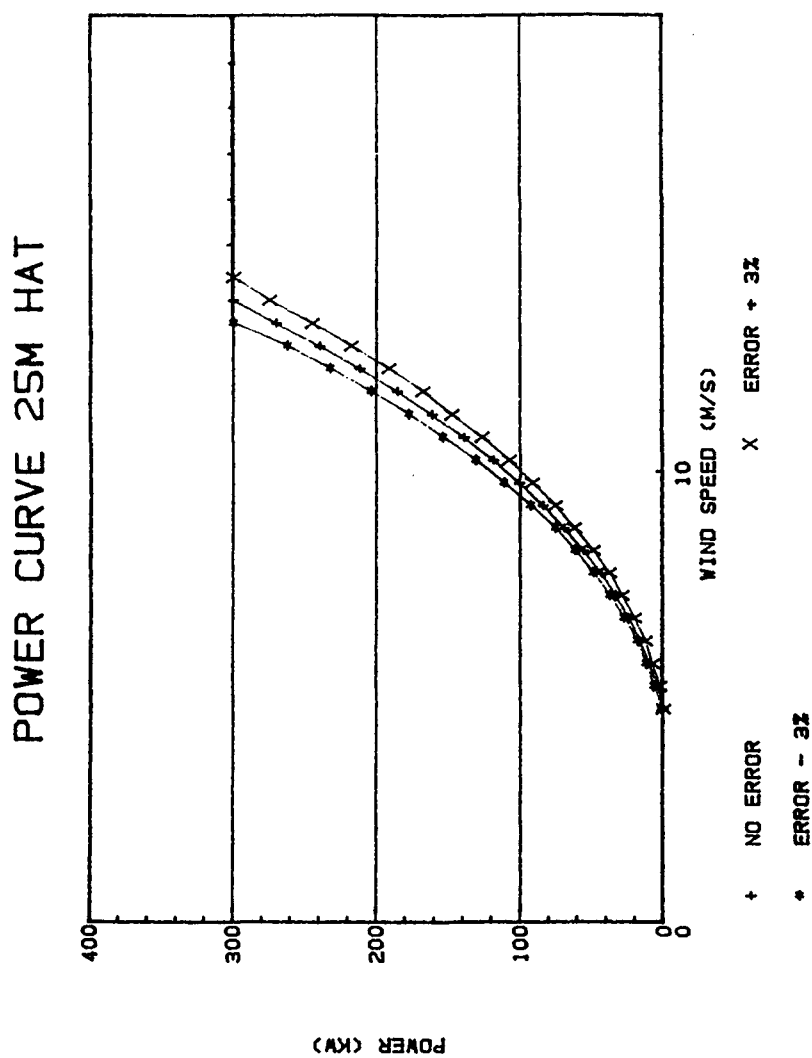


Fig. 7.1. Calculated power curves with -3, 0, +3% error in wind speed.

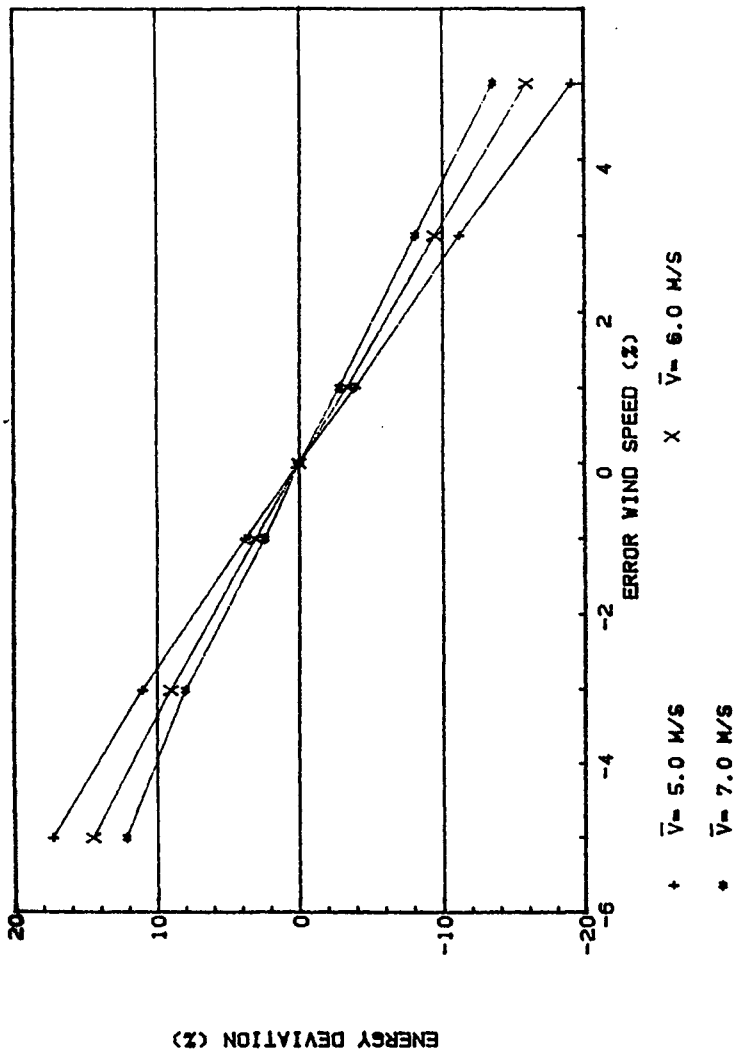


Fig. 7.2. Deviation in annual energy output due to wind speed errors.
Calculated with power curve of fig. 7.1.

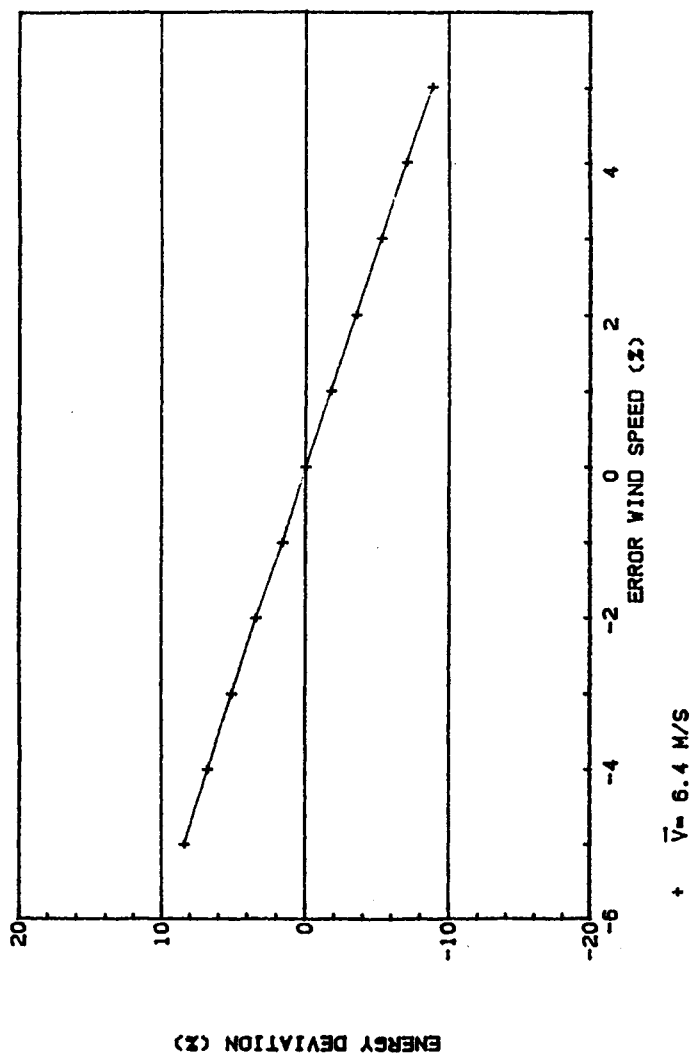


Fig. 7.3. Deviation of annual energy output due to wind speed errors.
Calculated with power curve of fig. 3.9.

8. MACHINE CONDITIONS AND POWER SENSOR ERRORS

8.1. Machine conditions

We have to look at four groups of machine-related errors. Firstly, machines of one specific type could have a scatter of properties. This could e.g. have to do with inaccuracies in blade profiles, blade angles, pitching mechanism, yawing mechanism. Secondly, the machine could be changing properties during the measurement as exemplified by dirty blades, wear in bearings, changes in cut-in control etc. Thirdly, it is not trivial to handle discontinuities as cut-in and change from one generator to the other. Fourthly, climatic parameters other than wind speed influence the power curve.

8.1.1. Deviations from average machine properties

We do not know of attempts to examine differences in behaviour of different machines of the same type. A study of this is very expensive and cannot be done in this context. Therefore no uncertainty can be ascribed to this effect. It is recommended always to note on the power curve, which fabrication number the measurements refer to and to make clear in the test, that other machines of the same type may deviate. For parameters, that may be changed (e.g. blade angle, setting of pitch control mechanisms, yaw misalignment) it is recommended to measure these parameters and state the results on the power curve.

8.1.2. Changes in machine properties during measurements

It is known that power curves change as the machines age. Dirty blades can mean heavy losses of production. The rate of degradation can be very different depending on environmental conditions. We have heard wind farm operators claim that cleaning blades each second week improves average electricity production by 20%. Also here we do not have information that allows us to ascribe an uncertainty.

It is recommended, that each test station look for special problems with dirt at their site. An idea of the problem can be obtained by dividing all measurements of one machine into two groups, first half and second half of the measurements. Calculate the power curve and the annual power produc-

tion expected for one wind speed distribution for both groups and compare the two predictions. It has to be checked, that the two predictions have not been influenced by too different (random?) selections of wind directions, as site inhomogeneities can introduce considerable differences also (chap. 3).

8.1.3. Discontinuities in power curve

Where discontinuities in the power curve exist, like e.g. at cut-in, cut-out, and generator change a special problem is to treat measurement points, where the change of the state of the system has happened at some random time within the averaging time. At e.g. generator change, the same wind speed bin could contain some values with only small generator, some with large generator. These two situations will quite likely give different power averages. With shift of generator within the averaging period some mean value between the two above-mentioned extremes will be the result. If total experiment time is long enough, these 3 situations will be statistically leveled out. The shift situation will however increase the power spread within the bin and thus lengthen the required total measurement time.

The final mean value in such situations, where hysteresis is normally occurring (i.e. the point of switching between two states is different when coming from above than when coming from below), will however depend on the wind regimes that happened to occur during the tests. That may be different from the distribution at the site where an energy production prediction has to be made. This gives an uncertainty. It may be expected to lead to small errors for the common electricity producing machines, but it has been found that very substantial hysteresis errors may arise for water-pumping machines. Methods should be developed to deal with such problems.

The possibility outlined in 8.1.2. of dividing all data into an early and a late group again gives an indication of the seriousness. If the two power curves are very different around the shift-wind-speed you need longer measurement time.

8.1.4. Influence of climate

Climatic parameters other than wind speed can influence the power curve. It has been observed ([17],[18]) and is being further studied at DFVLR/WISA, that rain changes the power curve very considerably (bad power curve with wet blades). The effect is thought to be due to changes in the aerodynamic properties of the airfoil by a water film. Even stronger effects occur with iced blades. It is recommended that data during rain are not included. Atmospheric stability could have an influence, but has not been studied. With stable atmosphere a strong stratification can take place, meaning that almost any windprofile can be found. In such situations measurements would be very dubious. It is no easy matter to treat this problem, so at the moment no recommendations can be given. Icing situations should of course also be excluded from the measurement (blades can change quite a bit, cup anemometers could be partly frozen, thereby changing calibration).

8.2. Watt-meter error

The power meter ought to be a 3-phase meter, as it is quite likely that either the grid or the windmill generator are not symmetric in the 3 phases. If a 3-phase meter is used its error is usually given reliably by the manufacturer, and is quite small (power measurement errors do not multiply as the velocity error of chap. 7).

It should be noted, however, that power meter accuracies often refer to percentage of the full range. If such an accurate meter, installed at a test station, is used for a wind turbine of rated power far below the full power of the meter, highly inaccurate measurements may result. Such situations should be avoided by all means.

When calculating the error propagation into a yearly energy production prediction, the relative error may be higher than the apparent Wattmeter error, because the relative error of the instrument at the actual power output will be decisive rather than the nominal % of full range.

8.3. Reproducibility

In several instances we have recommended to look at subsets of power curve data. In fig. 8.1 an example of this is shown. For the WM17S machine, which was also used in chapter 3, the full drawn curve is the final power curve for the full data set (fig. 3.9). The points are for 3 separate power curve runs out of a total of 20 runs. These shorter runs usually do not cover the complete wind speed range needed. The measured points have therefore been supplemented with points from the final power curve. The separate runs do, however, show deviations in the range, where it matters, i.e. at the most probable wind speeds. Yearly power predictions from each run have been evaluated as follows:

Table 8.1. Subsets of power curve data, WM17S, yearly production predictions (class 1, 24 m hub height).

run	averaging time (sec)	wind direction	prediction (kWh/hr)
WM17S/850906	600	200°	189.000
/850904	600	270°	192.800
/850705	600	320°	187.400
/850705/30	30		188.500
WM17S/final	600		187.400

data: courtesy of T.F. Petersen [38].

One example is of course not enough for making final statements, as many things could play a role in creating deviations (terrain and wind direction (chap. 3), changes in machines (chap. 8), rain or dirt (chap. 8), climatic effects (chap. 2+8) etc.. It does, however, show a remarkable reproducibility considering the large possible uncertainties we have pointed out. It also shows a useful way of getting an idea of the specific sources of uncertainty by each test station.

We do recommend in general, that test stations during a wind turbine test do add to the data evaluation as a routine, that each run is finished with a power curve evaluation and drawing. Further that the prediction calculation is done for each run, as the yearly prediction is convenient for keeping track of possible troubles, as it represent one number rather than a curve, whose uncertainty is hard to interpret.

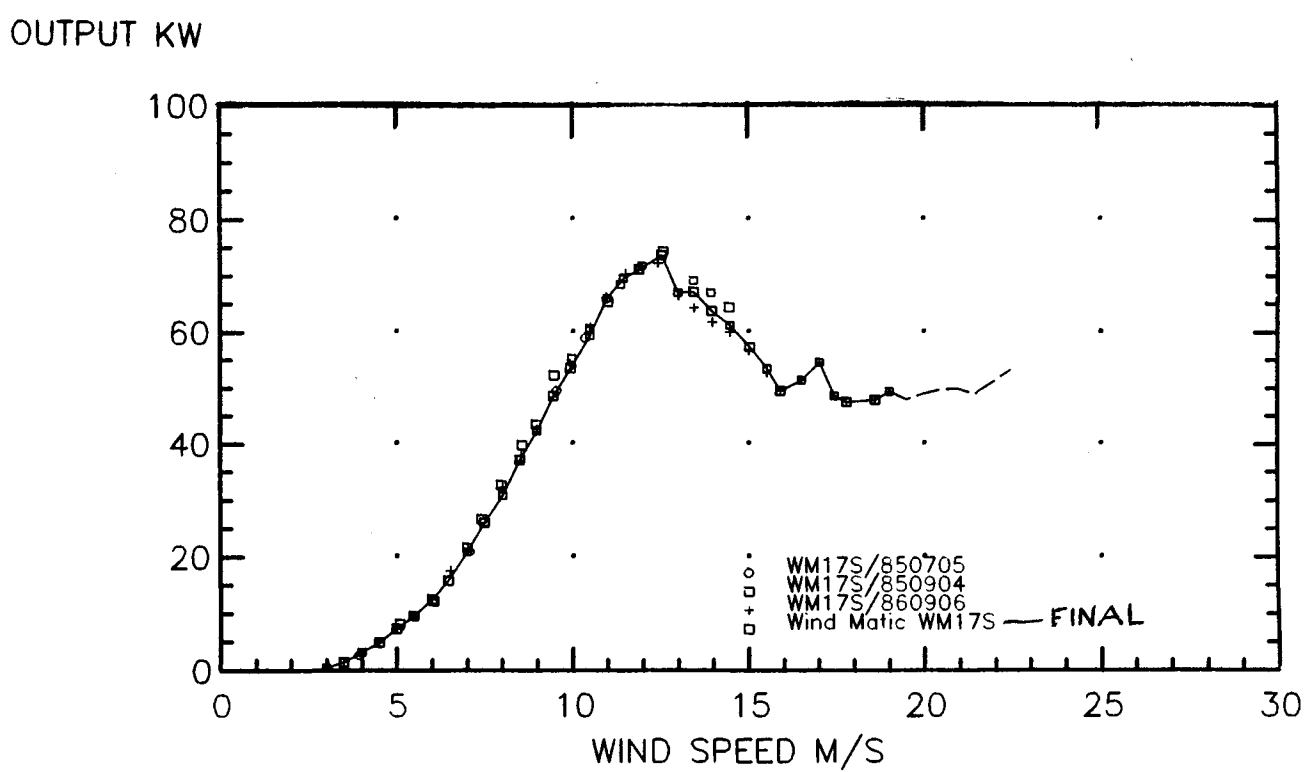
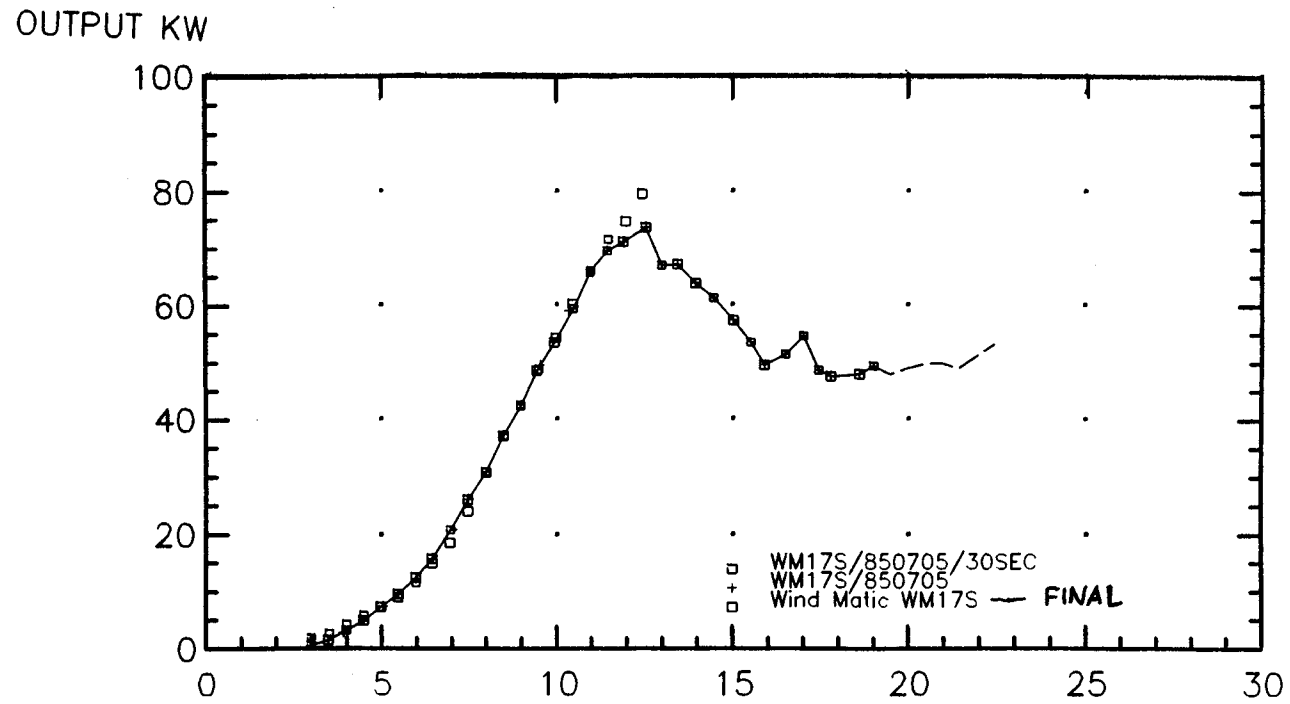


Fig. 8.1. Power curves of the same machine measured at different times.

9. CONCLUSION AND RECOMMENDATIONS

The philosophy of this report is to look at power curve errors as 3 groups:

- 1) machine related and power sensor errors,
- 2) wind speed measurement and
- 3) representativity of the wind speed (see chap. 2).

9.1. Recommendations on machine related errors

It is recommended to note on a measured power curve the fabrication number of the machine to indicate that other machines of the type may differ. Variable parameters should be measured and noted on the curve.

In the future an examination of scatter in machine properties would be useful.

It is recommended to avoid special climatic conditions like rain, icing or stable atmosphere. Keep the blades clean, if your site has problems with dirt. Check, that the machine does not change during the measurement. This can be done by subdividing the data into two subsets and doing power predictions on each.

At discontinuities in the power curve be careful to measure sufficiently long time to reduce hysteresis errors. Avoid stable wind profiles and other extreme conditions.

Ascertain that the power meter has an appropriate ($<3\%$) accuracy over the power range of the machine. Preferably use a 3-phase wattmeter of good quality. Otherwise an uncertainty must be evaluated for the possible electrical asymmetry between the 3 phases.

9.2. Recommendations on cup anemometer calibration and errors

In chapter 7.7. a series of recommendations pertaining to the cup anemometer was given. They cover cup-anemometer construction, running-in and calibration. Furthermore the anemometers should be carefully calibrated and an intercalibration between test stations is recommended. Finally, it is recommended, that the power curve error should be stated

as an uncertainty in the yearly power production prediction using a 7 m/s Raleigh distribution.

It is finally recommended to sharpen the IEA-recommendation on cup anemometer accuracy to 2% instead of 5%, as the multiplier for changing this error into an energy production prediction error is large (2-4).

9.3. Representativity of wind measurement

This is by far the most difficult part and the biggest source of error. The terrain effects discussed in Chapter 3.1. could give rise to considerable inaccuracies, if only the IEA recommendations are followed.

These only exclude $\pm 45^\circ$ around the direction, where the mast is right behind the turbine. Otherwise at present IEA assumes the terrain to be homogeneous, which is not normally the case.

It is recommended that the test stations examine their terrain with the evaluation of the velocity uncertainty in mind.

We are not in a position to recommend any one of the methods discussed (wind tunnel modelling, field measurements or computer modelling) over the other, as their value has not been validated sufficiently.

It is recommended, though, that dubious wind directions are reviewed critically and excluded, if it cannot be shown, that they are alright. The IEA-recommendation on direction should be changed to a more restrictive one accordingly.

An extended use of the comparisons between power curves and yearly predictions evaluated for each single run (sect. 8.3) is also recommended. When used over a period of time, keeping track of the average wind direction for each run, this will give indications of dubious directions.

It is recommended that the IEA-recommendation of cup anemometer height accuracy is sharpened to $\pm 5\%$ of hub height.

On turbulence/non-linearity effects it is recommended not to use the correction on power curves for power prediction purposes, but to state the level of turbulence during the measurements. It should be stated in the test reports, that turbulence was not corrected for. It is left for the power curve user to do his own correction, if his site has different tur-

bulence characteristics than the test station site.

For aerodynamic power curves it is recommended to use the method of chapter 3.2, taking into account that power curves are not u^3 -curves as is normally assumed where using the $3(\sigma/u)^2$ -correction. Likewise $\overline{u^3}$ -binning to correct for turbulence is not to recommend.

It is recommended to use RC-filtering of power and wind speed, preferably at an early stage in order to avoid aliasing.

On lack-of-correlation problems, that may introduce power curve bias or scatter, a set of requirements on averaging time is given in section 5.4.4. For power prediction purposes it is recommended that the IEA-recommendations on averaging time (10 mins), on experiment time (3000×10 min. periods) and on the distribution in wind speeds (i.e. the number of samples per bin) is adhered to. Under these conditions the spread of the data in the bins is expected to be small with respect to the other errors. We recommend, however, to check this by computing the standard deviations of the bin values and the resulting error in power prediction. The table of results should also contain the number of points per bin and the standard deviation per bin.

For variable speed machines, though, it is recommended to consider, whether the IEA averaging time allows you to disregard a correction for response time during the measurements (see sect. 5.3.2.3.).

There may be possibilities for faster measurements, in particular by choosing shorter averaging times than 10 minutes. Such possibilities, however, need further study along the lines pointed out in chapter 5.

9.4. Further work

It is clear from this report that many details are still unclear, e.g. the site specific problems. Also comparisons with, and assessment of other existing standards for power performance measurements (in particular of the AWEA, USA [39] and the CSA, Canada [40]) still have to be made.

In general we recommend further work along the following main lines:

- investigation of the items, which have been mentioned in this report as requiring further study;
- setting-up a comprehensive set of recommendations in the form of a draft for a European power performance measurement standard.

9.5. General conclusion

A simple overall outline of the relative importance of various error sources could look as follows.

group	source	basic error	prediction error
machine and power sensor	machine machine/climatic power sensor	should be avoided - < 2%	- - < 2%
wind sensor	cup anemometer	< 2%	< 8%
representativity	terrain (mean)	< 10%	< 40%
	turbulence/non-linearity	< 5%	< 20%
	turbulence/statistical		< 10%

A recent paper by Frand sen and Hausfeld [41] has discussed many of the problems treated here. They have as we focussed on the terrain effect (representativity) as the major source of errors.

The numbers in the above table represent worst cases and should not be used as uncertainties. But they do show the relative importance of work in the different areas, when evaluating/avoiding the respective error source.

Clearly the terrain warrants careful work. We do believe that it is possible to make acceptable measurements if sufficient care is taken.

Finally, it is recommended as the most important recommendation: always state the uncertainty- and also its progression into power prediction calculations.

REFERENCES

- [1] Progress Report No. 1 on "Power Curve Computation and Accuracy of Power Curve Measurements", Risø, The test station for wind-mills, December 1985.
- [2] R.E. Akins, Wind Characteristics for Field Testing of Wind Energy Conversion Systems, SAND-78-1563 (1979).
- [3] E.L. Petersen (Risø National Laboratory), private communication (1986).
- [4] P.E.J. Vermeulen, A wind tunnel study of the flow field over the SWECS test site at ECN Petten, Report TNO-82-014908 (November 1982).
- [5] J.W.M. Dekker, Bruikbare windrichtingen voor efficiëntiemetingen aan de 25 m HAWT, Internal ECN memorandum (Dec. 1979).
- [6] P.E.J. Vermeulen, J.W.M. Dekker, Wind tunnel and full-scale measurements of the wind field over low-relief topography at ECN Petten, Report TNO-84-02607 (March 1984).
- [7] H.P. Irwin, M.A. Lodge, Wind Speed Distribution over a 1:500 Scale Model of The Atlantic Wind Test Site, North Cape, Prince Edward Island, Report AWTS (March 1980).
- [8] E.L. Petersen, I. Troen, S. Frandsen, K. Hedegaard, Windatlas for Denmark, Report Risø-R-428 (January 1981).
- [9] P.E.J. Vermeulen, H. Hoogeveen, J.A. Leene, Energieopbrengsten van windturbines - een Handboek voor berekeningen, MT-TNO Apeldoorn and CvE Delft, voorlopige versie (Oktober 1983).
- [10] P. Lundsager, S. Frandsen, C.J. Christensen, Analysis of Data from the Gedser Wind Turbine 1977-1979, Report Risø-M2242 (August 1980).
- [11] H.T. Mengelkamp, Comments on the measurement of wind turbine performance curves, Paper at 4th International Meeting of Test Stations for SWECS, Lannion (May 1984).
- [12] T.F. Petersen, private communication (1986).
- [13] S. Frandsen et al. (editors), Expert group study on Recommended practices for wind turbine testing and evaluation, 1. Power Performance Testing, IEA, 1st edition 1982.
- [14] J.P. Molly, communication at IMTS-meeting AWTS Canada (August 1985).

- [15] J. Wieringa, P.J. Rijkoort, Windklimaat voor Nederland, Staats-uitgeverij Den Haag (1983).
- [16] J.P. Molly, private communication, Schnittlingen (May 1986).
- [17] Howden staff, private communication, N.E.L. (May 1986).
- [18] S. Frandsen, C.J. Christensen, On wind turbine power measurements, Proceedings Third International Symposium on Wind Energy Systems, BHRA, p. 207 (Aug. 1980).
- [19] L. Kristensen, S. Frandsen, Model for power spectra of the blade of a wind turbine measured from the moving frame of reference, J. Wind Eng. & Industr. Aerodyn. 10, 249 (1982).
- [20] J.B. Dragt, Load fluctuations and response of rotor systems in turbulent wind fields, Proc. Conf. Wind Power '85, SERI/CP-217-2902, p. 67 (Aug. 1985). Extended version: report ECN-172 (Oct. 1985).
- [21] A.J.M. van Wijk, W.C. Turkenburg, Windturbines als vermogensbron, Report NSS-85-16, Rijksuniversiteit Utrecht (June 1985).
- [22] J.S. Bendat, A.G. Piersol, Random Data: Analysis Measurements Procedures, Wiley-Interscience (1971).
- [23] N. Jenkins, private communication (1986).
- [24] D. Infield, Accuracy of Power Curve Measurements, Part 2 of a RAL/ERG report for CEC-DGXVII, presented at Schnittlingen IMTS-meeting (Sept. 1986).
- [25] T.E. Hausfeld, High Performance Airfoil Final Test Results, Proc. Conf. Wind Power '85, SERI/CP-217-2902, p. 76 (Aug. 1985).
- [26] J.B. Dragt, On the systematic errors in the measurement of the aerodynamic performance of a WECS by the method of bins, Report ECN-141 (Nov. 1983).
- [27] Th. van Holten, J.L. Kooman, Meting van de C_p - λ kromme van wind-turbines in de buitenlucht, Memorandum M-427 Technische Hogeschool Delft (Sept. 1982).
- [28] G. Stacey, P.J. Musgrove, The performance of the Rutherford 6 meter diameter VAWT, including the effects of various timing techniques and averaging periods, Wind Energy Conversion 1984, Proc. 6th BWEA Wind Energy Conf., Cambridge University Press (March 1984).
- [29] J.W.M. Dekker, C.M. de Groot, Bepaling van vermogens- en axiaal-krachtcoëfficiënten van de 25 m HAT, ECN, Petten.
Restricted distribution report ECN-85-151 (Sept. 1985).

- [30] H. Cramér, Mathematical Methods of Statistics, Princeton University Press.
- [31] J.W.M. Dekker, C.M. de Groot, Subroutine BING02 in PLTDCS, Unpublished internal note, ECN (Febr. 1984).
- [32] M.A. Borja, R.E. Borja, P.A. Parkman, A proposed method for processing data on WECS testing, Proc. Conf. Wind Power '85, SERI/CP-217-2903, p. 333 (Aug. 1985).
- [33] Private communications by A.C. Hansen and R. Richards.
- [34] A.P.W.M. Curvers, J.J. Schuurman, unpublished ECN memorandums (1986).
- [35] F. Rasmussen, private communication (1986).
- [36] N.E. Busch, L. Kristensen, Cup Anemometer Overspeeding, J. Appl. Meteorology, 15 (No. 12), 1328 (Dec. 1976); also in: N.E. Busch et al., Meteorological Field Instrumentation, Report Risø-R-400 (Jan. 1979).
- [37] S. Frandsen (editor), Summary report from the IEA expert meeting on Recommended Practices for Wind Turbine Performance Testing, Risø contract report (Feb. 1981).
- [38] T.F. Petersen, private communication (1986).
- [39] American Wind Energy Association, Standard performance testing of wind energy conversion systems, AWEA 1.1-1985.
- [40] Canadian Standards Association Preliminary Standard F417-M1986 Wind Energy Conversion Systems - Performance, CSA (March 1986).
- [41] S. Frandsen, T. Hansfeld, The application of uncertainty theory to power performance measurements, Paper presented at Wind Energy Expo '86, Cambridge MA (Sept. 1986).

ANNEX A

Site Descriptions

To support in particular the terrain effect discussion in chapter 3, in this chapter you will find maps and photographs from the test stations as follows:

ECN, Petten, Holland

Risø, Denmark

NEL, Glasgow, UK

RAL, Oxford, UK

VUB, Belgium (Bruxelles + Zeebrugge)

DFVLR, Schnittlingen, Germany

CWD, Holland (Eindhoven, Almere, Vriesenveen)

AWTS, PEI, Canada

Chalmers, Göteborg, Sweden

The photographs requested from the test stations were: 8 pictures from the main test pad around the horizon to form a panoramic view of the surroundings. It should be self-explanatory, which pictures represent that idea.



Fig. A.1.1 ECN, Petten, 1:25000 map.

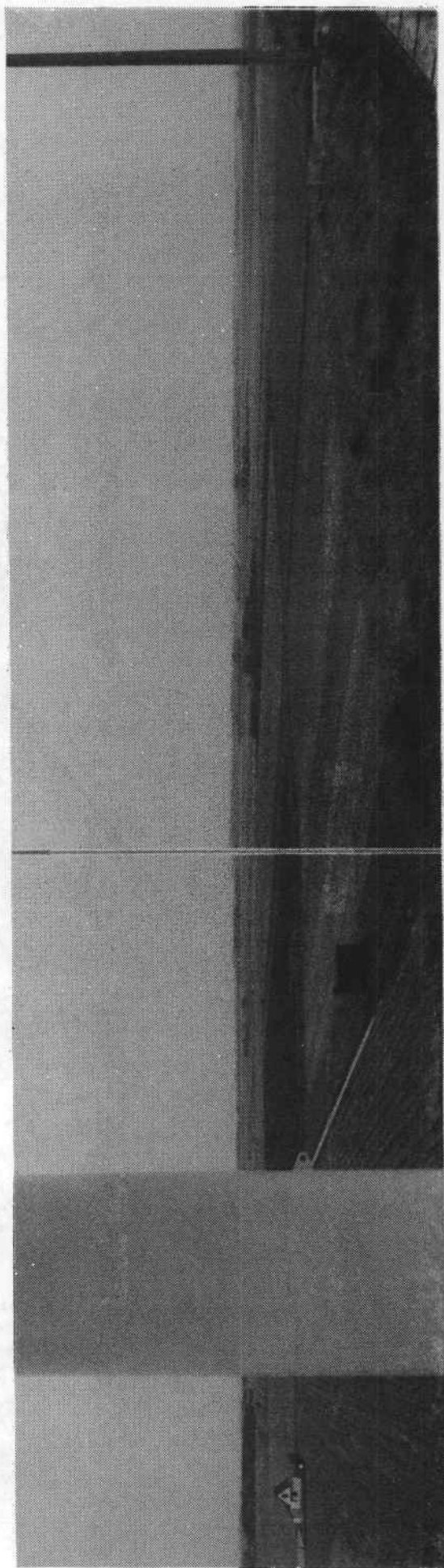
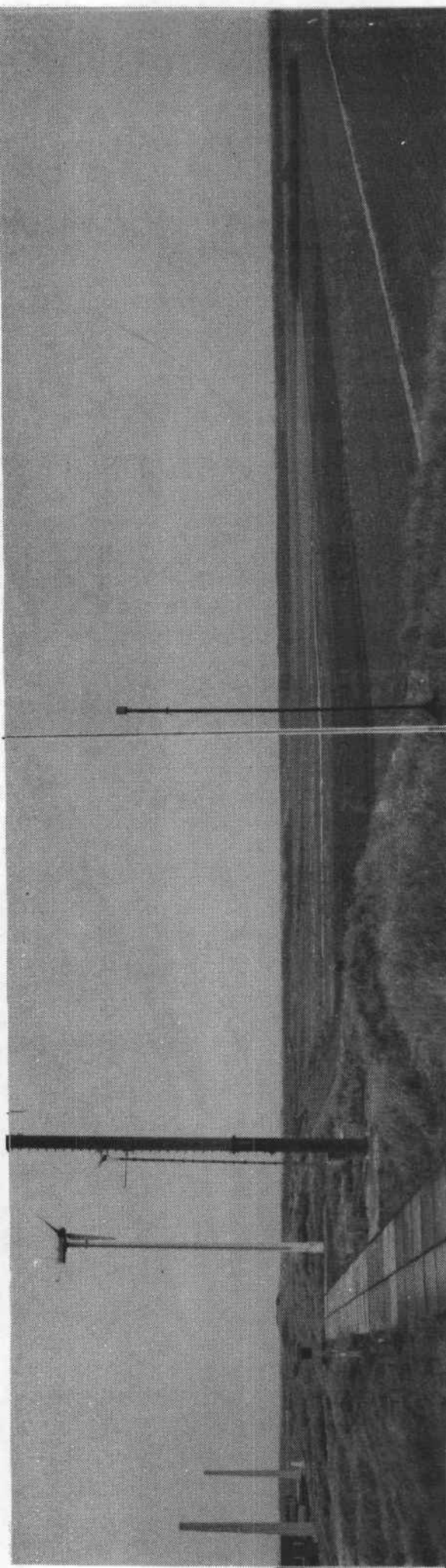


Fig. A.1.2 ECN, panoramic view, NE over E.

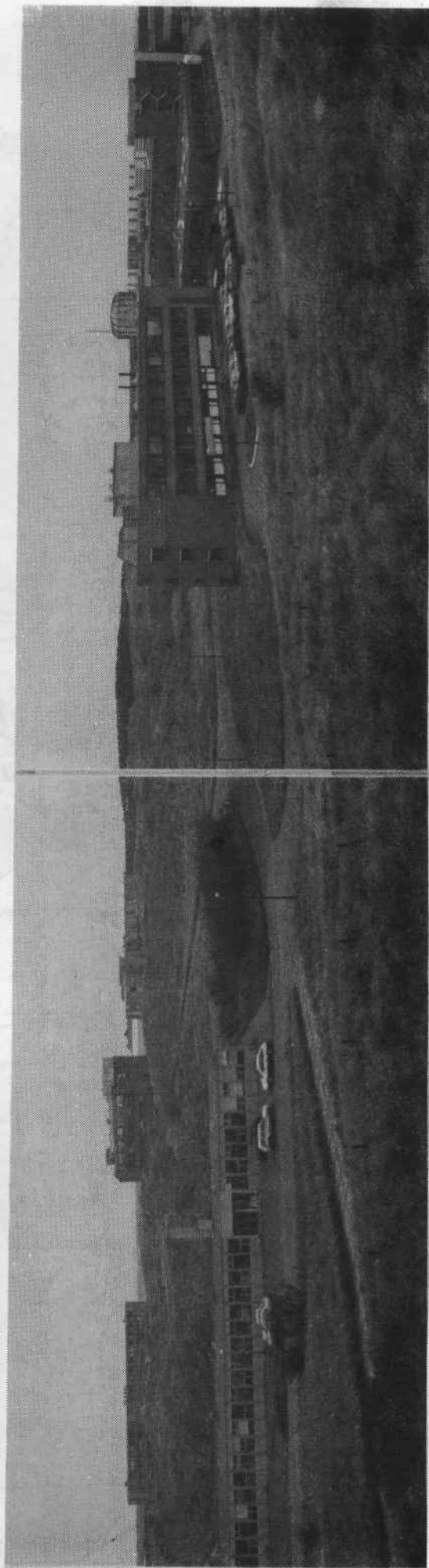
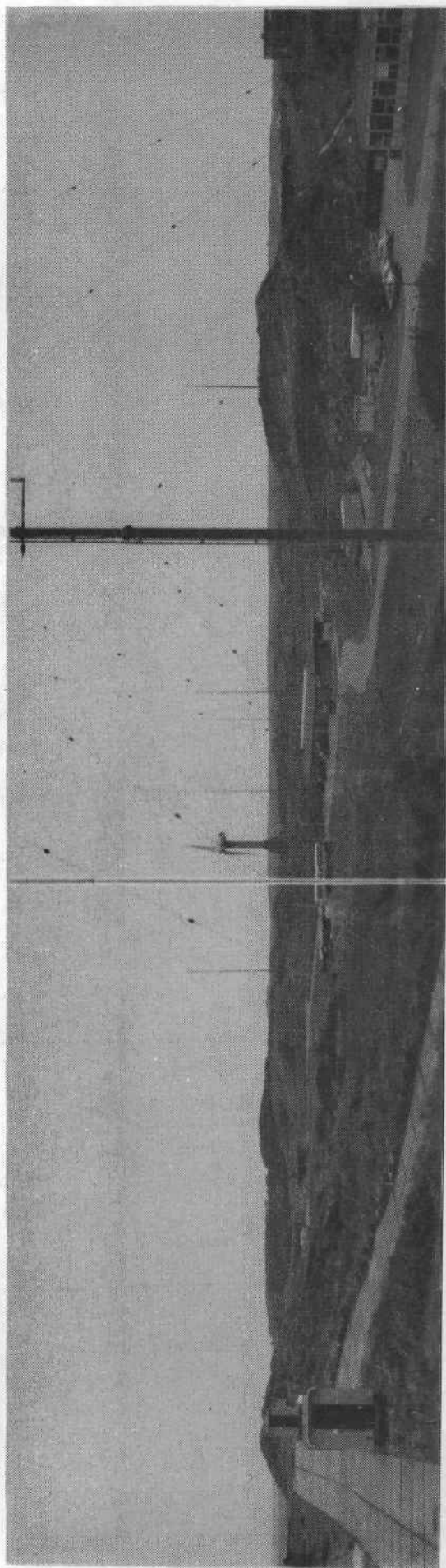


Fig. A.1.1.3 ECN, panoramic view, SW over W

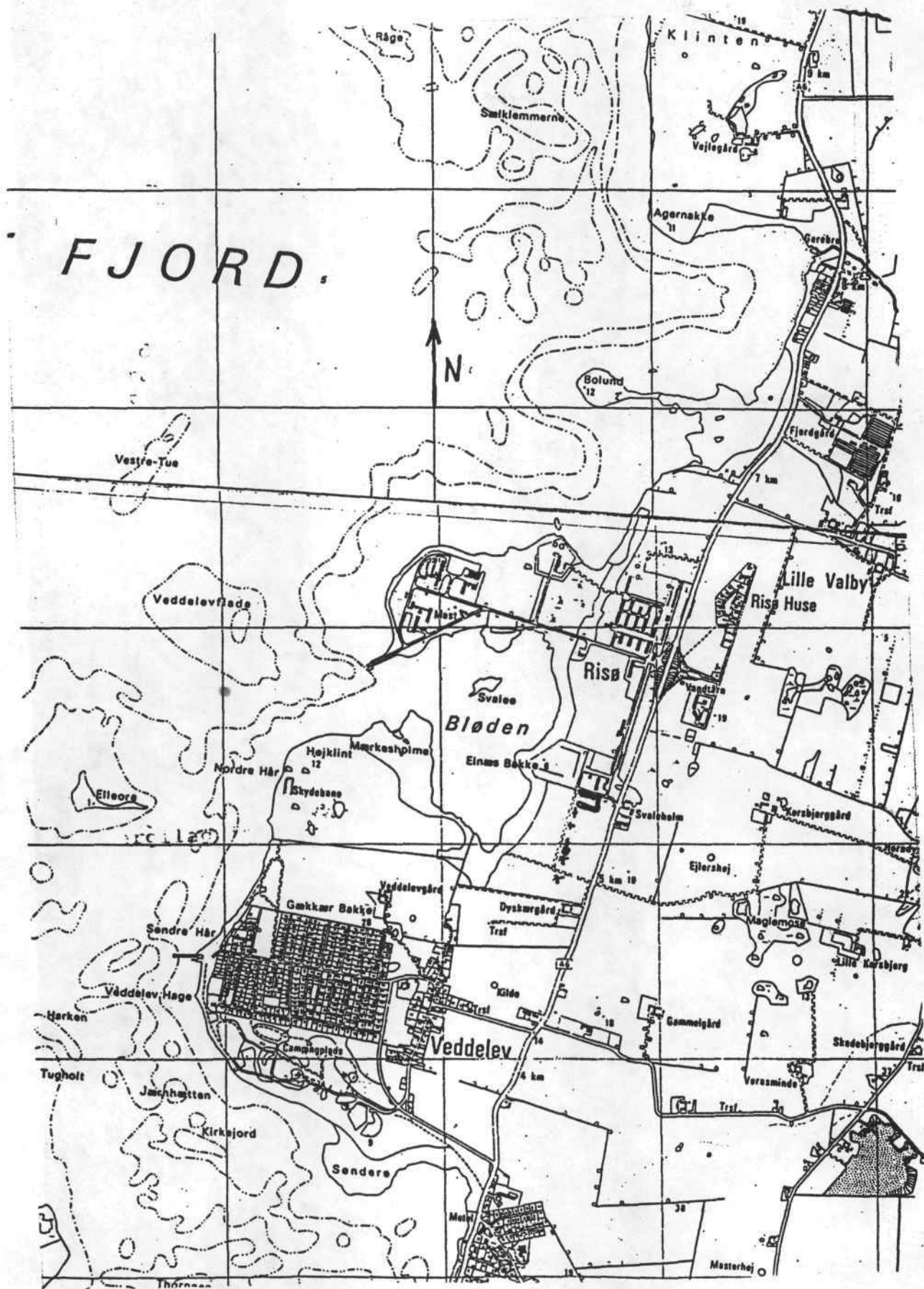


Fig. A.2.1 RISØE, 1:25.000 map

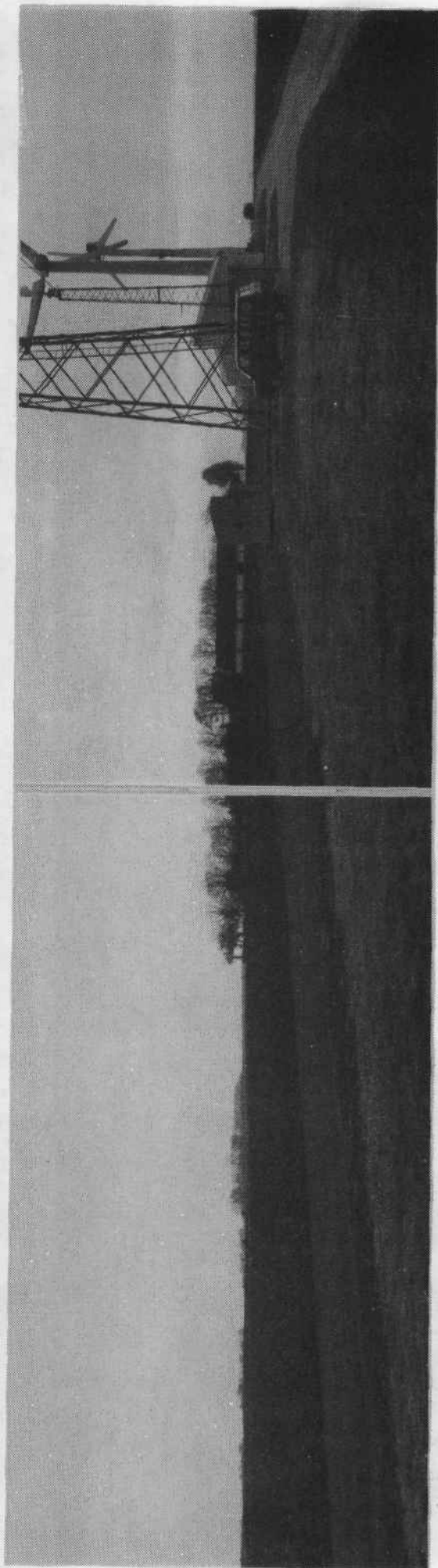
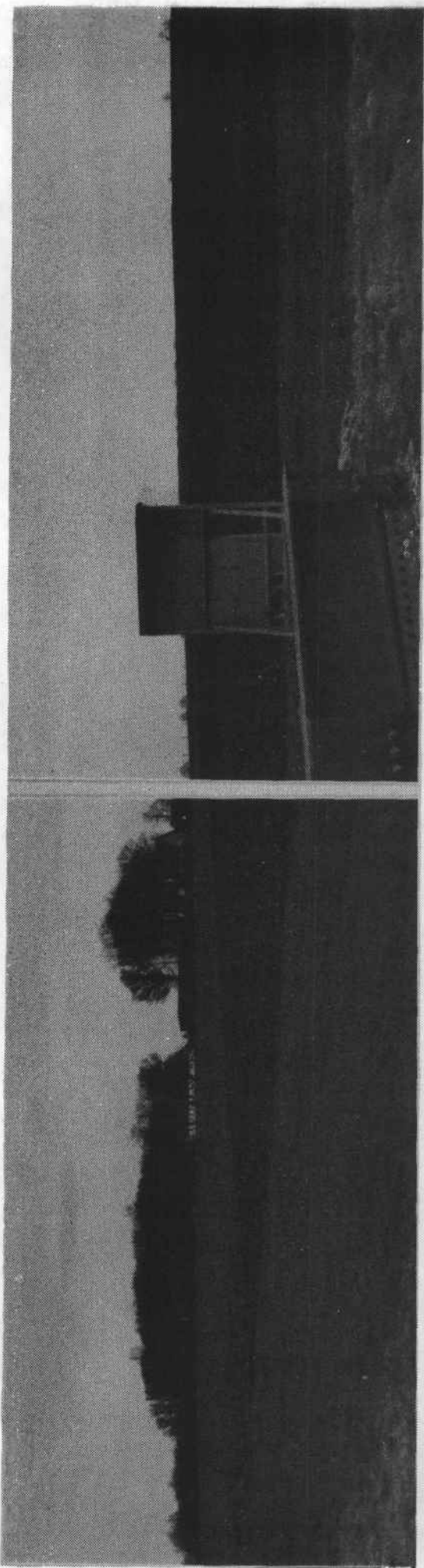


Fig. A.2.2 RISOE, panoramic view, NE over E.

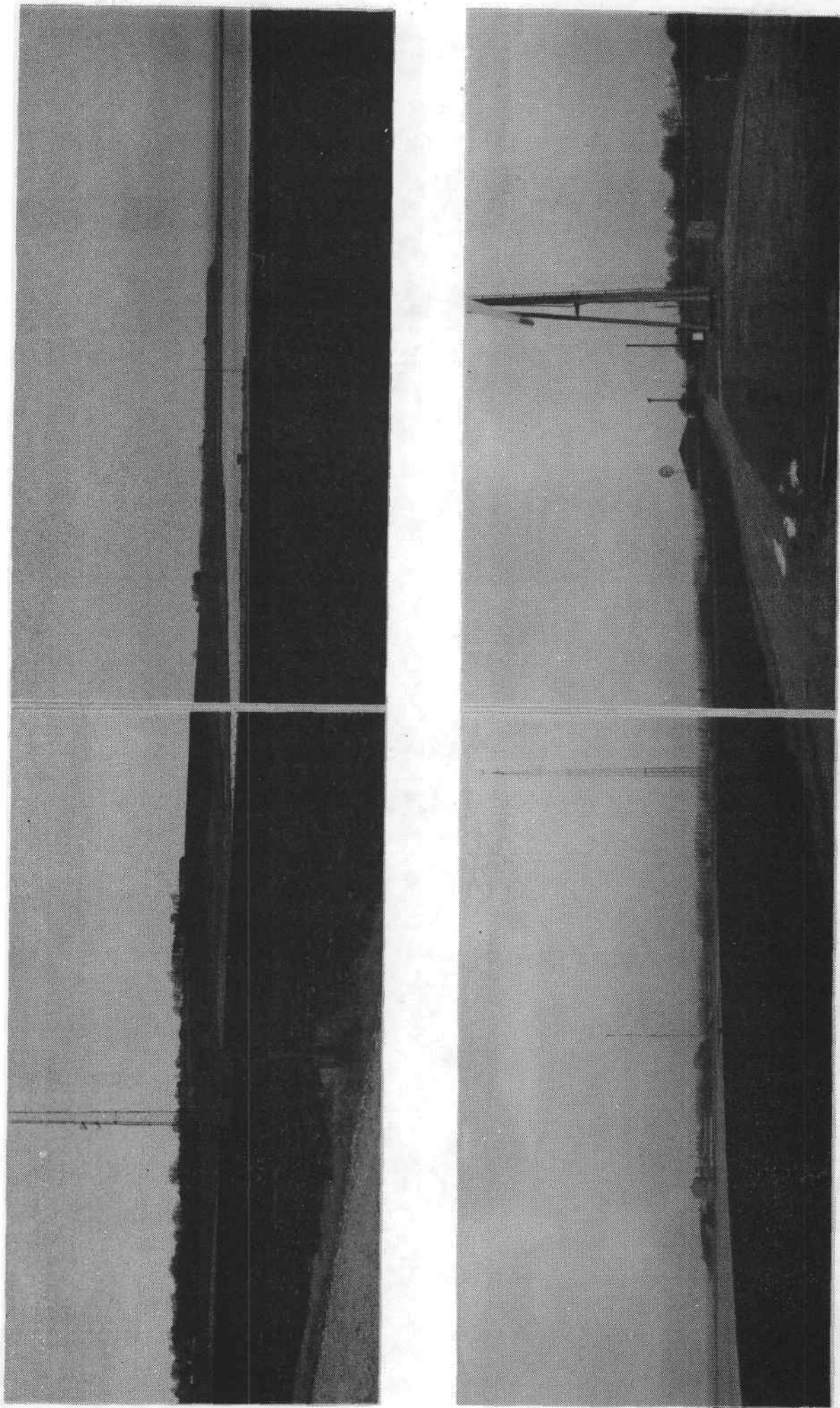


Fig. A.2.3 RISOE, SW over W

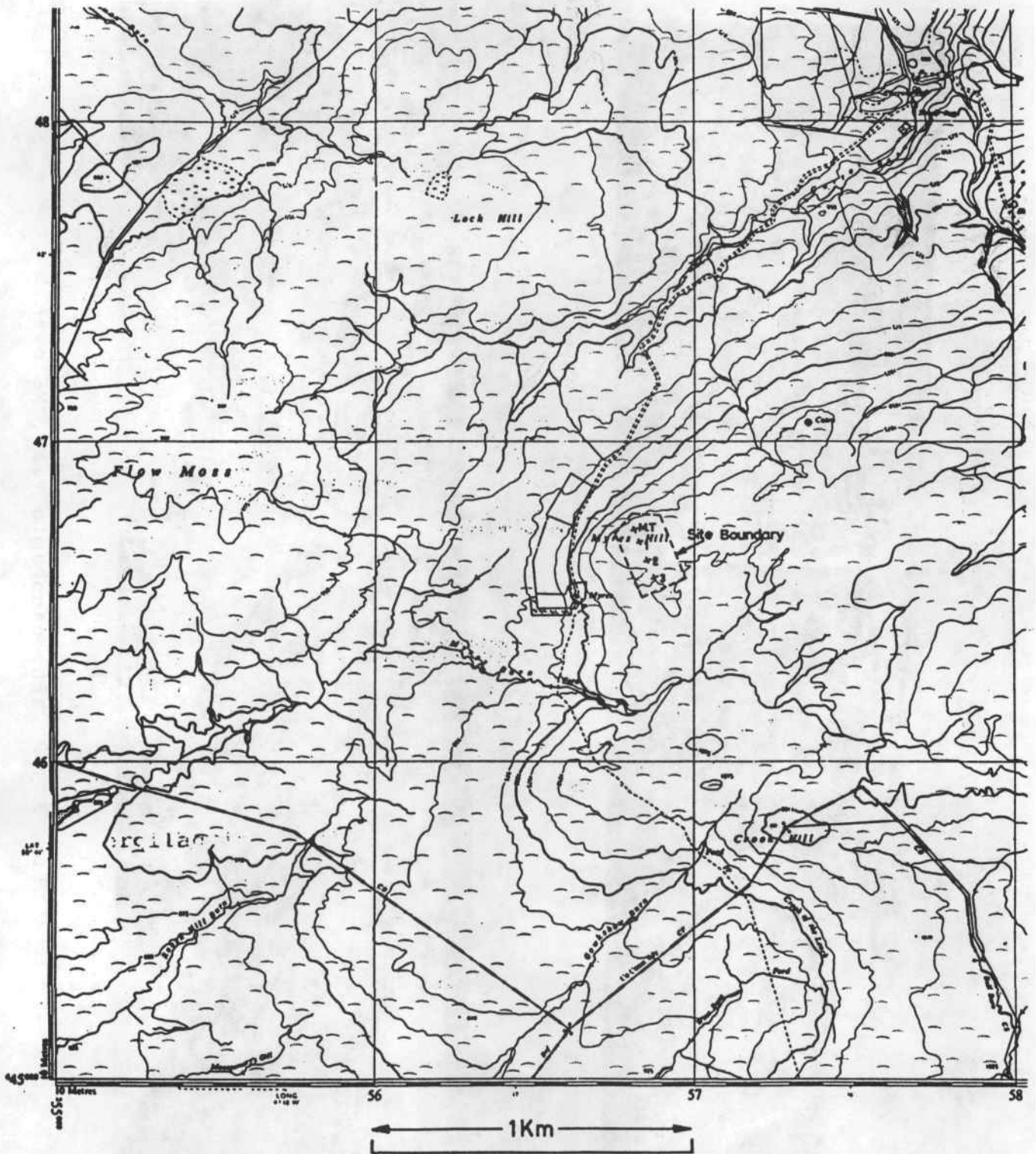


Fig. A.3.1 NEL, 1:10.560 map, contour interval 25' (≈8 m)

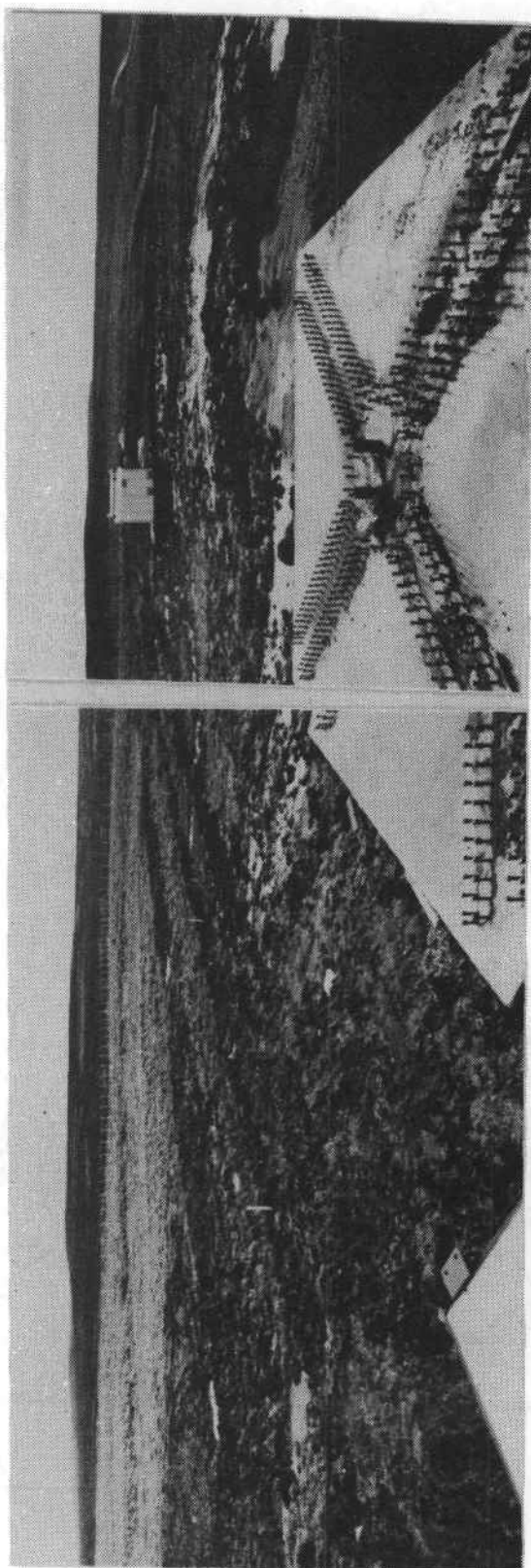
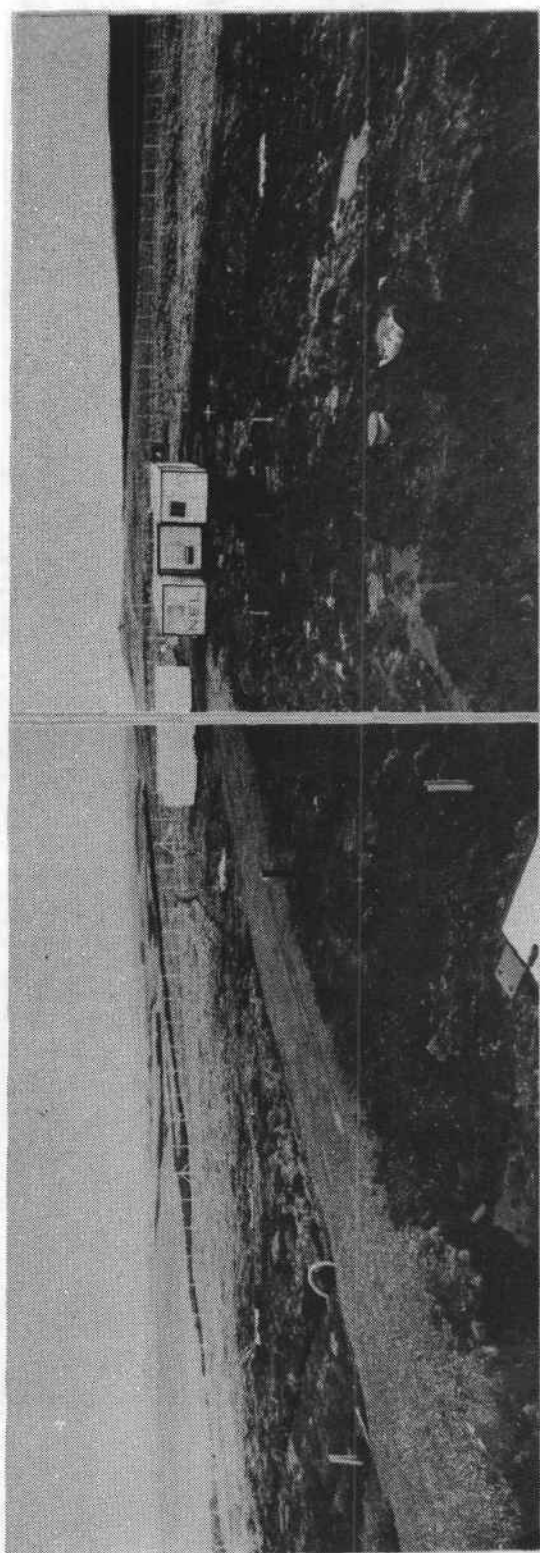


Fig. A.3.2 NEL, panoramic view, NE over E

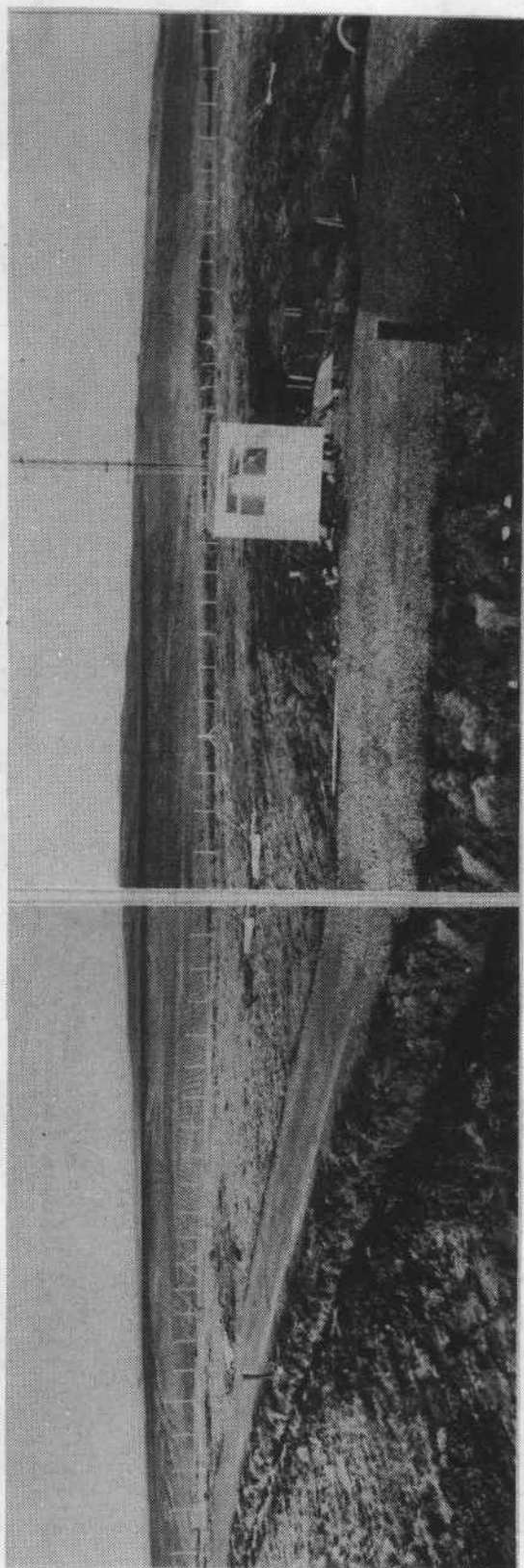
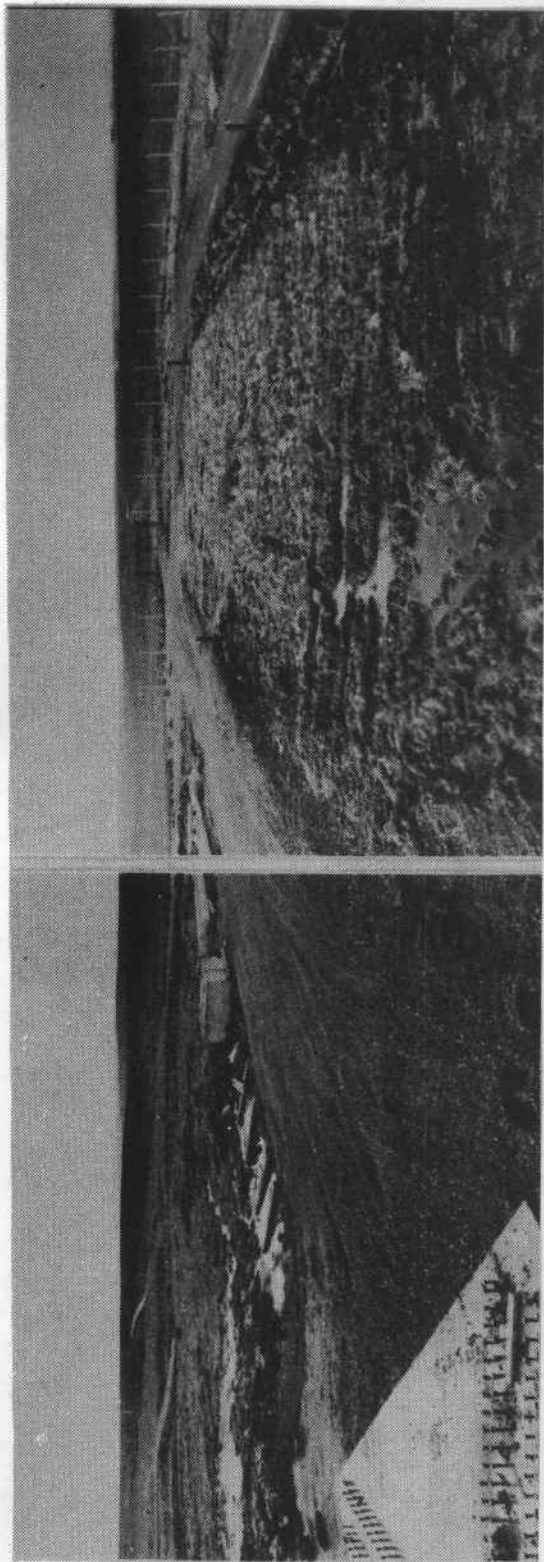


Fig. A.3.3 NEL, SW over W



Fig. A.4.1 RAL, UK, 1:50.000, map
contour interval 10 m.



Fig. A.4.2. RAL Test Station view looking W SW

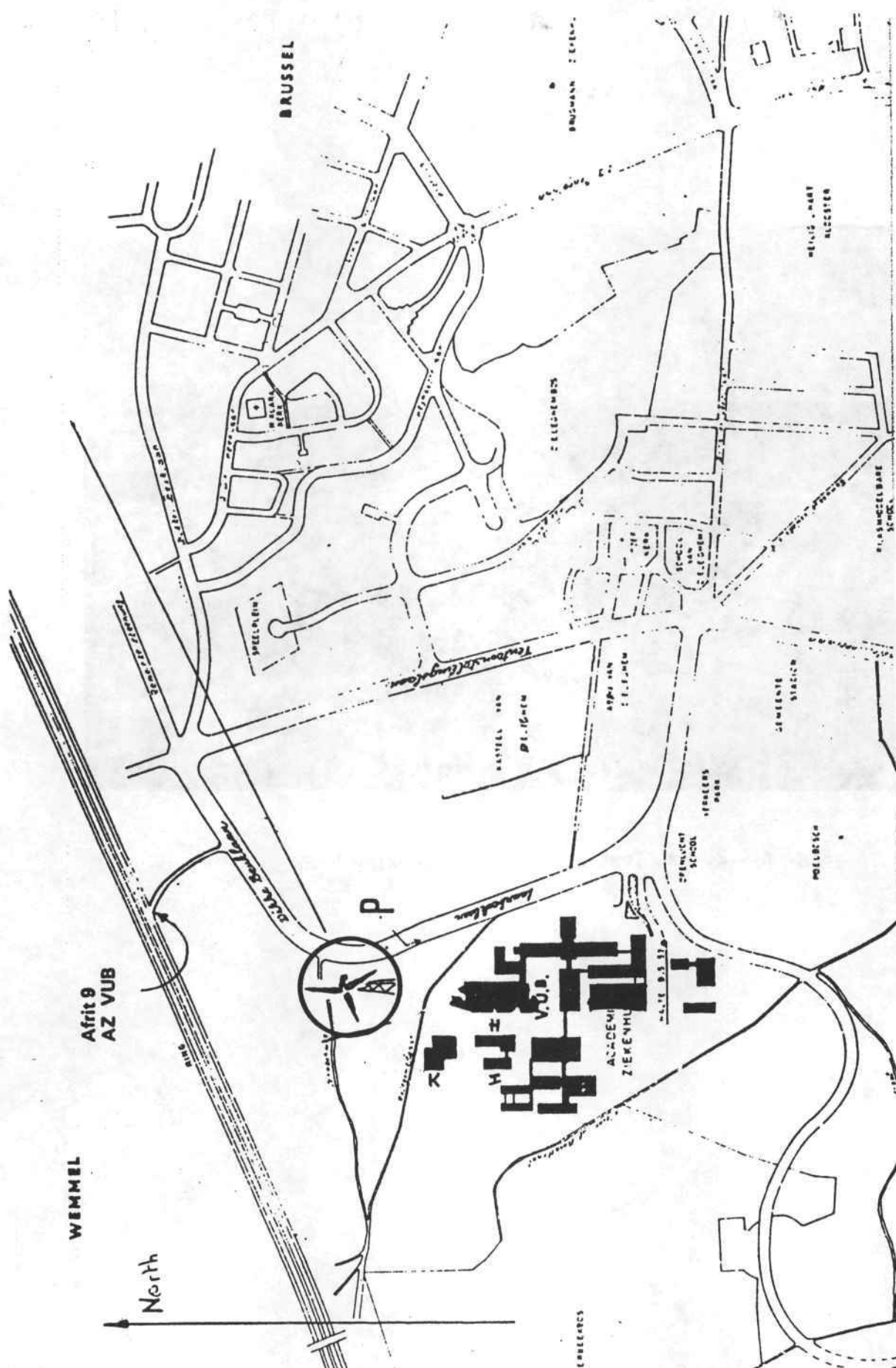
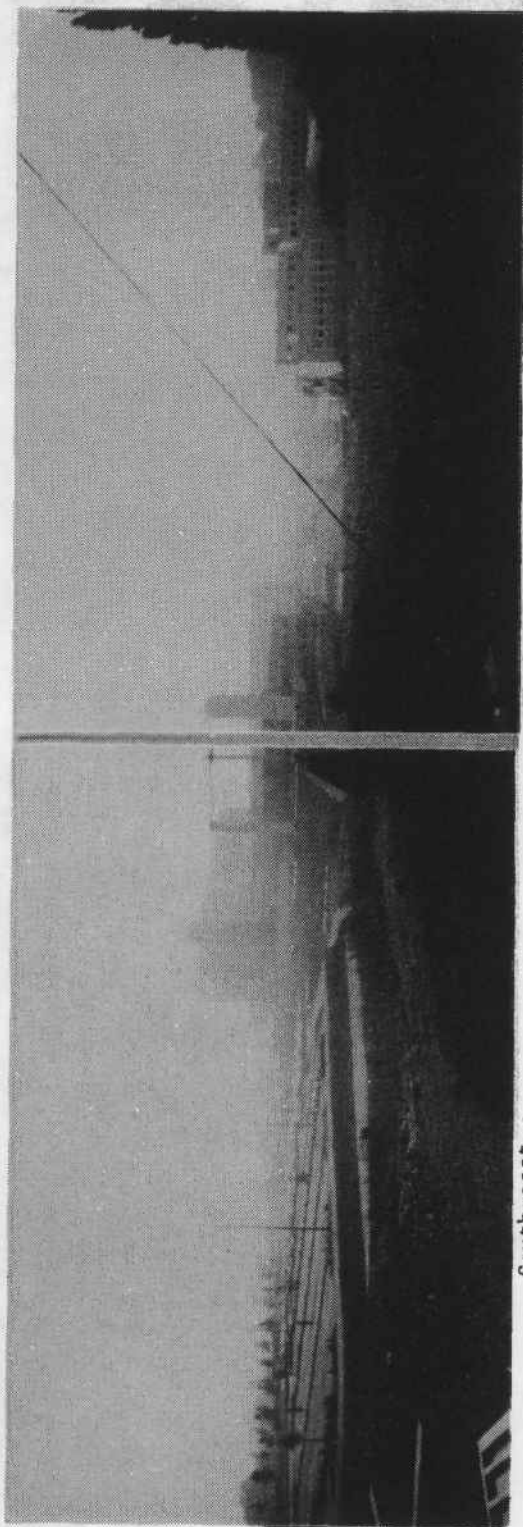
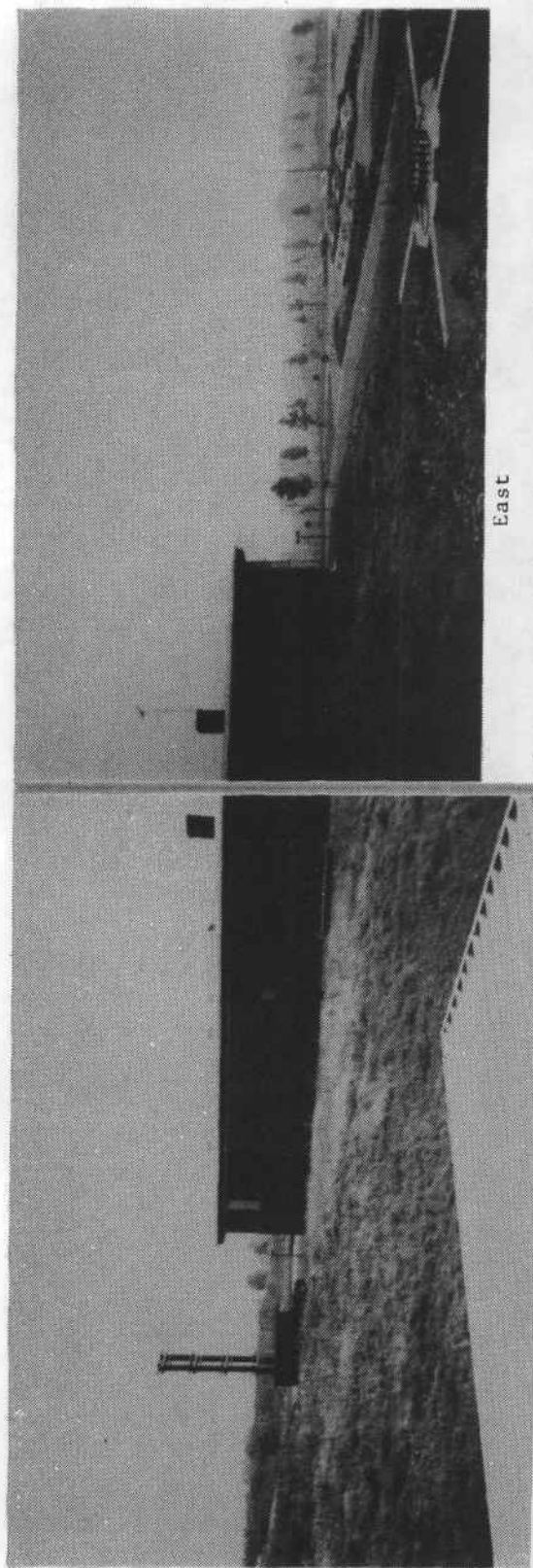


Fig. A.5.1 VUB, Bruxelles, map.



South-east

Fig. A.5.2 VUB, panoramic view, NE over E.

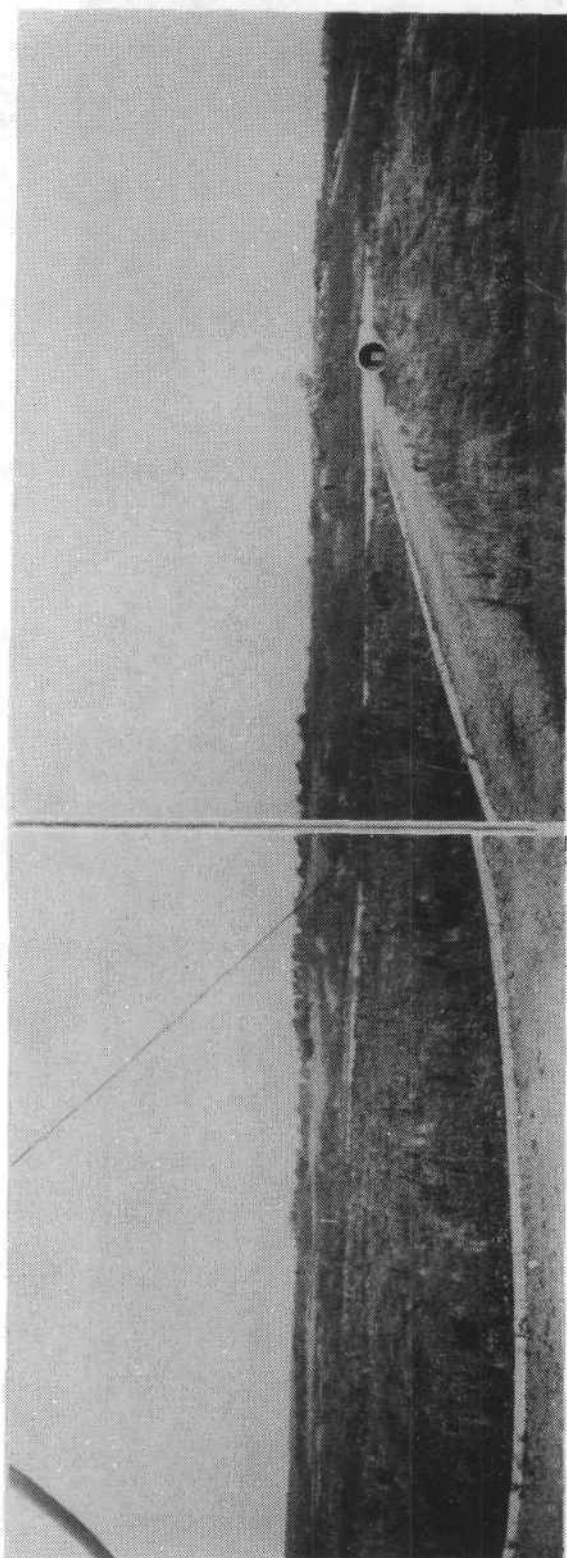
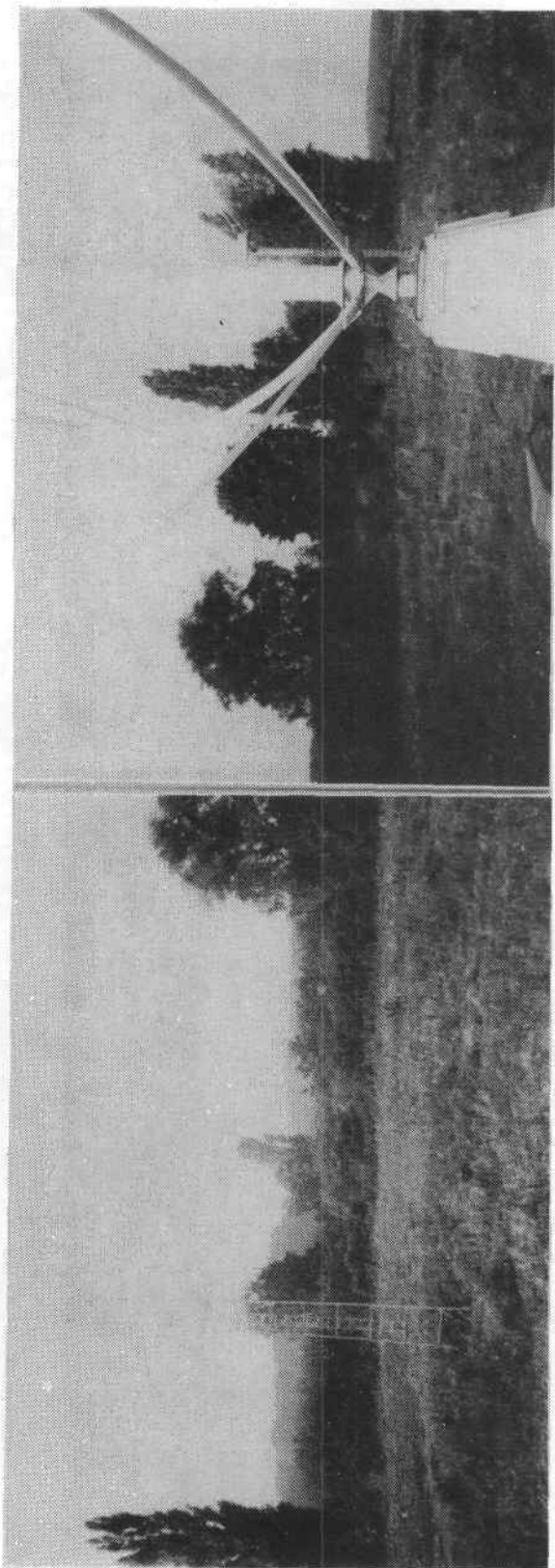


Fig. A.5.3 VUB, SW over W.

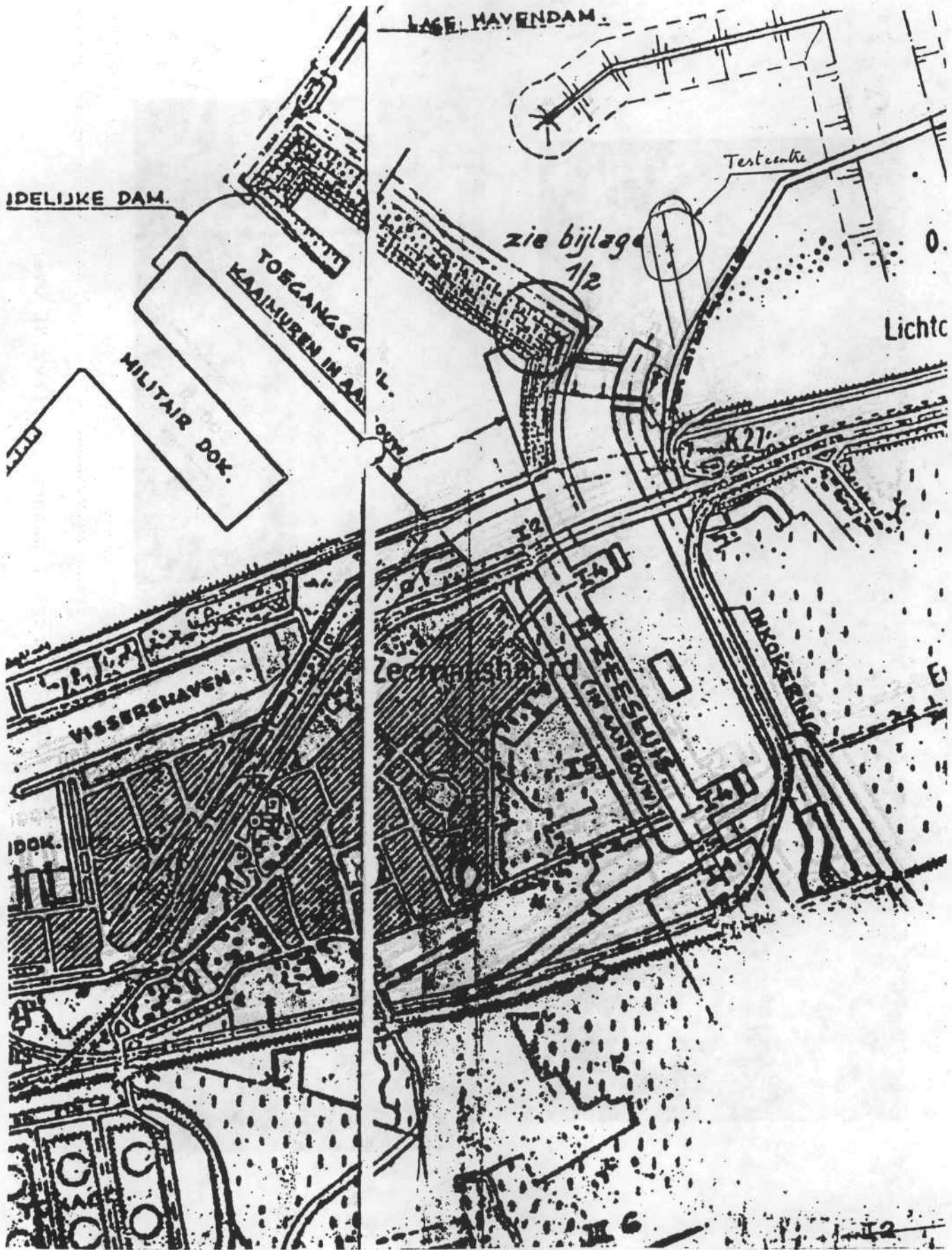


Fig. A.5.4 VUB, Zeebrugge, map.

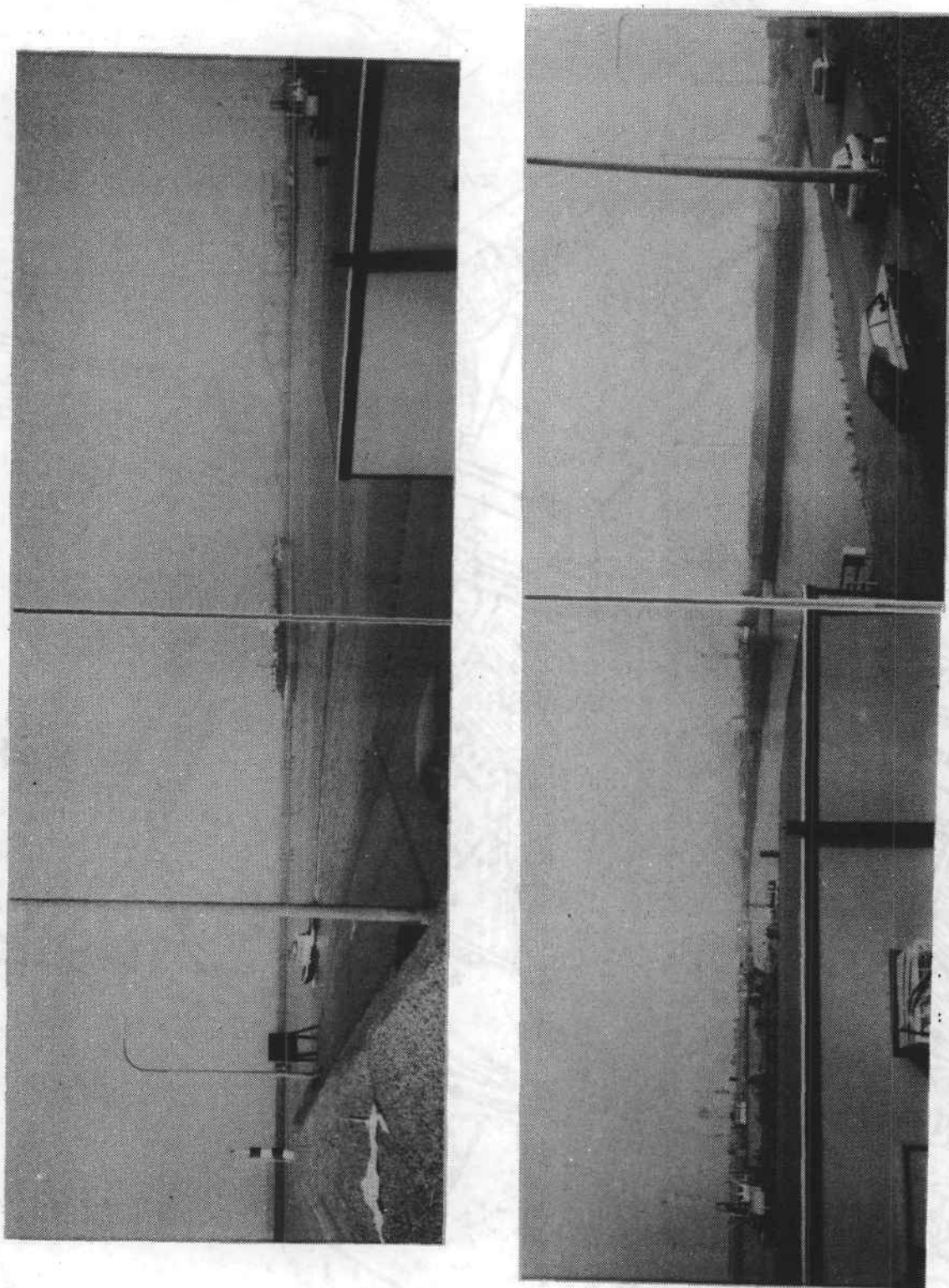


Fig. A.5.5 VUB, Zeebrugge, panoramic view, NE over E.

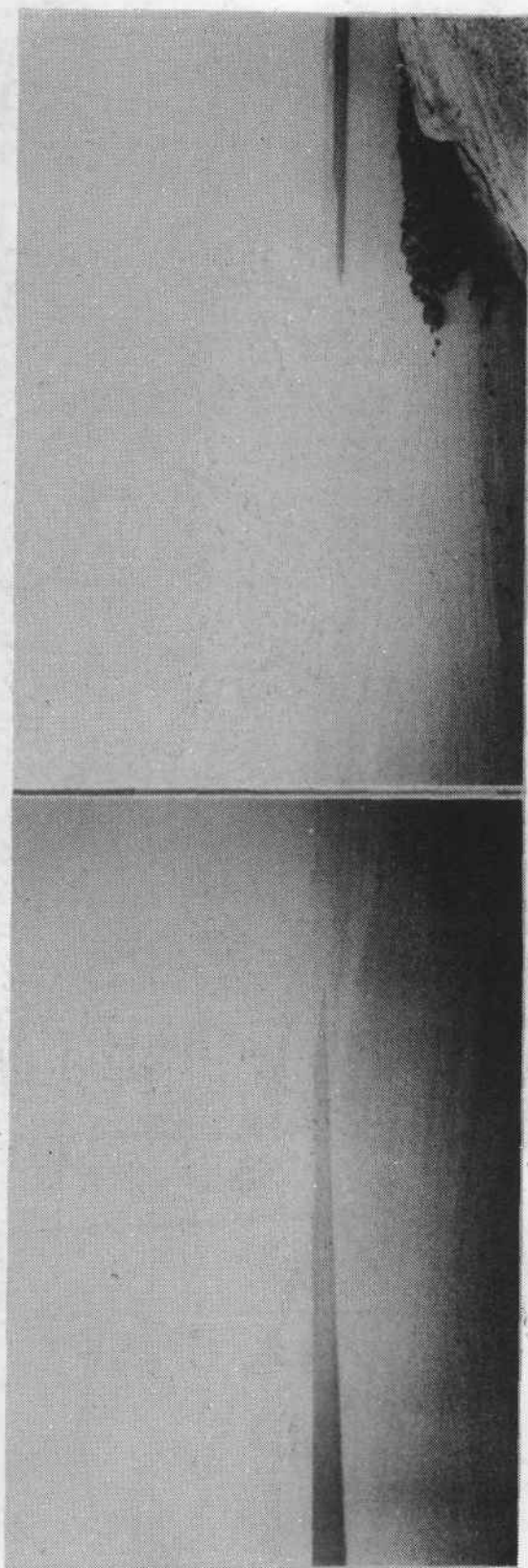
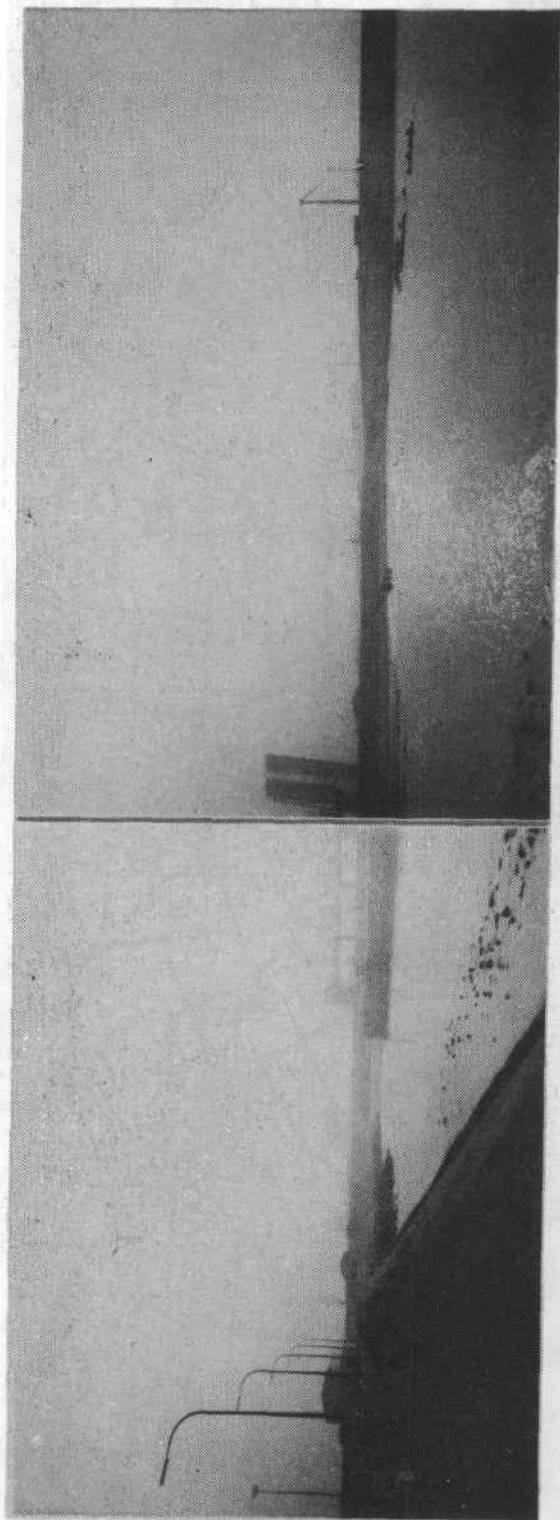


Fig. A.5.6 VUB, Zeebrugge, SW over S.

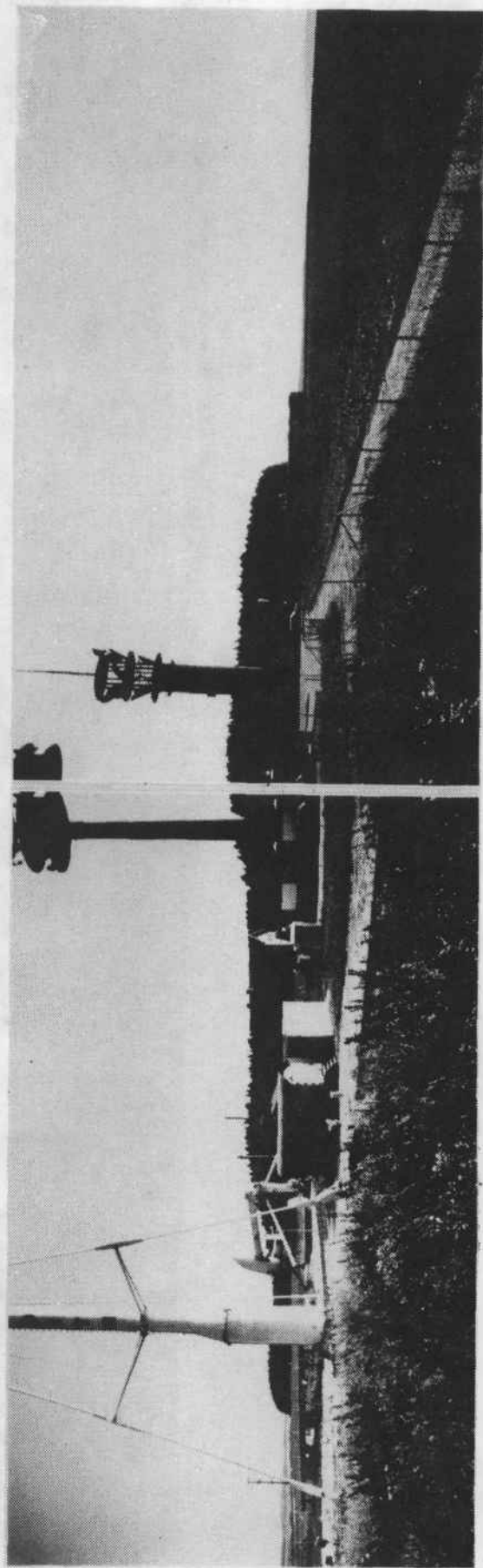
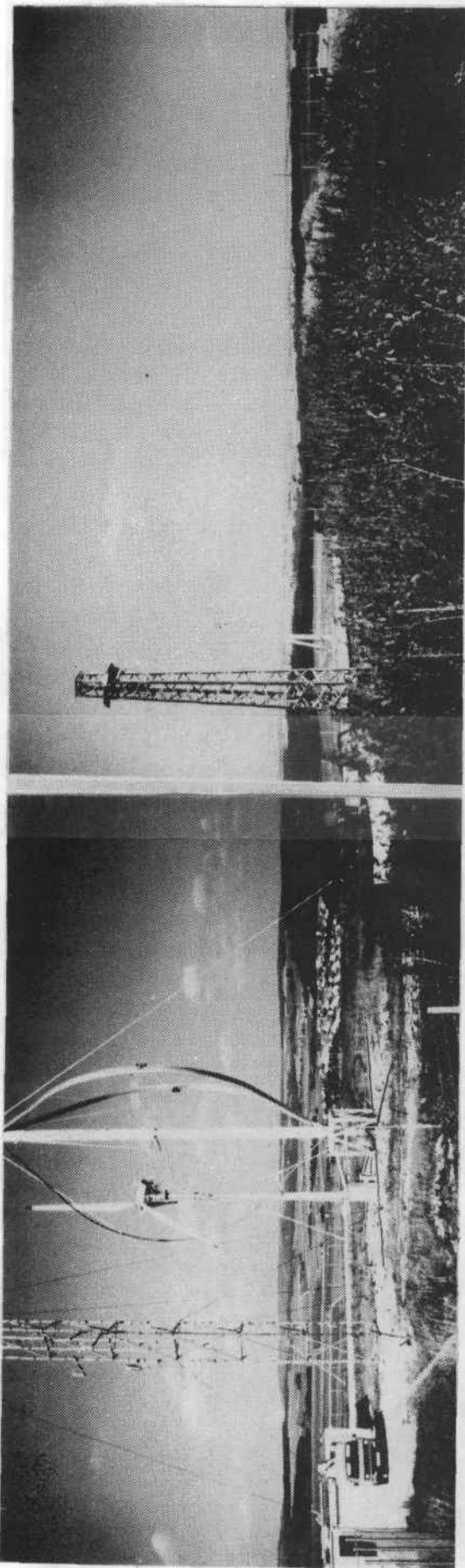


Fig. A.6.2 Schnittlingen, panoramic view, NE to SW over E.

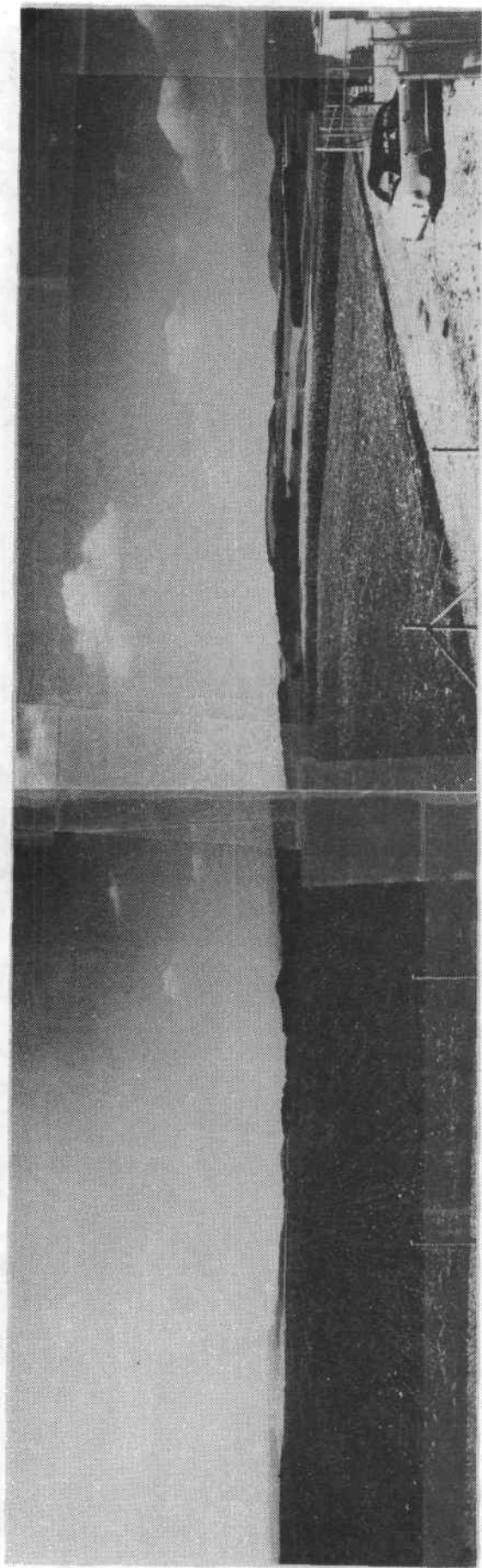


Fig. A.6.3 Schnitttlingen, W to NW

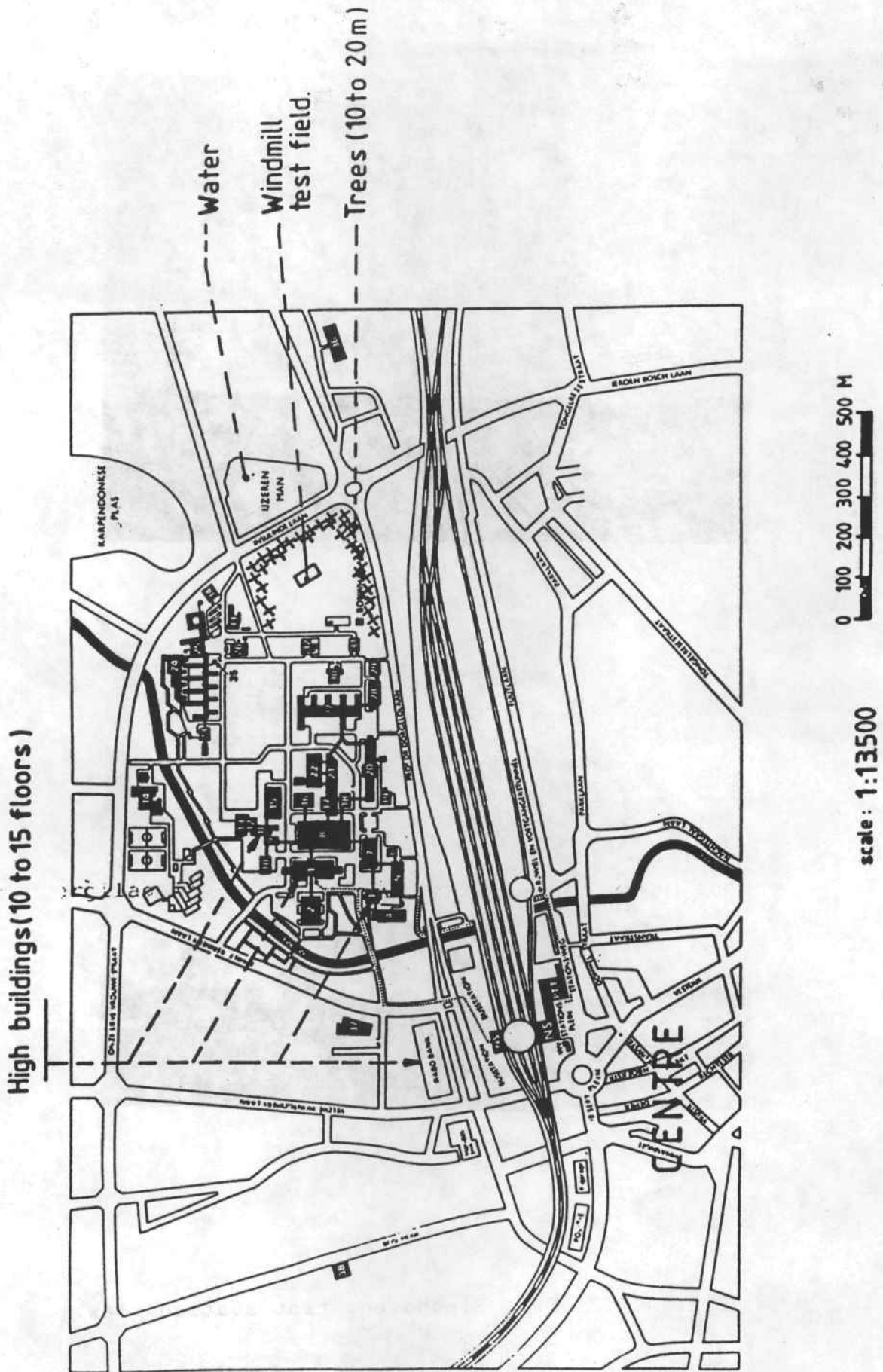


Fig. A.7.1 CWD, Eindhoven, NL, 1:13500 map.

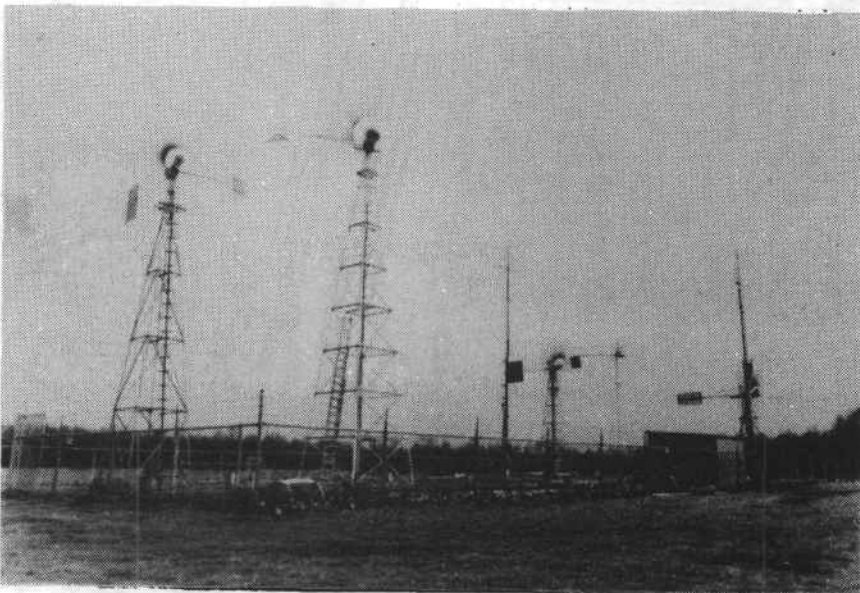
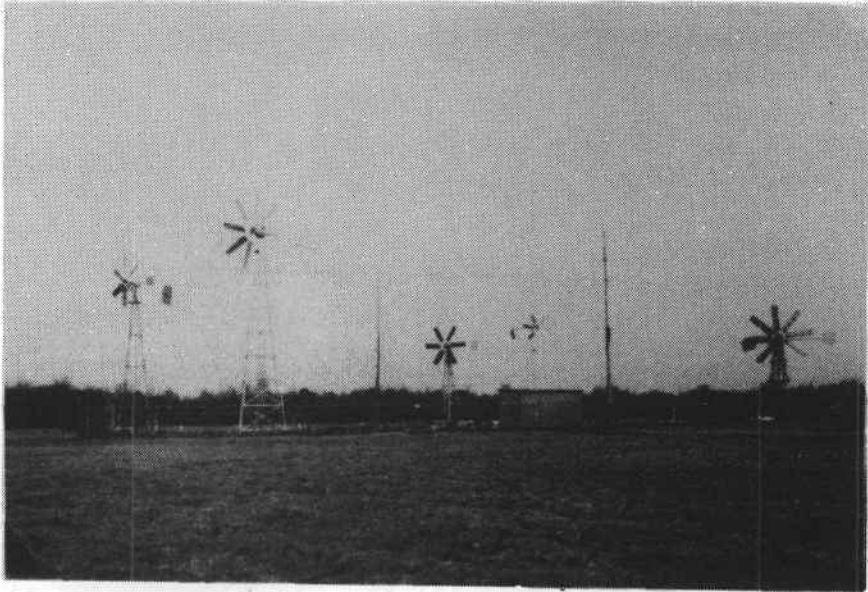


Fig. A.7.2 CWD, Eindhoven, test station view.

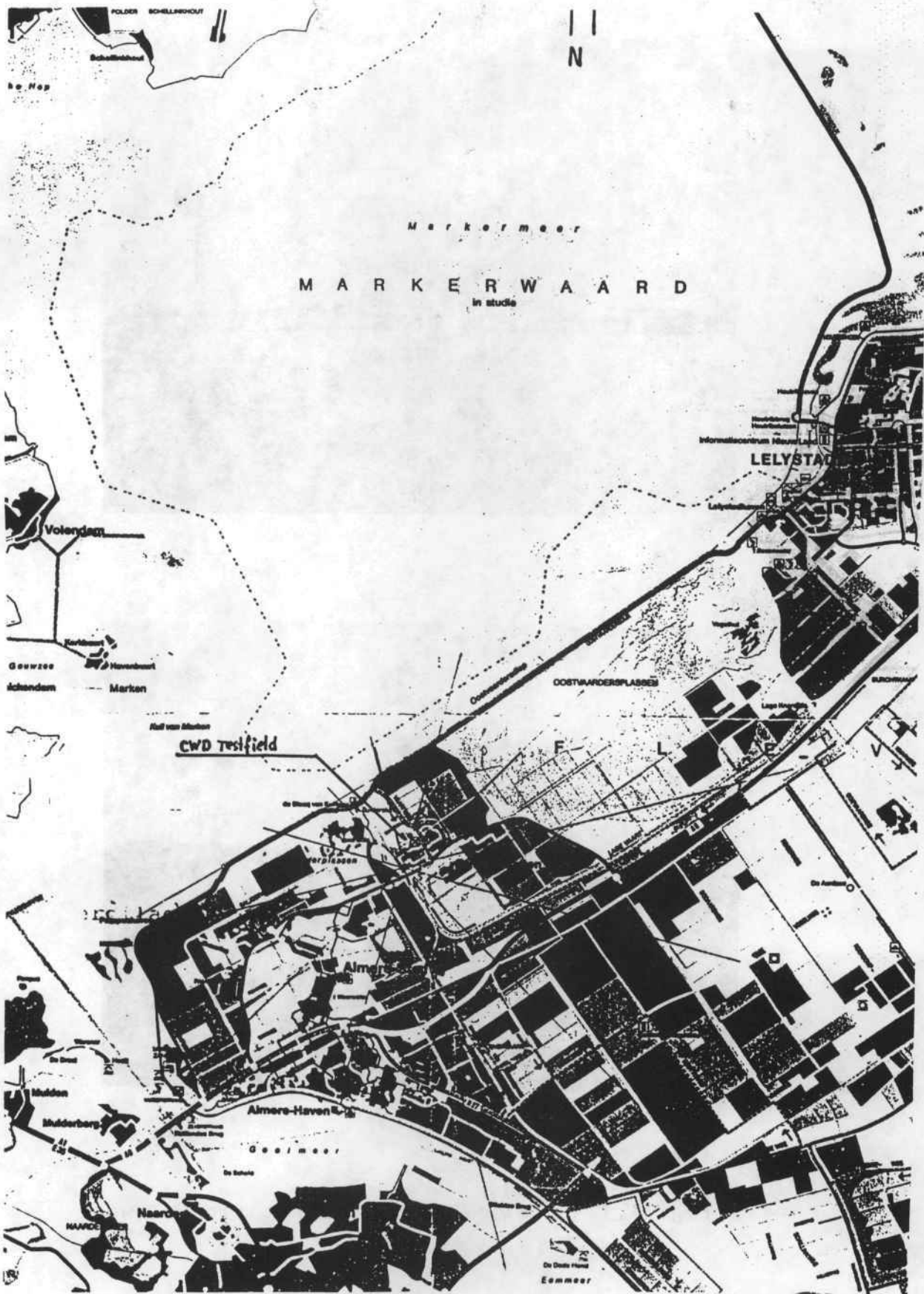


Fig. A.7.3 CWD, Almere, NL, map.

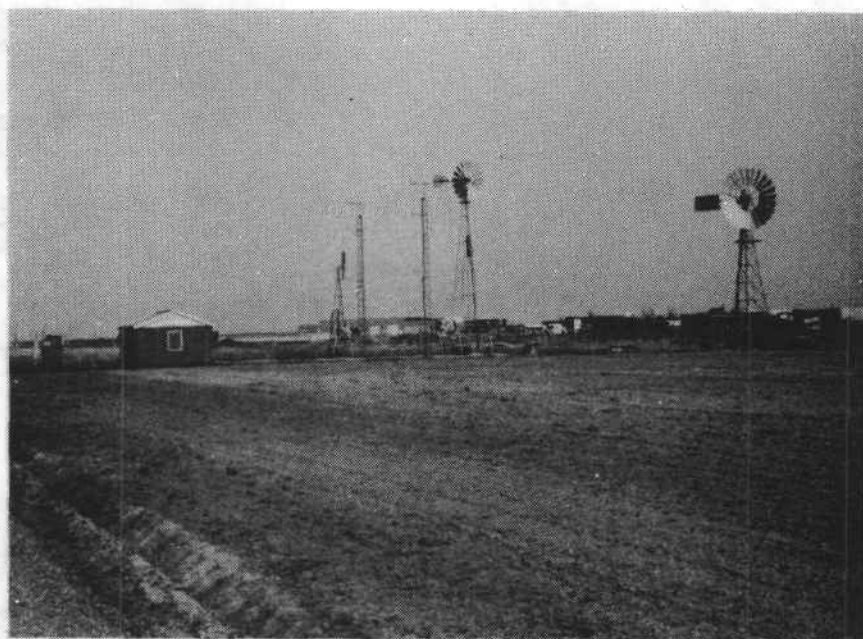
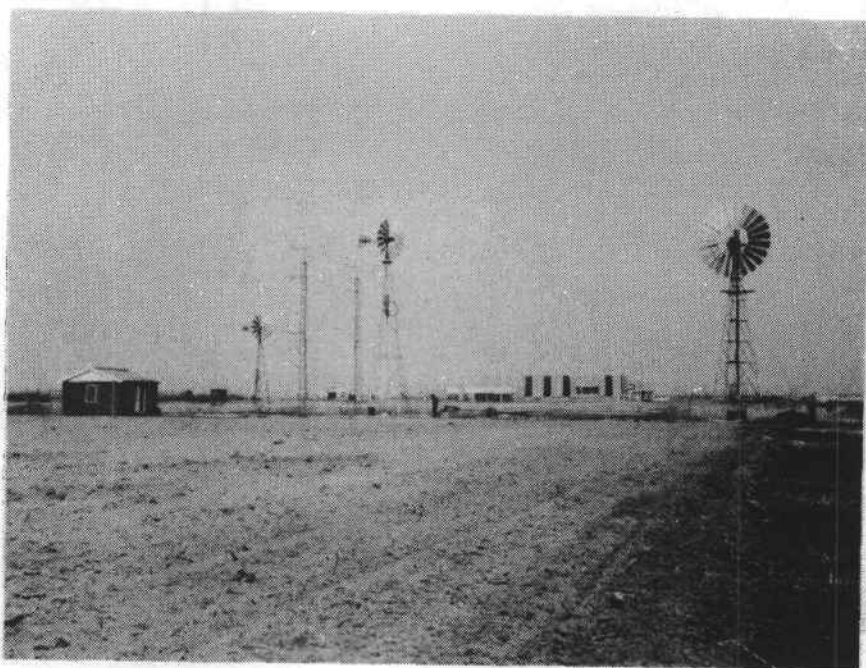
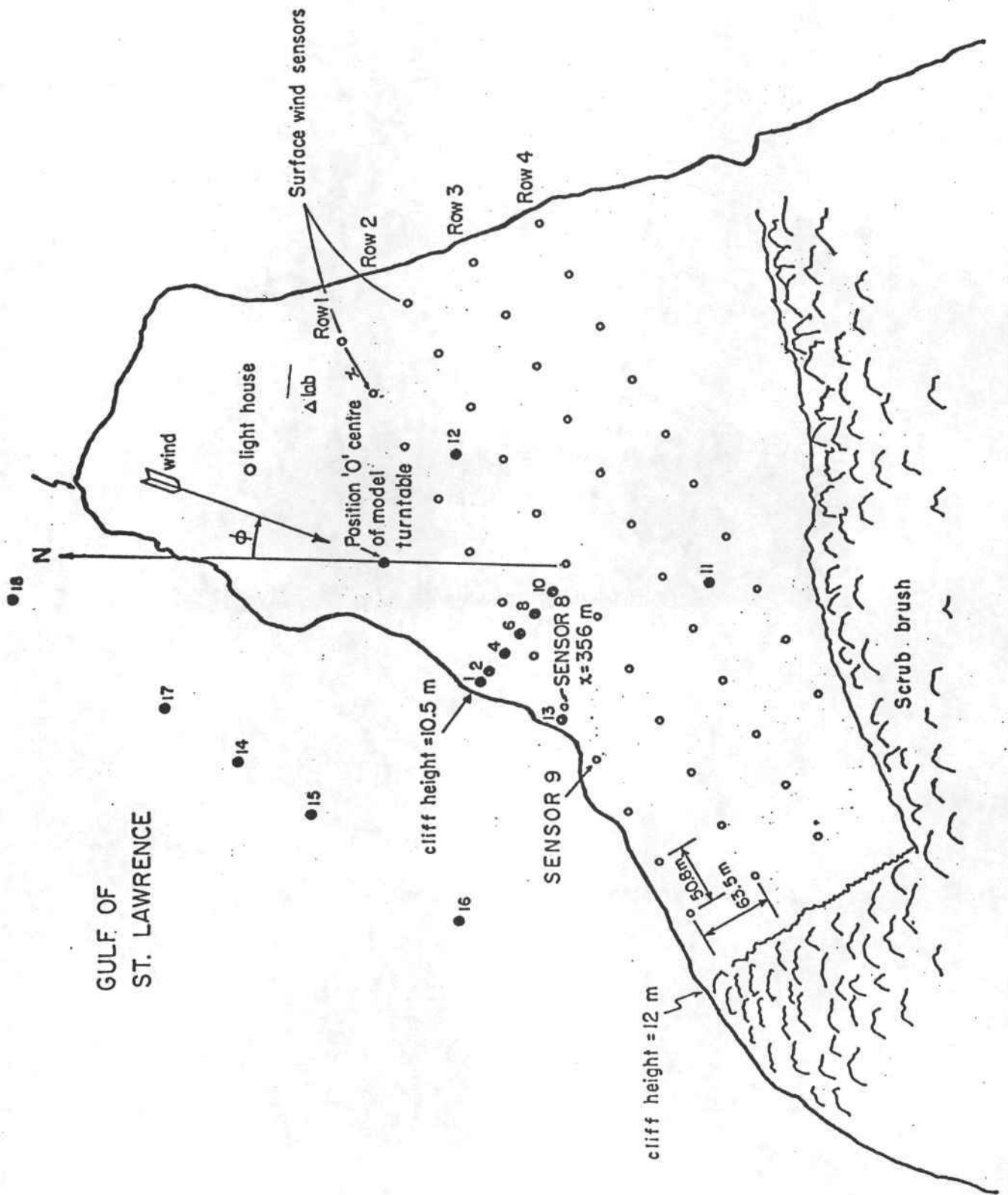


Fig. A.7.4 CWD, Almere, test station view

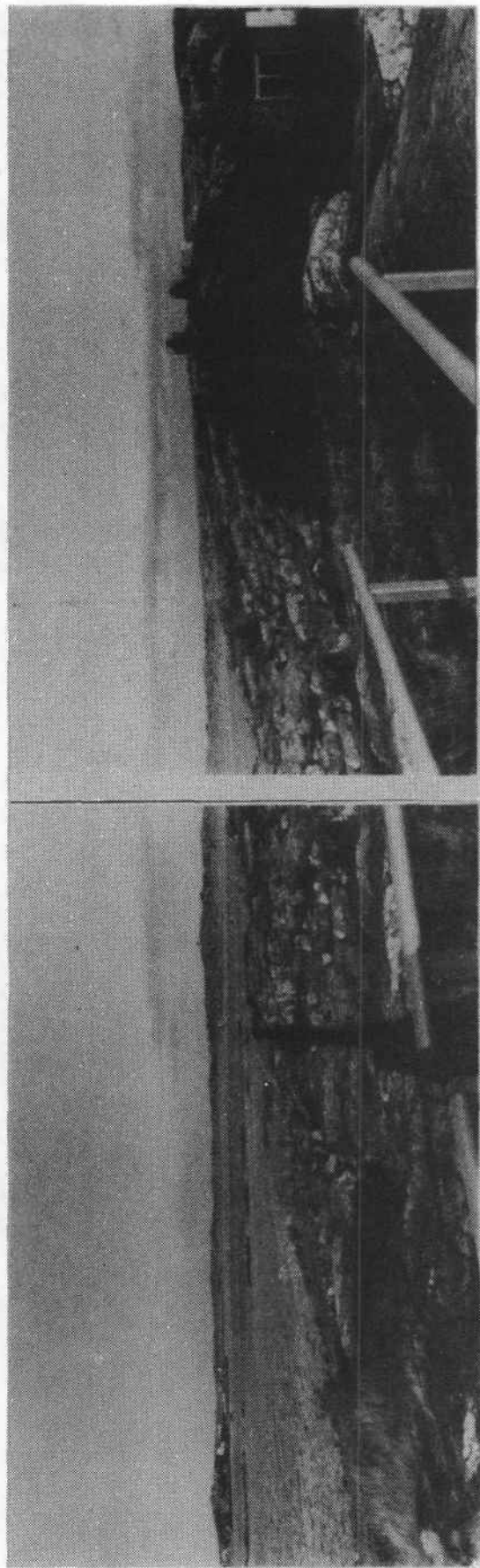


Fig. A.7.5 CWD, Vriezenveen, test station view.



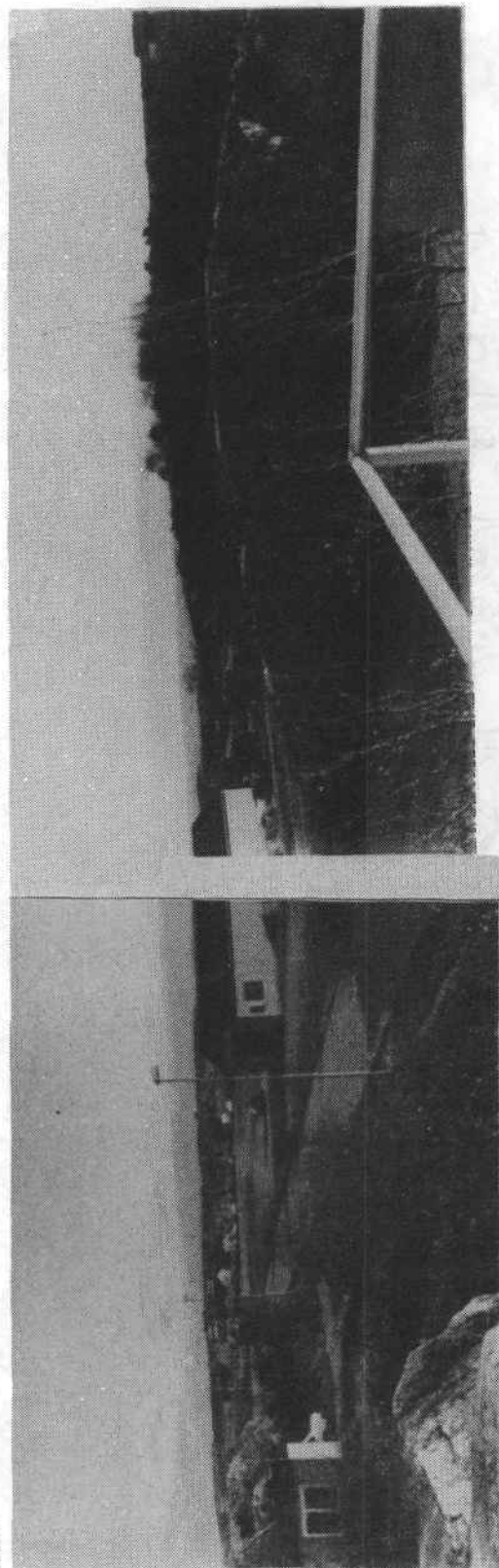
ATLANTIC WIND TEST SITE, NORTH CAPE, PRINCE EDWARD ISLAND

Fig. A.8.1 AWIS, Canada, 1:5000 map



EAST

NORTHEAST



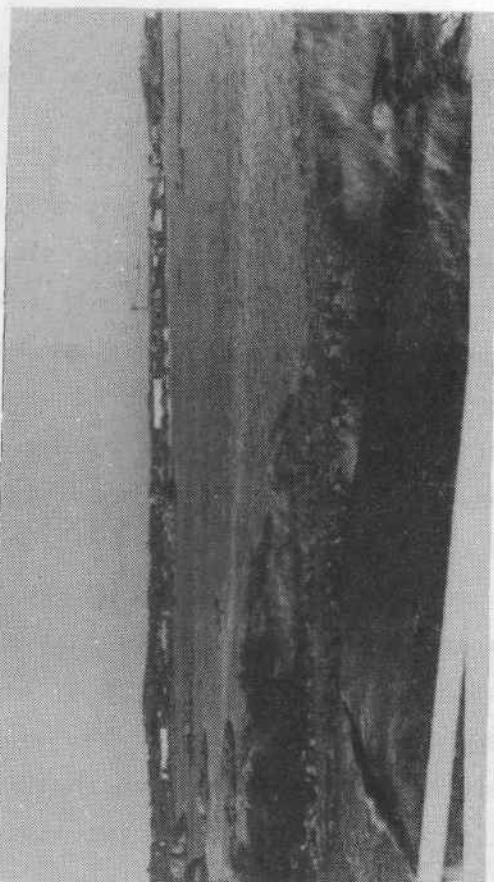
SOUTH

SOUTHEAST

Fig. A.9.2 Chalmers, panoramic view, NE over E



WEST



NORTH

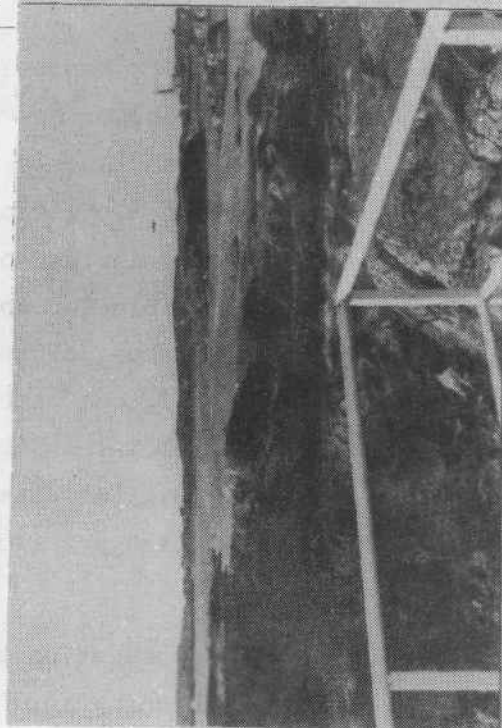
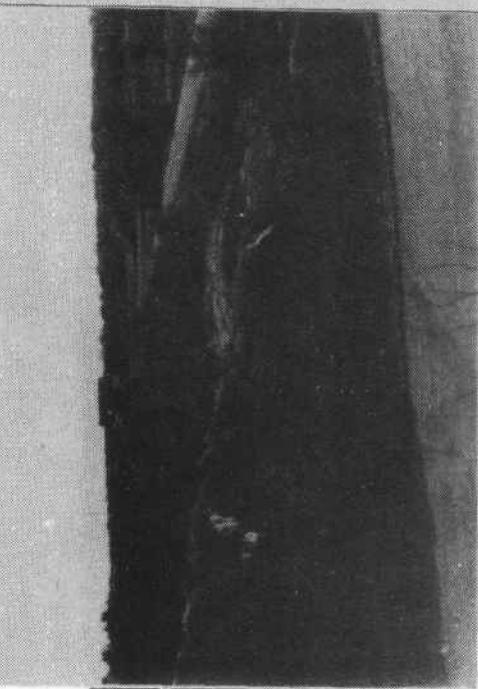


Fig. A.9.3 Chalmers, SW over W

ANNEX B

Benchmark exercise for power curve measurement

As part of the project the feasibility has been investigated of a benchmark test on the estimation of the power curve from real tape-recorded wind speed and power signals. The intercomparison of the results would provide a practical view on some of the existing inaccuracies. This test would serve as one of the preliminary steps for a round-robin tour of a small wind turbine for power performance testing. The desirability for such a round-robin tour in a later stage has been discussed for some time in the international test station cooperation and in the discussions with CEC. To make such a tour successful it would be a necessity that possible differences in results are not due to effects that can be tested separately, in particular

- differences in methods of data analysis,
- differences in anemometer calibrations.

Feasibility of test on these two topics has been studied. This section gives the result of the former item; annex B reports on the latter.

All participants in the project expressed their willingness to take part in a benchmark test for power curve estimation. It was checked what equipment is available for such a test. It would be most direct to use analog tape (FM recorded), giving signals to be fed directly into the data analysis system instead of the sensor signals.

This turned out to be impossible for most of the test stations: only two of them can read such a tape, plus one on a temporary loan basis. In nearly all cases digital tapes can be read and used for the test, though software provisions are required to feed them properly into the process. Digital data would circumvent some of the differences in test station practices, namely signal conditioning and sampling (see section 4.3).

There is a great deal of agreement on the bin method of analysis. All stations use velocity binning for 10 minute averaging time. The bin widths are different, but all can be translated into the

IEA bin width specification. The differences between test stations lie much more in the choice of acceptable/non-acceptable wind directions. There are also differences in extra information, computed above the mean values.

This brings us to the conclusion that the only benchmark test possible at this moment would consist of using a common digital tape at the different places, where the data are averaged to 10 minute data, which go into the same bin analysis. Essential aspects as signal handling and selecting or discarding data are not tested. No differences are to be expected that lead to insight into inaccuracies and errors. Therefore, we propose not to perform this particular benchmark test.

Instead, another test may be suggested here. Apart from the IEA-like specifications, there exist a lot of other non-standard methods, as treated in chapter 6. It is quite conceivable that in future other standards for power curve estimation will be needed, next to a basic 10-minute standard. This may be desirable for other purposes than energy production estimation, namely

- aerodynamic testing (where better velocity definition is a requirement),
- fast first-look power curves, e.g. for prototypes, but not for commercial purposes (if at all possible!).

For such purposes it is worthwhile to compare several methods of chapter 6 using the same input data. This requires data tapes obtained under a variety of wind conditions, which are used to obtain power curves through power binning, variations in regression techniques, with corrections for lack-of-correlation, or by frequency matching, etc.

It might be advisable to do this for different wind turbine types. The experience obtained will be a prerequisite for the special standard(s) mentioned.

We propose that actions are started for such an activity. Bringing suitable measurement sets together would be a task for several test stations in cooperation. Performing the actual analyses can probably best be done by only one institute with suitable hardware and software facilities.

ANNEX C

Proposal for the comparison of the accuracy of wind speed measurements at the wind turbine test stations

In pursuance of the ultimate goal of arriving at common certification and licensing agreements for wind turbines in the EEC member states, it will be essential for the national wind turbine test stations to formulate and adopt common standards of testing. Part of this will involve ensuring that measurement standards are derived and adhered to. The most important quantity of interest, in the study of wind energy conversion systems, is wind speed. Most other quantities, e.g. wind pressures, shaft torques, power levels, etc. are very sensitive to changes in wind speed, and it is therefore vital to measure it as accurately as possible. The work proposed in this document deals with the subject of measurement of wind speed and will involve an intercomparison of the calibration accuracies and response characteristics of the "standard" cup anemometers at present in use in the existing test stations. A previous joint-test site project, which involved an appraisal of the accuracy of the measurement of power-performance curves for wind turbines has highlighted the necessity to carry out work in this area. The work however is relevant, not only to power performance appraisal, but also to fatigue evaluation, wake studies and turbulence assessment.

It is proposed that each of the participating test stations should supply an anemometer for study. Changes in anemometer behaviour due to running-in and wear of rotor bearings will be evaluated. Each of the anemometers will be subjected to a detailed steady-state calibration at each of the calibration facilities available to the stations. This exercise will highlight possible, facility specific, inaccuracies. Further work will involve evaluation of distance constants, using wind tunnels, for both step increases and step decreases in wind speed. Free atmospheric studies, which will necessitate the purchase of a sonic anemometer, will be conducted, and will involve work at all test stations. The purpose of this investigation will be to define correction functions for each anemometer/test site combination which will allow the power spectra measured by a particular anemometer at a particular test station to be modified so as to im-

prove the accuracies of the power estimates. An investigation into the effect of rain on rotor behaviour will also be undertaken.

The proposal has been worked out in fuller details and submitted to the CEC by the UK National Engineering Laboratory.

Title and author(s) Accuracy of Power Curve Measurements C.J.Christensen, Risø and J.B.Dragt, ECN	Date November 1986					
	Department or group Meteorologi and Windenergy The Test Station for Windmills					
	Groups own registration number(s) 					
	Project/contract no. EEC, DGXVII, 84/B/7033/11/004/17					
<table border="1"> <tr> <td>Pages 136</td> <td>Tables</td> <td>Illustrations</td> <td>References</td> <td>ISBN 87-550-1307-4</td> </tr> </table>		Pages 136	Tables	Illustrations	References	ISBN 87-550-1307-4
Pages 136	Tables	Illustrations	References	ISBN 87-550-1307-4		

Abstract (Max. 2000 char.)

This report represents a start on the problem of reaching comparability and common acceptability of power curves measured at the different test stations. The problem is essential for establishing a future common set of certification rules. Such common rules in turn will serve the need for opening the internal market for windmills within the EEC. A few non-EEC members of the international IMTS cooperation between test stations have taken part in the project. This has been welcomed, as it will help opening the global market too.

Through the examination of a large number of error source, the test site specific errors were found to be the most important source of uncertainty. This has to do with how well an anemometer in a mast separated from the windmill represents the wind speed that drives the windmill. Three factors create this importance. First, when calculating the progression of errors from a power curve error into an uncertainty on the yearly production prediction, a multiplier of 2-4 must be applied to the velocity uncertainty. Secondly, turbulence induces errors. Thirdly, the terrain around the windmill is almost never homogeneous enough to avoid a flow distortion, that induces errors in the wind speed chosen to represent the driving speed.

A host of measures to be taken by the test station are recommended, aiming at reducing the uncertainties. Without an effort in this direction, the power prediction uncertainty can well be up to 25-30%. But it ought to be possible to reduce this uncertainty to a level of 5-10%.

It is recommended, that the power prediction error is calculated and quoted for a Rayleigh distribution with 7 m/s average wind speed.

Descriptors - EDB;

ACCURACY; ANEMOMETERS; BELGIAN ORGANIZATIONS; CALIBRATION; CANADIAN ORGANIZATIONS; DATA COVARIANCES; DATA PROCESSING; EFFICIENCY; ERRORS; GERMAN FR ORGANIZATIONS; INTERLABORATORY COMPARISONS; INTERNATIONAL COOPERATION; MEASURINGSMETHODS; NETHERLANDS ORGANIZATIONS; PERFORMANCE TESTING; POWER GENERATION; RISOE NATIONAL LABORATORY; STANDARDIZATION; STATISTICS; SWEDISH ORGANIZATIONS; TOPOGRAPHY; TURBULENCE; UNITED KINGDOM ORGANIZATIONS; VELOCITY; WIND; WIND TURBINES

Available on request from Risø Library, Risø National Laboratory, (Risø Bibliotek, Forskningscenter Risø),
 P.O. Box 49, DK-4000 Roskilde, Denmark.
 Telephone 02 37 12 12, ext. 2262. Telex: 43116, Telefax: 02 36 06 09

**Available on request from
Riss Library,
Riss National Laboratory, P. O. Box 49,
DK-4000 Roskilde, Denmark
Phone (02) 37 12 12 ext.2262**

**ISBN 87-550-1307-4
ISSN 0418-6435**